DISSERTATION

ROLE OF MECHANISTIC TARGET OF RAPAMYCIN (mTOR) SIGNALING IN THE CRUSTACEAN MOLTING GLAND

Submitted by

Ali Moftah M. Abuhagr

Department of Biology

In partial fulfillment of the requirements

For the Degree of Doctor of Philosophy

Colorado State University

Fort Collins, Colorado

Fall 2012

Doctoral Committee:

Advisor: Donald L.Mykles

Deborah M. Garrity
Anireddy N. Reddy
Norman P. Curthoys

ABSTRACT

ROLE OF MECHANISTIC TARGET OF RAPAMYCIN (mTOR) SIGNALING IN THE CRUSTACEAN MOLTING GLAND

Regulation of the molt cycle in decapod crustaceans is mainly controlled by the X-organ/sinus gland complex (XO/SG) and the Y-organ (YO). Molt-inhibiting hormone (MIH), secreted by the XO/SG complex, suppresses production of molting hormone (ecdysteroids) by a pair of YOs. In the blackback land crab, *Gecarcinus lateralis*, molting can be induced by eyestalk ablation (ESA) or autotomy of 5 or more walking legs (multiple leg autotomy or MLA). During the molt cycle, the YO transitions through four physiological states: "basal" state at postmolt and intermolt; "activated" state at early premolt; "committed" state at mid premolt and "repressed" state at late premolt. The basal to activated state transition is triggered by a transient reduction in MIH; the YOs hypertrophy, but remain sensitive to MIH. The main hypothesis is that up-regulation of mechanistic Target of Rapamycin (mTOR) signaling, which controls global translation of mRNA into protein, is necessary for YO hypertrophy and ecdysteroidogenesis. cDNAs encoding mTOR, Rheb, Akt (protein kinase B) and p70 S6 kinase (S6k) were cloned from blackback land crab, *G. lateralis*, and green shore crab, *Carcinus maenas*. All four genes were expressed in all tissues examined. mTOR appears to be involved in YO activation in early premolt, as rapamycin inhibited YO ecdysteroidogenesis *in vivo* and *in vitro*. In addition, the expression of *Gl-elongation factor 2* (*EF2*), *Gl-mTOR*, and *Gl-Akt* increased significantly in YOs from premolt, suggesting that an increase in protein synthetic capacity is necessary for YO activation. A putative transforming growth factor-beta (TGFβ) appeared to be involved in the transition of the YO from the activated to committed state, as SB431542, an Activin receptor

antagonist, lowered hemolymph ecdysteroid titers in mid premolt animals and abrogated the premolt increases in *Gl-EF2*, *Gl-mTOR*, and *Gl-Akt* mRNA levels. By contrast, molting had no effect on *Cm-EF2*, *Cm-mTOR*, *Cm-Rheb*, *Cm-Akt*, and *Cm-S6k* expression in *C. maenas* YOs.

Unlike *G. lateralis*, adult *C. maenas* was refractory to ESA. ESA caused a small increase in hemolymph ecdysteroid titers, but animals did not immediately enter premolt. Some ES-ablated animals molted after many months, but most failed to molt at all. We hypothesized that other regions of the nervous system, specifically the brain and/or thoracic ganglion, were secondary source(s) of MIH. Nested endpoint RT-PCR showed that MIH transcript was present in brain and thoracic ganglion of intermolt crabs. Sequencing of the PCR product confirmed its identity as MIH. Real time PCR was used to quantify the effects of ESA on MIH expression in brain and thoracic ganglion on *C. maenas* red and green color morphs. ESA had little effect on MIH transcript levels, indicating that MIH was not regulated transcriptionally by the loss of the eyestalks. The data suggest that MIH secreted by neurons in the brain and thoracic ganglion is sufficient to prevent molt induction when the primary source of MIH is removed by ESA. There was also no effect of ESA on the expression of *Gl-EF2* and mTOR signaling components in *C. maenas* YOs.

ACKNOWLEDGMENTS

I thank God, the Creator, ALLAH, for the abilities that I have been given and the opportunities in life to accomplish my degree. And I am grateful for the chance to learn and study the creation from the knowledge that has been given to mankind. And I ask that it be accepted in the balance of my good deeds “Ameen”. Recite in the name of your Lord who created, Created man, who taught by the pen, Taught man that which he knew not (Quran, Alaq, Chapter 96).

I deeply thank my advisor Dr. Donald Mykles for his guidance, time, and support and for understanding of my situation as a foreign student. I also thank my committee members Dr. Deborah Garrity, Dr. Anireddy Reddy and Dr. Norman Curthoys for their encouragement and guidance. My thanks also go to the past and present crab lab members Dr. Joseph Covi, Dr. Kyle MacLea, Kathy Cosenza, Natalie Pitts and Megan Mudron.

I would like to thank our Islamic community in Islamic Center of Fort Collins Colorado and my two close friends Weal Elflah and Mohammed Albaqami.

Finaly, I thank my parents and siblings for their sacrificing, prayers and supplication. I also thank my wife, sons Hatem and Anas and my daughter Asra for their patience and continuous support without which I would not succeeded.

TABLE OF CONTENTS

CHAPTER ONE

INTRODUCTION

A brief background on the crustacean molt cycle:

Decapod crustaceans grow by periodic molting that is essential for growth, reproduction and metamorphosis (Skinner, 1962). According to Drach (1939), the molt cycle is divided into five stages, A to E based on the structure and hardness of the exoskeleton. In land crab, *Gecarcinus lateralis*, the duration of the molt cycle is four to six months in juveniles and one or two years in adults. After ecdysis stage E comes stage A, which lasts one to two days. During this stage, gastroliths are dissolved and epidermal cell size is decreased. In stage B the muscle in chela grows and the endocuticle layer is formed. Stages C_1 to C_4 comprises all of the cycle except for a 30-day premolt stage, D_0 through D_4 and a brief postmolt stage (A and B) (Skinner, 1962). In the stages C_1 and C_2 the endocuticle layers are calcified and thickened. At the end of stage C_3 the membranos layer of exoskeleton is formed, which completes the synthesis of the exoskeleton. Intermolt, or stage C_4, is the longest period in the molting cycle. In response to internal and external cues, the animal enters premolt, which is divided to 5 substages D_0 to D_4. In stage D_0 claw muscle atrophies and gastrolithes begin forming. In stage D_1 the epidermis separates from the old exoskeleton (apolysis), thickens and begins secretion of the outer layers of the exoskeleton. Through stage D_2 hemolyph ecdysteroid concentrations increase and the epidermis secretes new epicuticle and exocuticle. During stage D_3 hemolyph ecdysteroid concentrations reach a peak and the hemolymph turns pink in stage D_4, due resorption of astaxanthin from the old exocuticle. Actual ecdysis, or shedding of the old exoskeleton, occurs at stage E and lasts up to 1 day (Skinner, 1985).

Environmental conditions can affect the molt cycle. Many factors such as feeding, migration, and reproduction are known to have close links with the molt cycle of crustaceans (Caddy, 1987). Temperature and salinity can affect the timing and frequency of molting in crustaceans (Hughes et al., 1972; Dall and Barclay, 1977; Chang; Bruce, 1980; Skinner, 1985). The shrimp *Macrobrachium rosenbergii* has a protracted post-molt period under nutrient-poor conditions (Peebles, 1977). In American lobster, *Homarus americanus*, higher temperature shortens the molt cycle, while lower temperature delays molting in the fiddler crab, *Uca pugnax* (Passano, 1960). Studies on other types of crustaceans reported that larger crustaceans have a longer intermolt period than smaller ones of the same spices under a given conditions (Small and Habard, 1967). In several different euphausiid crustaceans under controlled conditions, both temperature and body size act to adjust the length of the intermolt period in the molting cycle (Fowler et. al., 1971).

Endocrine control of the molting cycle in decapod crustaceans:

In decapod crustaceans, molting is controlled by the X-organ/sinus gland complex, a neurosecretory center in the eyestalks (ES). The complex secretes molt-inhibiting hormone (MIH), a neuropeptide that suppresses production of molting hormone (ecdysteroids) by a pair of molting glands (Y-organs or YOs) located in the anterior of the body (Fig. 1.1) (Spaziani et al., 2001; Covi et al., 2009). Molt-inhibiting hormone (MIH) represses YO ecdysteroidogenesis by increasing intracellular cAMP and cGMP (Covi et al., 2009; Nakatsuji et al., 2009). The data support the organization of the signaling pathway into a cAMP/Ca^{2+}-dependent “triggering” phase and a NO/cGMP-dependent “summation” phase linked by calmodulin (CaM) (Mykles et al., 2010; Lee and Mykles, 2006; Covi et al., 2011) (Fig. 1. 2). This is similar to the signaling mechanism that stimulates fluid secretion in *Drosophila* Malpighian tubules by the decapeptide

cardioacceleratory peptide 2b (Kean et al, 2002; Cazzamali et al., 2003). YOs express a Ca^{2+}/CaM-dependent NO synthase (NOS) and a NO-sensitive guanylyl cyclase (GC-I) (Kim et al., 2004 and Lee et al., 2007), and GC-I agonists (NO donors and YC-1) can inhibit YO ecdysteroidogenesis (Covi et al., 2008; Mykles et al., 2010). Phosphorylation of mammalian NOS reduces its activity; dephosphorylation by calcineurin enhances activity (Kone, 2001). NOS is phosphorylated in the activated YO, which is consistent with inactivation of NOS by protein kinases in the absence of MIH (Lee and Mykles, 2006).

The YO is a dynamic organ that changes over the molt cycle. The YO goes through four physiological states during the molt cycle (Fig. 1. 4), that are mediated by endocrine and autocrine factors. A reduction in MIH triggers the transition from the basal state in intermolt to the activated state in early premolt. TGFβ factor triggers the transition from the activated state to the committed state in mid premolt and high ecdysteroids trigger the transition from the committed state to the repressed state in late premolt (Chang and Mykles, 2011).

MIH suppresses ecdysteroidogenesis by the YO during intermolt (Fig. 1. 5), but the YO becomes refractory to MIH during premolt. In *Carcinus maenas* and *Procambarus clarkii*, the sensitivity to MIH declines during premolt and is least sensitive to MIH by the end of mid premolt and late premolt (Chung and Webster, 2003; Nakatsuji and Sonobe, 2004). In *G. lateralis* and *C. maenas* YOs, expression of NOS and GC-Iβ is up-regulated in response to an acute and chronic withdrawal of MIH and other neuropeptides by Eyestalk ablation (ESA) (McDonald et al., 2011).

Ecdysteroids are polyhydroxylated steroids synthesized from cholesterol by the YO. Hydroxylations at C25, C22, C2, and C20 are catalyzed by cytochrome P-450 mono-oxygenases, which are encoded by the Halloween genes Phm, Dib, Sad, and Shd, respectively, in insects

(Gilbert and Rewitz, 2009; Hopkins, 2009; Mykles, 2010). Orthologs of Phm, Dib, Sad, and Shd occur in the *D. pulex* genome (Rewitz and Gilbert, 2008; Markov et al., 2009; Niwa et al, 2010), and a cDNA encoding Phm (Mj-Phm) has been cloned from prawn, *M. japonicas* (Asazuma et al., 2009). Mj-Phm is a target of eyestalk neuropeptides, as its expression in the YO is increased as much as 7-fold during premolt and is decreased about 2.5-fold by sinus gland extract and rMIH (Asazuma et al., 2009). Inactivation involves conversion of ecdysteroids to polar metabolites and conjugates, which are eliminated in the urine and feces. The antennal gland is the major route for excretion of ecdysteroids synthesized by the YO (Mykles, 2010).

The mechanistic Target of Rapamycin (mTOR) signaling and its role in molting in arthropods:

The mechanistic target of rapamycin (mTOR) is now the center of substantial research in regulation cell growth, in mTOR signal are linked to human diseases, including some types of cancer (Albanella et al., 2007). The mTOR pathway is highly conserved among all metazoans and functions as a nutrient sensor for cellular growth (Proud, 2009). mTOR is crucial for growth, aging, development, reproduction, and metamorphosis in insects (Layalle et al., 2008; Grewal, 2009; Bjedov et al., 2010; Teleman, 2010). mTOR increases the ecdysteroid biosynthetic capacity of the prothoracic gland (PG) during premolt. Nutrients and insulin-like peptides (ILPs) activate mTOR, which phosphorylates components of the protein synthetic machinery, such as p70-S6 kinase (S6k) and eIF4E-binding protein (4EBP1) to increase translation of mRNA (Fig. 1. 6) (Proud, 2009; Teleman, 2010). Insulin stimulates ecdysteroidogenesis in the PG of *Bombyx mori* (Gu et al., 2009). Binding of ILP to an insulin receptor activates a signal transduction cascade involving PI3K, PDK1, and Akt protein kinases. mTORC1 is activated by the Rheb GTP-binding protein, and is inactivated when Rheb-GTPase activating protein (Rheb-GAP or

TSC1/2) stimulates the hydrolysis of GTP to GDP by Rheb (Fig. 1. 3). Rheb-GAP is inhibited when phosphorylated by Akt. Insulin-like peptide signaling prevents the hydrolysis of GTP by Rheb through the inhibition of Rheb-GAP, thus keeping mTOR in the active state (Fig. 1. 3) (Teleman, 2010). Genetic studies on *Drosophila melanogaster* have shown that the ILP/mTOR pathway controls PG size and ecdysteroidogenic capacity (Colombani et al., 2005; Mirth et al., 2005; Layalle et al., 2008). Over-expressing Rheb-GAP inhibits PG growth (Colombani et al., 2005; Mirth et al., 2005; Layalle et al., 2008). Conversely, over-expressing PI3K, an upstream activator of Akt, stimulates PG growth (Colombani et al., 2005; Mirth et al., 2005).

There is little information on the mTOR pathway in crustaceans. Shrimp nervous tissue and lobster hepatopancreas produce peptides with insulin-like properties (Hatt et al., 1997; Gallardo et al., 2003), while an IGF is expressed in the androgenic gland of crayfish and prawn (Manor et al., 2007; Ventura et al., 2009). An insulin receptor tyrosine kinase and a phosphotyrosyl protein phosphatase have been characterized in crustacean tissues (Lin et al., 1993; Chuang and Wang, 1994; Kucharski et al., 1999). A cDNA encoding S6k was cloned from *Artemia* and is up-regulated during embryonic development (Santiago and Sturgill, 2001).

Two methods can induce molting: ES ablation (ESA) and multiple leg autotomy (MLA). MLA resembles “natural” molting, as animals successfully completing ecdysis. Regenerating limbs in MLA provide measure of the progress events in the crabs. The measure is defined as the R index (calculated as the length of the regenerate x 100/carapace width), which increases from 0 to ~23 prior to ecdysis (Fig. 1. 7) ESA is an effective and convenient method, as the XO/SG complex is the primery source of MIH (Skinner and Graham, 1972; Yu et al., 2002).

The goal of this project is to examine the role of mTOR signaling in the regulation of the molting gland (Y-organ). We hypothesize that a major target of MIH and TGFβ pathways is the

mTOR complex, which controls global translation of mRNA into protein in animal cells. This dissertation is organized into five chapters. Chapter one is an introduction. Chapter two reports the cloning and characterization of cDNAs encoding four mTOR signaling components in decapod crustaceans. Chapter three describes the role of the mechanistic target of rapamycin (mTOR) and TGFβ signaling in the crustacean Y-organ during the molt cycle. Chapter four reports how *C. maenas*, is refractory to molt induction by eyestalk ablation and multiple leg autotomy. Chapter five is a summary and suggests future areas of investigation.

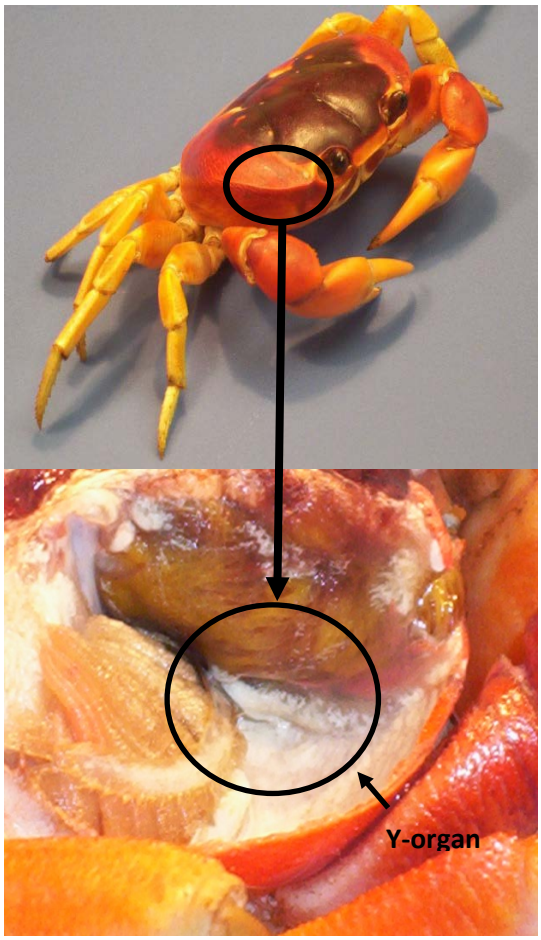

Figure 1. 1. Blackback land crab, *G. lateralis*. The molting gland, or Y-organ, is located in the cephalothorax, anterior to the branchial chamber.

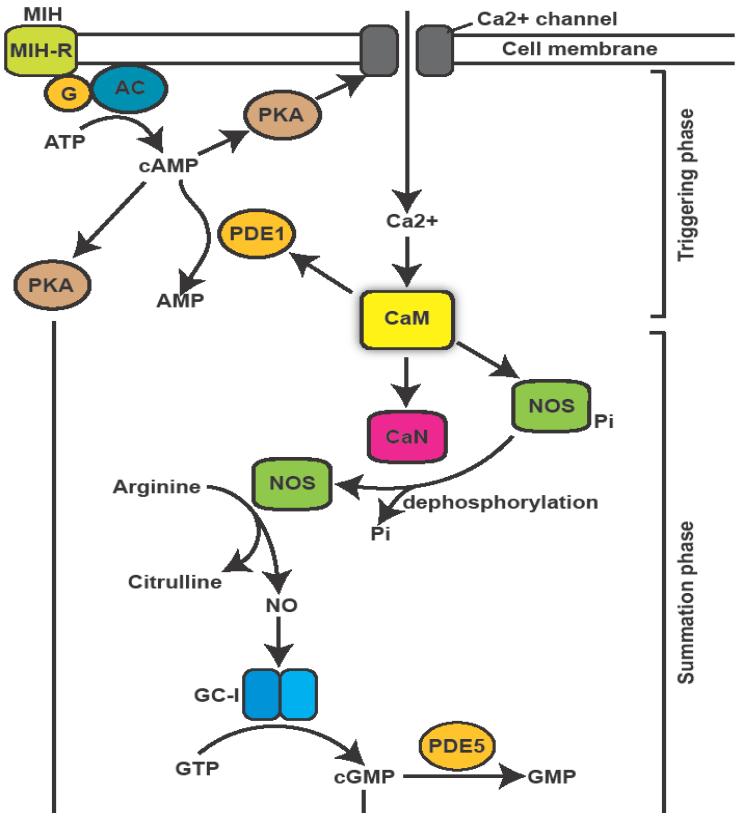

Figure 1. 2. Proposed MIH signaling pathway regulating ecdysteroidogenesis in decapod crustacean molting gland. The ‘‘triggering’’ phase is initiated by binding of MIH to a G protein-coupled receptor (MIH-R) and activation of adenylyl cyclase (AC); cAMP increases intracellular Ca^{2+} via cAMP-dependent protein kinase (PKA) phosphorylation of Ca^{2+} channels. Sensitivity to MIH is determined by phosphodiesterase 1 (PDE1) activity, which varies during the molting cycle. The ‘‘summation’’ phase is mediated by NO and cGMP. Calmodulin (CaM) links the two phases by activating NO synthase (NOS) directly and indirectly via calcineurin (CaN). Dephosphorylation of NOS by CaN can potentially prolong the response to MIH. CaM can also activate PDE1 to inhibit the triggering phase (PDE1 can also hydrolyze cGMP, thus inhibiting the summation phase). cGMP dependent protein kinase (PKG) inhibits ecdysteroidogenesis. Chronic activation of PKA may directly inhibit ecdysteroidogenesis. Chronic elevated intracellular cAMP can inhibit ecdysteroidogenesis directly, perhaps by inhibiting protein synthesis. Other abbreviations: G, G protein; GC-I, NO-sensitive guanylyl cyclase; PDE5, cGMP PDE (Chang and Mykles, 2011).

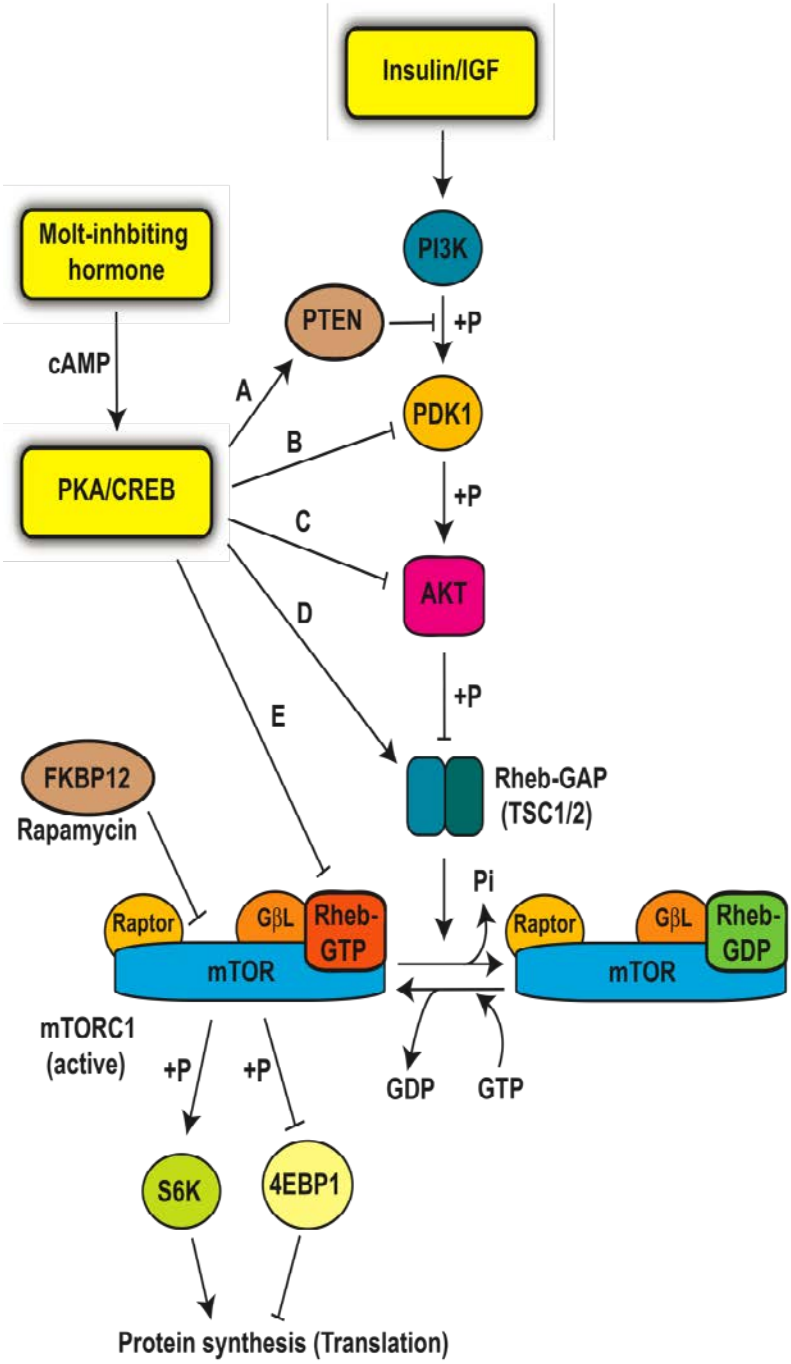

Figure 1. 3. Regulation of mTORC signaling pathway. Rheb-GAP (TSC1/2) inactivates mTORC1 by promoting the hydrolysis of GTP to GDP. Rapamycin inhibits mTORC1 via binding to FKBP12. Insulin/IGF signaling (PI3K, PDK1, & Akt) activates mTORC1 by inhibiting Rheb-GAP. We hypothesize that Mstn/Smad signaling inhibits mTORC1 by altering expression and subsequent phosphorylation of insulin/IGF signaling components, either through up-regulation of PTEN (A) and/or Rheb-GAP (D), down-regulation of PDK1 (B), Akt (C), and/or Rheb (E), or a combination of any or all (Wullschleger et al., 2006; Proud, 2009).

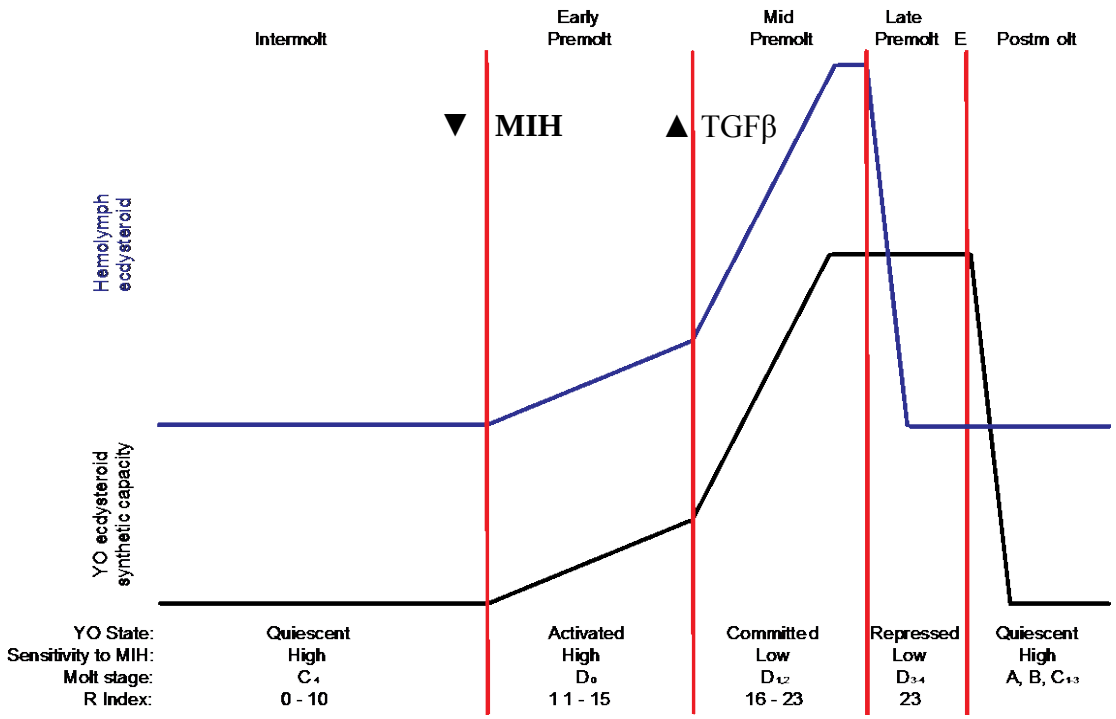

Figure 1. 4. Hormonal regulation of molting. YO transitions through four physiological states (basal, activated, committed, and repressed) during the molt cycle. Diagram shows the relationship between molt stage, YO state (transitions indicted by vertical red lines), YO sensitivity to MIH, limb regeneration (R index), YO ecdysteroidsynthetic capacity (black line), and hemolymph ecdysteroid titer (blue line). YO activation is triggered by a reduction in MIH (▼ MIH); YO commitment involves a putative TGFβ factor (▲ TGFβ) (from Chang and Mykles, 2011).

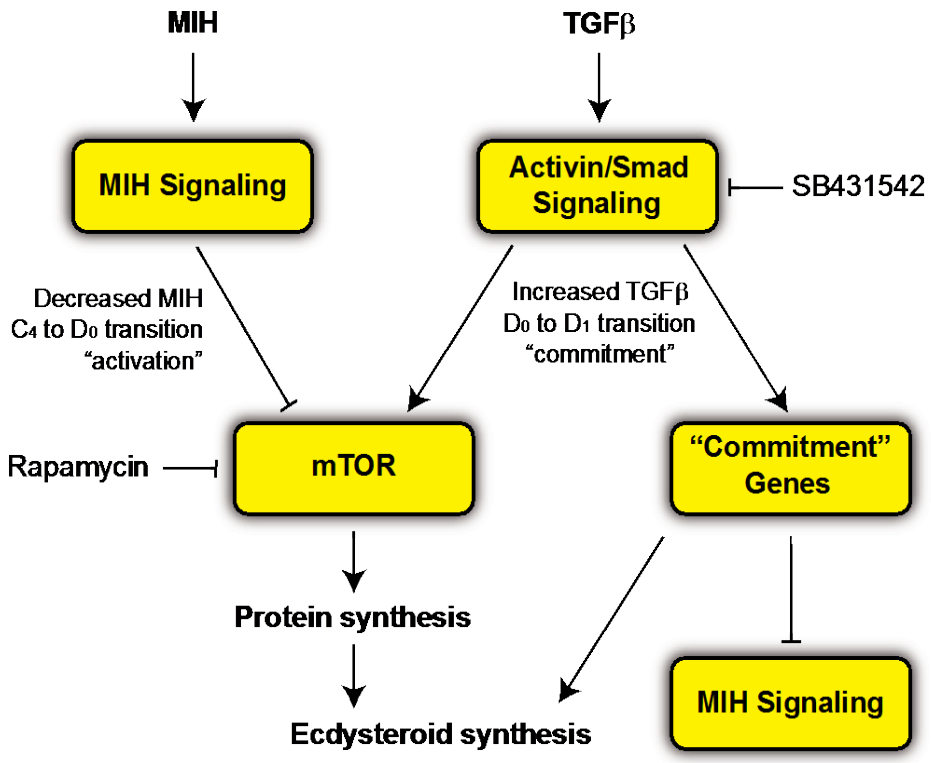

Figure 1. 5. Signaling pathways controlling YO ecdysteroid synthesis. MIH inhibits YO during intermolt. At mid premolt a putative TGFβ factor produced by the activated YO stimulates mTOR and "commitment" genes that inhibit MIH signaling and stimulate ecdysteroid biosynthetic enzymes. Rapamycin inhibits mTOR and SB431542 inhibits TGFβ.

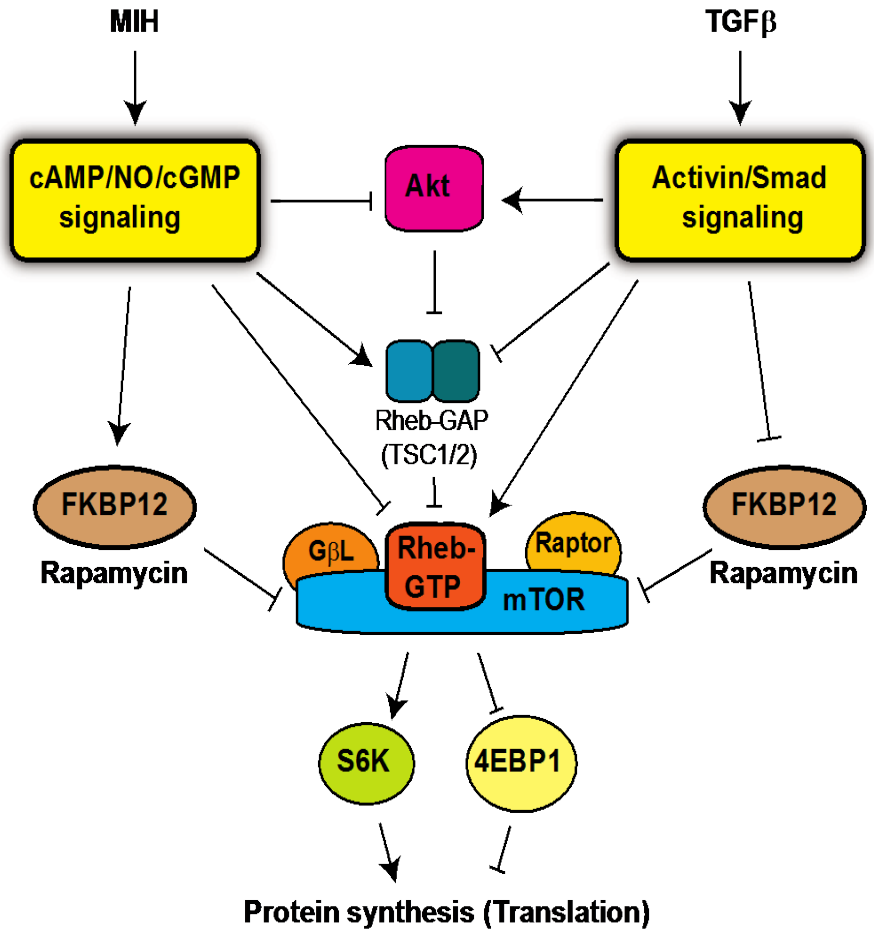

Figure 1. 6. Hypothetical control of mTOR by MIH and TGFβ in the crustacean YO. The mTORC1, composed of mTOR, Raptor, and GβL, regulates translation by phosphorylating S6K and 4E-BP1. mTORC is activated by Rheb-GTP; Rheb-GAP inactivates mTORC1 by promoting the hydrolysis of GTP. Rapamycin inhibits mTORC1 via binding to FKBP12. MIH signaling may inhibit mTOR by inhibiting Akt or Rheb and/or activating Rheb-GAP or FKBP12. TGFβ signaling may stimulate mTOR by having the opposite effects on Akt, Rheb-GAP, Rheb, and/or FKBP12.

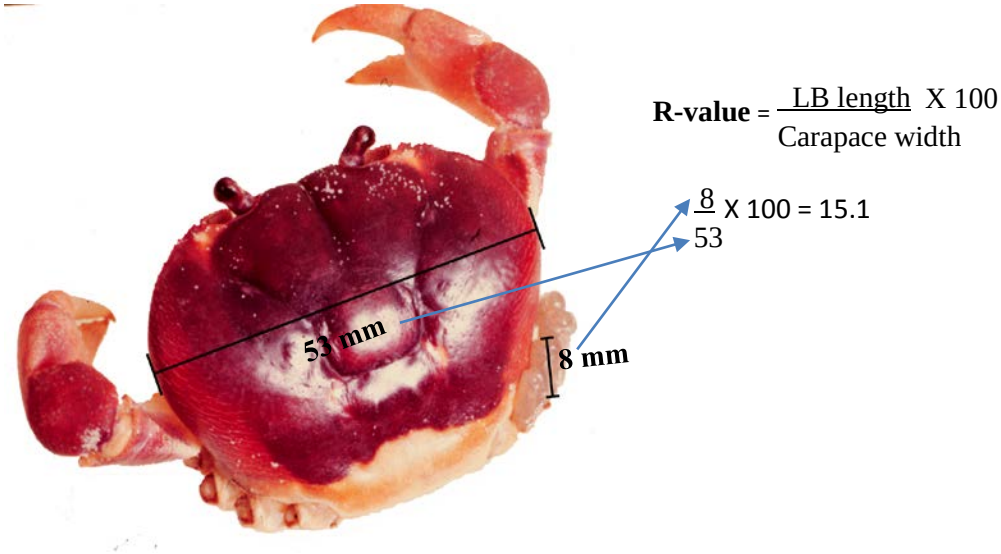

Figure 1. 7. Blackback land crab *Gecarcinus lateralis*, showing autotomized limbs on the left side, and limb buds on the right side. The formula for calculating the Regeneration value (R-value) is shown.

CHAPTER TWO

CLONING AND CHARACTERIZATION OF CDNAS ENCODING MECHANISTIC TARGET OF RAPAMYCIN (mTOR) SIGNALING COMPONENTS IN DECAPOD CRUSTACEANS

SUMMARY

The mechanistic Target of Rapamycin (mTOR) is a highly conserved protein kinase controlling cell growth in multicellular animals. It controls the rate of translation of mRNA into protein by phosphorylating p70 S6 kinase (S6k) and eIF4E-binding protein-1. Rheb (Ras homolog expressed in brain) and Akt (protein kinase B) are important regulators of mTOR. Growth in crustaceans requires the periodic shedding of the exoskeleton, a process known as molting or ecdysis. Thus, tissue growth is linked to molting, which is regulated by ecdysteroids produced by a pair of molting glands (Y-organs, YO) located in the cephalothorax. During premolt, YOs hypertrophy and increase production of ecdysteroids. We hypothesize that up-regulation of mTOR signaling is necessary for the growth of the YO and other tissues associated with molting. cDNAs encoding mTOR, Rheb, Akt, and S6k were cloned from the blackback land crab, *Gecarcinus lateralis* and green shore crab, *Carcinus maenas*. The *G. lateralis* cDNA sequences were obtained by reverse transcriptase-polymerase chain reaction and rapid amplification of cDNA ends. The *C. maenas* cDNA sequences were obtained from expressed sequence tags (ESTs). Partial cDNAs encoded Gl-mTOR (3705 bp), Cm-mTOR (4031 bp), Gl-Rheb (983 bp), Gl-Akt (1461 bp), Cm-Akt (855 bp), Gl-S6k (1116 bp), and Cm-S6k (918 bp). A complete cDNA encoded Cm-Rheb (1543 bp). Identity/similarity of the deduced amino acid sequences of

the *G. lateralis* cDNAs to human orthologs were 69%/80% for mTOR, 64%/83% for Rheb, 62%/78% for Akt, and 75%/86% for S6k. Identity/similarity of the deduced amino acid sequence of the *C. maenas* cDNAs to human orthologs were 72%/81% for mTOR, 66%/81% for Rheb, 58%/73% for Akt, and 77%/88% for S6k. The four genes were expressed in all tissues examined, indicating the importance of this pathway in regulating protein synthesis in all cells.

INTRODUCTION

The mechanistic Target of Rapamycin (mTOR) pathway is highly conserved among all metazoans; it functions as a nutrient sensor for cellular growth and is up-regulated in mammalian cancers (Proud, 2009; Zoncu et al., 2011; Dodd and Tee, 2012; Gentzler et al., 2012; Laplante and Sabatini, 2012; Zhou et al., 2012). mTOR is crucial for growth, aging, development, reproduction, and metamorphosis in insects (Bjedov et al., 2010; Gibbens et al., 2011; Gu et al., 2012; Mirth and Shingleton, 2012). mTOR increases the ecdysteroid biosynthetic capacity of the insect molting gland (prothoracic gland or PG). Nutrients and insulin-like peptides (ILPs) activate mTOR, which phosphorylates components of the protein synthetic machinery, such as p70-S6 kinase (S6k) and eIF4E-binding protein-1 (4E-BP1) to increase translation of mRNA (Proud, 2009; Teleman, 2010). Binding of ILP to an insulin receptor activates a signal transduction cascade involving phosphoinositide 3-kinase (PI3K), 3'-phosphoinositide-dependent kinase-1 (PDK1), and Akt (Teleman, 2010).

mTOR is activated by the Rheb GTP-binding protein. mTOR is inactivated when Rheb-GTPase activating protein (Rheb-GAP or TSC1/2) stimulates the hydrolysis of GTP to GDP by Rheb-GAP is inhibited when phosphorylated by Akt. Insulin and ILP signaling prevents the hydrolysis of GTP by Rheb through the inhibition of Rheb-GAP, thus keeping mTOR in the

active state (Teleman, 2010). The ILP/mTOR pathway controls PG size and ecdysteroidogenic capacity (Teleman, 2010; Mirth and Shingleton, 2012). Overexpression of Rheb stimulates cell growth while knockdown of Rheb expression inhibits protein synthesis and cell growth in insects (Hall et al., 2007; Patel et al., 2003). Conversely, over-expressing PI3K, an upstream activator of Akt, stimulates PG growth (Colombani et al., 2005; Mieth et al., 2005). In addition, PI3K and mTOR inhibitors block PTTH-induced increases in ecdysteroid secretion in the PG (Gu et al., 2011; Gu et al., 2012).

Little is known about the insulin/mTOR pathway and its role in growth and development in crustaceans. Insulin-like peptides were reported in shrimp and lobster hepatopancreas (Hatt et al., 1997; Gallardo et al., 2003). An IGF is expressed by androgenic gland of crayfish and prawn (Manor et al., 2007; Ventura et al., 2009). Insulin receptor tyrosine kinase and phosphotyrosyl phosphatase are present in crustacean tissues (Lin et al., 1993; Chuang and Wang, 1994; Kucharski et al., 1999; Kucharski et al., 2002). A single study examined p70 S6 kinase in the brine shrimp, *Artemia franciscana*; it showed that S6k activity is present, and increases, in early preemergence development after quiescence, when protein synthesis is restored (Santiago and Sturgill, 2001).

The purpose of this study was to clone and characterize cDNAs encoding four key components of the mTOR signaling pathway (mTOR, Rheb, Akt and S6k) from the blackback land crab, *Gecarcinus lateralis*, and green shore crab, *Carcinus maenas*. cDNAs were obtained by reverse transcriptase-polymerase chain reaction (RT-PCR) and rapid amplification of cDNA ends (RACE). The tissue expression of the four genes was determined by endpoint RT-PCR.

MATERIALS AND METHODS

Animals

Adult blackback land crabs (*Gecarcinus lateralis*) were collected in the Dominican Republic and shipped via commercial air cargo to Colorado, USA. Animals were maintained at 27 ºC in 75-90% relative humidity with intermolt individuals kept in communal plastic cages lined with aspen bedding wetted with 5 p.p.t. Instant Ocean (Aquarium Systems, Mentor, OH). The crab environmental chamber was maintained in 12 h: 12 h light: dark cycle with twice-weekly animal feedings of carrots, iceberg lettuce, and raisins (Covi et al. 2010). These crabs molt approximately once a year. European green shore crabs (*Carcinus maenas*) were collected from the harbor at Bodega Bay, California. They were maintained under ambient conditions in the facilities of Bodega Marine Laboratory or were shipped to Colorado. In Colorado, animals were kept in aerated 30 ppt Instant Ocean at 20 °C and fed cooked chicken liver once a week. Instant Ocean was changed twice a week (or more if water became cloudy or there was a death in the cage) (Lee et al., 2007).

RNA purification and cDNA synthesis

Total RNA was isolated from land crab and green crab tissues using TRIzol reagent (Life Technologies, Carlsbad, CA) as described previously (Covi et al., 2010). Briefly, tissues (claw muscle, thoracic muscle, and gill) (50-200 mg) were homogenized in 1-2 ml TRIzol and centrifuged at 12,000 × g for 15 min at 4 ºC. Supernatants were phenol-chloroform extracted and RNA in the aqueous phase was precipitated using isopropanol (0.75 ml per 1 ml TRIzol reagent). RNA was treated with DNase I (Life Technologies), extracted twice with phenol:chloroform:isoamyl alcohol (25:24:1), precipitated with isopropanol, washed twice with 75% ethanol in DEPC water, and resuspended in nuclease-free water. First-strand cDNA was

synthesized using 1 µg total RNA in a 20 µl total reaction with SuperScript III reverse transcriptase (Life Technologies) and oligo-dT(20)VN primer (50 µM; IDT, Coralville, IA) as described (Covi et al., 2010). RNA was treated with RNase H (Fisher Scientific, Pittsburgh, PA) and stored at -80 ºC.

Cloning of cDNA encoding mTOR, Rheb, Akt, and S6k

RT-PCR and RACE were used to clone cDNAs encoding Cm-mTOR, Cm-Rheb, Cm-Akt, and Cm-S6k on the basis of sequence determined by multiple sequence alignment of several ESTs from each organism, courtesy of the Mount Desert Island Biological Laboratory (Towle and Smith, 2006). Sequence for each open reading frame was verified by RT-PCR using cDNA prepared as above. All primers were synthesized by IDT.

RT-PCR and RACE were used to clone the Gl-mTOR, Gl-Rheb, Gl-Akt, and Gl-S6k cDNAs. cDNAs synthesized from claw muscle, thoracic muscle, and gill RNA were pooled and used for PCR. PCR was conducted using 0.5 µl of the first strand cDNA as template and forward (10 pmol) and reverse (10 pmol) primers shown in Table 2. 1. For Rheb, specific primers directed against the green crab (*C. maenas*) were used. All the other genes used degenerate primers (Table 2. 1) designed using iCODEHOP (Boyce et al., 2009) or by hand using multiple sequence alignments of homologous proteins and a codon chart. PCR reactions used GoTaq Green master mix (Promega, Madison, WI). After denaturing the cDNA at 96 ºC for 3 min, 35 cycles of PCR were completed with the following program: 96 ºC for 30 s, lowest annealing temperature of a primer pair (see Table 2. 1) for 30 s, and 72 ºC for 30 s to 1 min. Final extension was for 7 min at 72 ºC. Amplified fragments, verified as single bands by 1% agarose gel electrophoresis, were purified using the GeneJet PCR Cloning Kit (Fermentas), ligated into the pJET1.2 vector using the CloneJet PCR Cloning Kit (Fermentas), and, after insert

verification by PCR with vector primers, sequenced using a T7 primer (Davis Sequencing, Davis, CA).

The FirstChoice RLM-RACE Kit (Applied Biosystems, Austin, TX) was used according to the manufacturer's instructions to amplify additional parts of the Gl-mTOR, Gl-Rheb, Gl-Akt, and Gl-S6k coding sequence using nested 5' and 3' RACE and primers shown in Table 2. 1. RACE conditions were as follows: 0.4 µl RACE template cDNA was used in each reaction, with 8 pmol of each gene specific (Table 2. 1) and kit primer and other components identical to the initial PCR reactions (see above). After denaturation at 94 ºC for 3 min, 35 cycles of 94 ºC for 30 s, lowest annealing temperature of a primer pair (Table 2. 1) for 30 s, and 72 ºC for 30 s to 1 min, were completed. Final extension was for 7 min at 72 ºC. Most of nested and 3' and 5'RACE PCR products were separated by 1% agarose gel electrophoresis, purified using the Gel Extraction Kit (QIAEX II, Qiagen), and sequenced by direct sequencing with sequence-specific primers (Davis Sequencing).

Tissue expression of EF2, mTOR, Rheb, Akt, and S6k mRNAs

End-point PCR was used to qualitatively assess the tissue distribution of Gl-elongation factor 2 (EF2; GenBank AY552550), Gl-mTOR (GenBank HM989973), Gl-Rheb (GenBank HM989971), Gl-Akt (GenBank HM989974), Gl-S6k, (GenBank HM989975), Cm-EF2 (GenBank GU808334; McDonald et al., 2011), Cm-mTOR (GenBank JQ864248), Cm-Rheb (GenBank HM989970), Cm-Akt (GenBank JQ864249), Cm-S6k (GenBank JQ864250). The Rheb sequences were reported in a recent publication (MacLea et al., 2012; see Appendix 1). Total RNA was purified from eyestalk ganglia, thoracic ganglion, YO, hepatopancreas, heart, claw muscle, thoracic muscle, midgut, hindgut, and testis as described above. All tissues were collected from intermolt adult male animals. Reactions contained 1 µl template cDNA and 5

pmol each of the appropriate expression primers (Table 2. 1) in GoTaq Green master mix (Promega). After denaturation at 94 ºC for 3 min, 30 or 35 cycles of 94 ºC for 30 s, lowest annealing temperature of a primer pair (see Table 1) for 30 s, and 72 ºC for 30 s, were completed. Final extension was for 7 min at 72 ºC. Cm-EF2 and Gl-EF2 used 30 cycles. After PCR was terminated, products were separated on a 1% agarose gel containing TAE (40 mM Tris acetate and 2 mM EDTA, pH 8.5). The gels were stained with ethidium bromide and visualized with a UV light source.

Analyses and software

Multiple sequence alignments were produced with ClustalX version 2.0.12 (Thompson et al., 1997) using deduced amino acid sequences. Illustrator 10 (Adobe Systems, San Jose, CA) was used for constructing/annotating graphs and figures.

RESULTS

Cloning and characterization of crustacean mTOR cDNAs

RT-PCR and 3' RACE were used to clone cDNAs encoding of the mTOR from *G. lateralis* and *C. maenas*. Initial RT-PCR using degenerate primers targeted to the kinase domain (Fig. 2. 1) produced a 664-bp product for Gl-mTOR that was ligated into a plasmid vector and used to transform *E. coli* cells. Plasmids were purified and sequenced. A ~779-bp product from 3' RACE using sequence-specific forward primers (Table 2. 1) encoded the 3' end of the open reading frame (ORF) and part of the 3' untranslated region (UTR). Nested RT-PCR was used to extend the 5' end for Gl-mTOR using Cm-mTOR forward primers with Gl-mTOR reverse primers (Table 2. 1). Two partial sequences (1543 bp and 1624 bp) for Cm-mTOR were obtained using sequence-specific primers (Table 2. 1) derived from an EST (GenBank DV642891). Nested RT-PCR was used to fill the gap between the two partials and 3' RACE was used to

obtain the 3' end of the ORF and part of the 3' UTR (Fig. 2. 1, 2. 3). Gel-purified PCR products were sequenced by direct sequencing (see Materials and methods).

The consensus DNA and deduced amino acid sequences for Gl-mTOR and Cm-mTOR are presented in Figs. 2. 2 and 2. 3, respectively. The cDNAs encoded the 3' part of the ORF containing the HEAT repeat, FKBP12-rapamycin-binding (FRB), FAT, serine-threonine protein kinase, and FATC domains (Fig. 2. 1; Table 2. 2). As human mTOR is 2549 amino acids, we estimate that about 43% of the Gl-mTOR ORF and about 44% of the Cm-mTOR ORF was obtained (Fig. 2. 1). The deduced sequences shared high degrees of identity and similarity to the human ortholog at the protein level (Table 2. 2), with even higher identity and similarity to insect orthologs. Multiple alignments of the deduced amino acid sequences from crustacean and insect species indicated high sequence identities in the HEAT repeat, FRB, FAT, kinase, and FATc domains (Fig. 2. 4).

Cloning and characterization of crustacean Rheb cDNAs

cDNAs containing the complete ORF of Gl-Rheb and Cm-Rheb were obtained from RT-PCR and RACE (MacLea et al., 2012). Cm-Rheb was cloned on the basis of sequence alignment of several ESTs (GenBank DV467211, DV944345, DV943723, DV642713 and DV642936) using RT-PCR with specific primers (Table 2. 1). The Gl-Rheb sequence was obtained by RT-PCR using primers designed from the Cm-Rheb sequence (Table 2. 1). The sequences contained the 5' UTR, ORF, and 3' UTR (Fig. 2. 5-2. 7; Table 2. 2). The DNA and deduced amino acids sequences for Gl-Rheb and Cm-Rheb are presented in Figs. 2. 6 and 2. 7, respectively.

Multiple sequence alignment of Rheb protein from crustacean and insect species indicated a high level of sequence identity. An EST encoding the Rheb protein in American lobster, *Homarus americanus* (Ha-Rheb; MacLea et al., 2012), was included in the analysis. The Rheb

cDNAs encoded 182 amino acid proteins with estimated masses of 20.2 kDa for Gl-Rheb, and 20.4 kDa for Cm-Rheb and Ha-Rheb. Sequence identity was particularly high within the G box motifs (G1–G5) in all the Rheb proteins (Fig. 2. 8). The lipid modification site at the C-terminus was also conserved in the arthropod Rheb proteins.

Cloning and characterization of crustacean Akt cDNAs

cDNA encoding Gl-Akt was obtained with RT-PCR using degenerate primers directed to conserved sequences in the kinase domain (Fig. 2. 9), which were identified from multiple sequence alignments of Akts from vertebrate and invertebrate species. An initial PCR product (~540 bp) was ligated into a plasmid vector and sequenced. 3' RACE and 5' RACE using sequence-specific primers to the initial PCR product (Table 2. 1) extended the ORF 5' to the initiation codon and 3' into the regulatory C-terminal domain (Fig. 2. 9). The Cm-Akt sequence was derived from ESTs using RT-PCR and 5' RACE. Attempts to obtain more of the 5' and 3' sequences by RACE were unsuccessful. The DNA and deduced amino acids sequences for Gl-Akt and Cm-Akt are presented in Figs. 2. 10 and 2. 11, respectively.

Multiple sequence alignment of crustacean and insect Akts indicate high levels of sequence identity. Identity/similarity to human Akt was 62%/78% for Gl-Akt and 58%/73% for Cm-Akt (Table 2. 2). Akt proteins from five arthropod species were highly conserved, showing high identity and similarity to each other, including the activation loop in the kinase domain (Fig. 2. 12).

Cloning and characterization of crustacean S6k cDNAs

cDNAs encoding S6k from *G. lateralis* and *C. maenas* were obtained from RT-PCR and RACE or from EST clones, respectively (Fig. 2. 13). For Gl-S6k, an initial RT-PCR product (678 bp) was obtained with nested degenerate primers targeted to conserved sequences in the

kinase domain (Fig. 2. 13), based on sequence alignments of S6k proteins from vertebrate and invertebrate species. The RT-PCR product was ligated into a plasmid vector and sequenced. 5' RACE and 3' RACE yielded additional 5' and 3' sequences, but the RACE products did not extend to the UTRs. Further attempts to obtain the 5' and 5' UTRs were unsuccessful. The Cm-S6k sequence was obtained by RT-PCR using sequence-specific primers, based on sequence alignments of several ESTs. The Gl-S6k cDNA encoded the N-terminal domain (NTD), kinase domain (KD) with kinase extension region (KE), and C-terminal domain (CTD) (Figs. 2. 13, 2. 14). The Cm-S6k cDNA encoded the kinase domain and portions of the NTD and KE domains (Figs. 2. 13, 2. 15).

The deduced amino acid sequences of the crustacean S6ks showed high degrees of identity and similarity to the human ortholog of each sequence (75%/86% identity/similarity for Gl-S6k and 77%/88% identity/similarity for Cm-S6k; Table 2. 2). A multiple sequence alignment of the two decapod S6k proteins with *D. pulex* S6k and two insect S6k proteins showed high sequence identity, including the activation loop and phosphorylation site within the catalytic domain.

Tissue expression of mTOR signaling components

Endpoint RT-PCR was used to determine the expression of mTOR, Rheb, Akt, and S6k in tissues from *G. lateralis* and *C. maenas*. EF2 was included as a constitutively expressed gene to assess RNA isolation and cDNA synthesis. All five genes were expressed in all tissues, including Y-organ, heart, skeletal muscle (claw and thoracic muscles), eyestalk ganglia, thoracic ganglion, hepatopancreas, midgut, hindgut, and testis (Fig. 2. 17).

DISCUSSION

The highly conserved insulin/IGF/mTOR signaling pathway is found in all metazoans and has an important role as a nutrient sensor (Proud, 2009) critical for growth and development in insects (Hietakangas and Cohen, 2009; Layalle et al., 2008; Maestro et al., 2009; Montagne et al., 2010; Walkiewicz and Stern, 2009) and other invertebrates (Soulard et al., 2009). Before this project, it was not clear whether components of this pathway would be regulated during the molt cycle of crustaceans, as is the case in insects, although a study of *Artemia* did demonstrate the increased expression of p70S6 kinase in emergence from quiescence (Santiago and Sturgill, 2001). In order to determine its function in crustaceans, we cloned mTOR pathway components representing four different genes from two crustacean species, *G. lateralis*, and *C. maenas* (Table 2. 2). All four genes were expressed in all tissues that were examined, indicating that the mTOR pathway is important in growth regulation in all cells.

The domain organization of mTOR is well conserved across animal phyla. It has a C-terminal catalytic domain bounded by the FRB (FKBP12 rapamycin binding) domain, FAT (FRAP, ATM, and TRRAP) domain, and protein HEAT repeats (Huntington, Elongation Factor 3, a subunit of PP2A and TOR) domain (Fig. 2. 1). The C-terminus of mTOR consists of the FATC (FRAP, ATM and TRRAP C-terminal) domain (Bosotti et al., 2000; Perry and Kleckner, 2003; Veverka et al., 2008).

The cDNAs of mTOR cloned from *G. lateralis* and *C. maenas* showed high levels of sequence relatedness when compared with the human protein (Table 2. 2). This level of relatedness was even higher when compared by BLASTX against top hits among arthropod sequences in the database (Fig. 2. 4). Gl-mTOR and Cm-mTOR contain all the important domains found in other mTOR proteins. The rapamycin binding domain, which is a key target

for FKBP12/rapamycin inhibition of inhibits kinase activity (Sonja et al., 2005). The kinase domain functions by phosphorylating serine and threonine residues on target proteins (Harris and Lawrence, 2003; Jacinto and Hall, 2003). The FAT domain consists of HEAT repeat-like α-helical structures and may function as a protein interaction platform (Perrt and Klechkner, 2003). The C-terminal FATC domain, which consists of an α-helix and a disulfide bonded loop, may regulate mTOR activity (Sonja et al., 2005).

mTOR associates with other proteins to form two complexes that differ in function. mTOR complex 1 (mTORC1) is composed of raptor, mLST-8, and other proteins (Dibble et al., 2009; Treins et al., 2009) and is regulated by growth factors, energy status, nutrients, and stress (Laplante and Sabatini, 2009). mTORC1 activates proteins that regulate translation initiation and elongation. Activation of protein biosynthesis by mTORC1 occurs via phosphorylation of ribosomal protein S6 kinase (S6k) and eukaryotic initiation factor 4E-binding protein 1 (4E-BP1) (Zoncu et al., 2001). mTOR complex2 plays a role in actin cytoskeleton reorganization. mTORC2 phosphorylates Akt that is induced by stimuli such as growth factors and hormones (Won and Estele, 2011).

Rheb is an important activator of mTOR and is highly conserved across phyla. Gl-Rheb and Cm-Rheb share the same functional domains with Rheb proteins from insects (Fig. 2. 5). The Rheb sequences contained the five G boxes necessary for GTP-binding and GTPase activity (MacLea et al., 2012). The lipid modification site (CAAX, where C = Cys, A = aliphatic residue, and X = any residue; reviewed in Wennerberg et al., 2005) is required for proper targeting to membranes and for the downstream effects of Rheb (Castro et al., 2003). The effector domain, or “switch I”, includes the G2 box and surrounding residues and is important for Rheb activation of mTOR (Ma et al., 2008). The effector domain mediates binding of Rheb to FKBP38, an

inhibitor of mTOR that is thought to reduce mTOR activity under nutrient or growth factor-poor conditions (Ma et al., 2008; Dunlop et al., 2009). However, there is contradictory evidence of the role of FKBP38 in the modulation of Rheb activity (Wang et al., 2008).

Akt is the central mediator of mTOR-dependent protein synthesis in response to growth factors (Marte and Downward, 1997; Toker and Newton, 2000; Xin et al., 2003). Akt belongs to the AGC kinase family, which is related to AMP/GMP kinases and protein kinase C (Masahito et al., 2004). Akt activates mTOR by phosphorylating TSC1/2, a GTPase-activating protein that inactivates Rheb (Laplante and Sabatini, 2012). It consists of an N-terminal pleckstrin homology (PH) domain, kinase domain (KD), and regulatory C-terminal (RC) domain (Chandra and Vincent, 2005). Gl-Akt and Cm-Akt share the same domain organization with Akt proteins from other species (Fig. 2. 9). The PH domain interacts with phosphatidylinositol (3, 4, 5) trisphosphate produced by phosphatidylinositol 3-kinase (PI3-kinase). Membrane binding allows phosphorylation by PDK1.

S6k is downstream effector of the mTOR signaling pathway involved in cell growth and cell proliferation (Laplante and Sabatini, 2012). S6k is also member of the AGC family of serine-threonine kinases that share high homology in the kinase domain (Grove et al., 1991; Zhao et al., 2007). Gl-S6k and Cm-S6k share the same domain organization as S6k proteins from other species (Fig. 2. 13). S6k activity is highly sensitive to rapamycin in the kinase extension (KE) domain in a conserved sequence called the hydrophobic motif (Alessi et al., 1988; Pullen et al., 1998). The rapamycin-sensitive phosphorylation is mediated by mTORC1, a complex consisting of mTOR, raptor and mLST-8 (Dibble et al., 2009; Treins et al., 2009). S6k has important role as mediator of negative feedback loops in the PI3K signaling network. Moreover, recent studies

have revealed that S6k impacts on Akt activation by phosphorylating the mTORC2 component, Rictor (Dibble et al., 2009; Treins et al., 2009; Julien et al., 2010; Tim and Ivan, 2011).

CONCLUSIONS

cDNAs encoding Rheb, mTOR, Akt, and S6k were cloned from the blackback land crab, *G. lateralis*, and green shore crab, *C. maenas*. The sequences were highly conserved with orthologs from insects and human and the genes were expressed in all tissues examined. The data indicate that the genes function in controlling tissue growth in decapod crustaceans. Now that these key components of the mTOR signaling pathway have been identified, future studies can be directed at gaining a mechanistic understanding of the interactions between ecdysteroids and the signaling pathways that control protein synthesis in the crustacean molting gland.

Table 2. 1. Oligonucleotide primers used in the cloning of mTOR signaling components from *G. lateralis* (Gl) and *C. maenas* (Cm). Abbreviations: deg, degenerate; F, forward; R, reverse; EF2, elongation factor 2; mTOR, mechanistic Target of Rapamycin; Rheb, Ras homolog expressed in brain; Akt, protein kinase B; S6k, p70 S6 kinase; IF, inner forward; IR, inner reverse; OF, outer forward and OR, outer reverse.

Primer	Sequence (5'-3')	Use	Annealing Temperature
Gl-mTOR degF	CCGCCAGTTCAGCARNGGRTCRTA	PCR	53 ºC
Gl-mTOR degR	GCAGGACGAGCGGBTNATGSARYT	PCR	53 ºC
Gl-Akt degF2	TGAACAACTTCACCGTGAARCARTGYCA	PCR	51 ºC
Gl-Akt degR1	TCGCCGCCGTTCACRTAYTCCAT	PCR	51 ºC
Gl-s6k degF2	TCGTGGACCTGGTGTAYGCNTTYCA	PCR	50 ºC
Gl-s6k degR1	TCTGCTTGGTGAACTTGSWRTCRAAYTG	PCR	50 ºC
Gl-Rheb deg OF1	ATGCCTCCMAARGAYAG	Nested PCR	45 ºC
Gl-Rheb deg IF2	AAAGTRGCCGTWATGGGC	Nested PCR	48 ºC
Gl-Rheb deg OR1	CTCRATCTCSAGGATGRCTC	Nested PCR	45 ºC
Gl-Rheb deg IR2	GATGRCTCKTGTGAAGATGTC	Nested PCR	48 ºC
Gl-mTOR 3' F1	TGCTGTGGTTCAAGAGTCCCT	3'RACE	58ºC
Gl-mTOR 3' F2	GCAAGATCATCCACATCGACTT	3'RACE	55ºC
Gl-Rheb 3' F1	CATCTACGACAAGATTCTCGAC	3'RACE	53 ºC
Gl-Rheb 3' F2	GCAAAGTCACAGTTCCTGTAG	3'RACE	53 ºC
Gl-Akt 3' F1	TGTCGTGAAAAGAGTAGCAACCAT	3'RACE	56 ºC
Gl-Akt 3' F2	CCTCAAGTATTCCTTCCAAACCAA	3'RACE	55ºC
Gl-Akt 3' F1	TTGCACTGGGTTACTTACACGAA	3'RACE	59ºC
Gl-Akt 3' F2	GAAGACATCTCCTACGGCTCA	3'RACE	60 ºC
Gl-Akt 3' F1	GCC TTG CAC TGG GTT ACT TAC ACG	3'RACE	56ºC
Gl-Akt 3' F2	TTC CAA ACC AAT GAC CGA CTC TGC	3'RACE	56ºC
Gl-S6k 3' F1	TGATGATGATGTGAGCCAATTCGA	3'RACE	56ºC
Gl-S6k 3' F2	ACA CAT GCC TTT CAC TCG TAA TTG	3'RACE	55ºC
Gl-S6k 3' F1	AACCTTCCACCCTACCTGACT	3'RACE	57ºC
Gl-S6k 3' F2	GTGGTGATGATGATGTGAGCCAAT	3'RACE	57 ºC
Gl-Rheb 5' R1	ACCTGCCGTGTCCACCAGCTC	5'RACE	60 ºC
Gl-Rheb 5' R2	GATCATAGCTGTCCACAAAC	5'RACE	60 ºC
Gl-Akt 5' R1	CTGGAGTACTTGAGTTGGATGTGC	5'RACE	57 ºC
Gl-Akt 5' R2	TTCCATCCATTCTTCCCTGTCACT	5'RACE	57 ºC
Gl-S6k 5' R1	TGATGCCCTCAGAGTGAAGATGTT	5'RACE	58 ºC
Gl-S6k 5' R2	AGTAGCTGAAAGTCTGATGGA	5'RACE	51ºC
Gl-S6k 5' R1	TGCCTGGGTTGACTGTACTGT	5'RACE	53ºC
Gl-S6k 5' R2	CAGGATGAGATATAGCTTACCA	5'RACE	58 ºC
Cm-mTOR OF1	AACGGTGGCATGAGAAGC	Nested PCR	55ºC
Gl-mTOR OR1	CGAGTTGGTAGACAGCGGAAT	Nested PCR	56ºC
Cm-mTOR IF2	ATGTGCGTGCTCAGATGG	Nested PCR	55ºC
Gl-mTOR IR2	TGATGAGCAGCGTGTTGACC	Nested PCR	58 ºC

Cm-mTOR OF1	AGAGATTACACAGACGCTCC	Nested PCR	53ºC
Gl-mTOR OR1	AACCAAACAGTCAGCAGG	Nested PCR	52 ºC
Cm-mTOR IF2	TCTGCACTACAAGGAGGAGG	Nested PCR	56 ºC
Gl-mTOR IR2	GAGATGGAGCGGATGAAC	Nested PCR	52 ºC
Cm-mTOR F1	CTTGGCAGAGTTCATGGAGC	PCR	56 ºC
Cm-mTOR R1	ACAGGTCATGCGATACGTGC	PCR	57 ºC
Cm-Rheb F1	ATGGGCAAAGTCACAGTTCC	PCR	62 ºC
Cm-Rheb R1	GTCAGGAAGATGGTGGCAAT	PCR	62 ºC
Cm-Akt F1	GATGATGCTCAACCTTAACGTG	PCR	54ºC
Cm-Akt R1	CACGTTAAGGTTGAGCATC	PCR	51ºC
Cm-S6k F1	GAAGGCGAAAGAAGAGTTCG	PCR	54ºC
Cm-S6kR1	ACGTCCGTCCCTTGACTCTC	PCR	58ºC
Cm-mTOR OF1	ACGAGAGCTGCTACAAGG	Nested PCR	54ºC
Cm-mTOR OR1	GTCTCTCCCATTACTACCCTTG	Nested PCR	53ºC
Cm-mTOR IF2	GAACTTTGAGGCAATAC	Nested PCR	44ºC
Cm-mTOR IR2	ATCCTGCCTCAAGTCCTC	Nested PCR	54ºC
Cm-mTOR 3’F1	AAAGCGTTCTGTGGTGGGTGAG	3’RACE	59ºC
Cm-mTOR 3’F2	TCCTGACCTGCTATTGACACTGCC	3’RACE	54ºC
Cm-Akt 3’F1	GCGTAAAGATGTGATTATTGAGCG	3’RACE	54ºC
Cm-Akt 3’F2	TGATGGAGTATGTCAATGGTGGAG	3’RACE	56ºC
Cm-S6k 3’F1	TCTTGGGTAGTTCTCCGTAGACAA	3’RACE	57ºC
Cm-S6k 3’F2	ACTCACCACTACTACTACACTCGG	3’RACE	57ºC

Table 2. 2. cDNA clones encoding mTOR signaling components from *G. lateralis* (Gl) and *C. maenas* (Cm). Abbreviations: mTOR, mechanistic Target of Rapamycin; Rheb, Ras homolog expressed in brain; Akt, protein kinase B; S6k, p70 S6 kinase.

Clone	Accession number	Source	Completeness	Size (bp)	Protein domain(s)	Identity (Similarity) to human ortholog
Cm-mTOR	JQ864248	EST	Partial	4031	Portion of HAET repeat, FAT, FRB, Kinase and FARC	72% (81%)
Cm-Rheb	HM989970	EST	Complete	1543	Complete ORF	66% (81%)
Cm-Akt	JQ864249	EST	Partial	855	PH and kinase	58% (73%)
Cm-S6k	JQ864250	EST	Partial	918	Kinase	77% (88%)
Gl-mTOR	HM989973	RT-PCR	Partial	3705	Portion of HAET repeat, FAT, FRB, Kinase and FARC	69% (80%)
Gl-Rheb	HM989971	RT-PCR	Complete except partial 3'UTR	983	Complete ORF	64% (83%)
Gl-Akt	HM989974	RT-PCR	Partial	1461	PH, kinase and RC	62% (78%)
Gl-S6k	HM989975	RT-PCR	Partial	1116	NTD, kinase and KE	75% (86%)

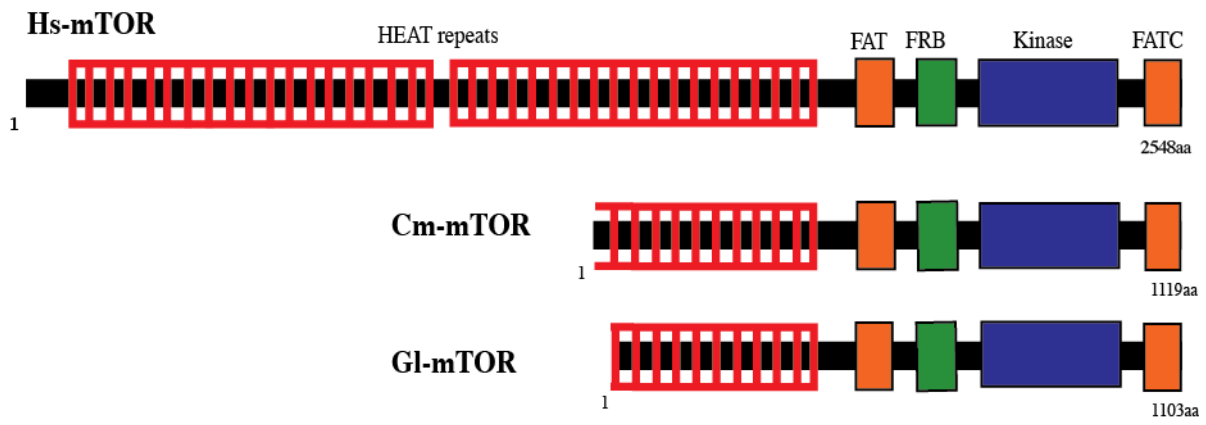

Figure 2. 1. Domain organization of mTOR. The complete mTOR protein from human (Hs-mTOR) is compared to the partial mTOR sequences from *G. lateralis* (Gl-mTOR) and *C. maenas* (Cm-mTOR). All share highly conserved HEAT repeats (Huntington, Elongation Factor 3, a subunit of PP2A and TOR), FAT (FRAP, ATM, and TRRAP), FRB (FKBP12 rapamycin binding), KD (kinase domain) and FATC (FRAP, ATM and TRRAP C-terminal) domains, indicated by red, orange, green, blue, and orange shading, respectively.

```
gtcctggagcacctcatctccatcaacaacaagcttggacagaaggaggctgctgctggg 60
 V  L  E  H  L  I  S  I  N  N  K  L  G  Q  K  E  A  A  A  G  20
ttgctggaatatgcccgcaagaacaaccgcactgacatgaaggtgcaggagcggtggcat 120
 L  L  E  Y  A  R  K  N  N  R  T  D  M  K  V  Q  E  R  W  H  40
gagaagttgcacgactgggaccaggccctccaggcatactccaccaagctggagacgcaa 180
 E  K  L  H  D  W  D  Q  A  L  Q  A  Y  S  T  K  L  E  T  Q  60
cctgatgaccttgccctcgtcctgggtcagatgaggtgtttggaggccctgggggaatgg 240
 P  D  D  L  A  L  V  L  G  Q  M  R  C  L  E  A  L  G  E  W  80
ggagagctgtacagtgtgtcatgcgagcgatggatgggaacgatgccagaggaggtgcgt 300
 G  E  L  Y  S  V  S  C  E  R  W  M  G  T  M  P  E  E  V  R  100
gctcagatgtcccgagtggctgcagcatcagcctgggggctgggggagtggagcatgatg 360
 A  Q  M  S  R  V  A  A  A  S  A  W  G  L  G  E  W  S  M  M  120
gaggagtacagccgctgcattccccgtgacaccaatgagggggccttctaccgtgctgtg 420
 E  E  Y  S  R  C  I  P  R  D  T  N  E  G  A  F  Y  R  A  V  140
ctggctgtacataaggaccaacatcacgtggcccagcagtatattgacacagcgagggat 480
 L  A  V  H  K  D  Q  H  H  V  A  Q  Q  Y  I  D  T  A  R  D  160
cttctggacaccgagctcactgccatggtaggagaaagttaccagcgtgcttacaactcc 540
 L  L  D  T  E  L  T  A  M  V  G  E  S  Y  Q  R  A  Y  N  S  180
atggtggcagtacagatgctggctgagctggaggaggtgattcagtacaagctggtgcct 600
 M  V  A  V  Q  M  L  A  E  L  E  E  V  I  Q  Y  K  L  V  P  200
gagcggaggccgcccattatacagatctggtgggagaggctgcaggggtgccaacgtgtg 660
 E  R  R  P  P  I  I  Q  I  W  W  E  R  L  Q  G  C  Q  R  V  220
gtggaggactggcagaagattctgcaggtgcgctcccttgtgttgtctcctcaggaggac 720
 V  E  D  W  Q  K  I  L  Q  V  R  S  L  V  L  S  P  Q  E  D  240
atgcggccgtggcttaagtttgcctcattgtgccgtaagtcaggtcgccttgccctctcc 780
 M  R  P  W  L  K  F  A  S  L  C  R  K  S  G  R  L  A  L  S  260
cacaagacactggtgcgtctccttggctgtgacccatccctcagcccctcccagcccctg 840
 H  K  T  L  V  R  L  L  G  C  D  P  S  L  S  P  S  Q  P  L  280
cccatcagccacccccacgtcacctaccagtactgcaaacacatctacacctacccacac 900
 P  I  S  H  P  H  V  T  Y  Q  Y  C  K  H  I  Y  T  Y  P  H  300
aggcgccaggaggcttatgggcgactgcagaagttcctccagttcttggctccggctgtg 960
 R  R  Q  E  A  Y  G  R  L  Q  K  F  L  Q  F  L  A  P  A  V  320
gttgtagtgggtggaggcaaccagaatggggacaacaagctacgtaaactagtttctcgt 1020
 V  V  V  G  G  G  N  Q  N  G  D  N  K  L  R  K  L  V  S  R  340
gtctacctcaagctgggtgaatggtatgagcagctacatggcttgaatgaagagaacatt 1080
 V  Y  L  K  L  G  E  W  Y  E  Q  L  H  G  L  N  E  E  N  I  360
gccaacatcctgacctactacactcacgccaaggacacagatgaaacctgctacaaggct 1140
 A  N  I  L  T  Y  Y  T  H  A  K  D  T  D  E  T  C  Y  K  A  380
tggcatgcctatgcctacatgaactttgaggcaatactcttctataaagggaagatggat 1200
 W  H  A  Y  A  Y  M  N  F  E  A  I  L  F  Y  K  G  K  M  D  400
gtcaagggagaggcacccaccacacctggggaggattcagcatcaggggcagctgctgtt 1260
 V  K  G  E  A  P  T  T  P  G  E  D  S  A  S  G  A  A  A  V  420
gtcacccccagcaagaagaggtcagctggggactttgcagtggcagcagtgaaagggttc 1320
 V  T  P  S  K  K  R  S  A  G  D  F  A  V  A  A  V  K  G  F  440
atccgctccatctccctgagtgacggcaacagcctgcaggacacactccgcctgctgact 1380
 I  R  S  I  S  L  S  D  G  N  S  L  Q  D  T  L  R  L  L  T  460
gtttggtttgagcatggtcaccagtctggggtgtatgaggctctggtggatggactcaag 1440
 V  W  F  E  H  G  H  Q  S  G  V  Y  E  A  L  V  D  G  L  K  480
accatacagattgacacctggctgcaggtcattcctcagttaattgctcggattgacacc 1500
 T  I  Q  I  D  T  W  L  Q  V  I  P  Q  L  I  A  R  I  D  T  500
cctcgttctctggtgtccaagctcatccaccagctgcttatggacatcggcaagcaccac 1560
 P  R  S  L  V  S  K  L  I  H  Q  L  L  M  D  I  G  K  H  H  520
cctcaggccctcatctaccccctcactgtagcagctaagtcctcagtggctgctcgttct 1620
 P  Q  A  L  I  Y  P  L  T  V  A  A  K  S  S  V  A  A  R  S  540
caggctgctgagaagatcctgaagaacatgagagaacactcagccaaccttgtacagcag 1680
 Q  A  A  E  K  I  L  K  N  M  R  E  H  S  A  N  L  V  Q  Q  560
gccatgatggtctcagaggaactgatccgcgtggctatcctgtggcatgagacatggcat 1740
 A  M  M  V  S  E  E  L  I  R  V  A  I  L  W  H  E  T  W  H  580
gagggtctggaggaggccagtcggctctactttggggaacgcaatgagtcagggatgttc 1800
 E  G  L  E  E  A  S  R  L  Y  F  G  E  R  N  E  S  G  M  F  600
cgcacactggagccgctgcatgccatgatggcacggggcccacagacactcaaggagatg 1860
 R  T  L  E  P  L  H  A  M  M  A  R  G  P  Q  T  L  K  E  M  620
tccttcaaccaggcctttgggcgggacctgaacgaggcgctggagtggtgtcgtcgctac 1920
```

```
 S  F  N  Q  A  F  G  R  D  L  N  E  A  L  E  W  C  R  R  Y  640
caacgctcgggcaacgtgcgcgagctgaaccaggcgtgggacctctactaccacgtgttt 1980
 Q  R  S  G  N  V  R  E  L  N  Q  A  W  D  L  Y  Y  H  V  F  660
cgccgaatctcccgcacgctgccgcaactcacctcccttgagctgcagagcgtctctccg 2040
 R  R  I  S  R  T  L  P  Q  L  T  S  L  E  L  Q  S  V  S  P  680
cggctgctccagtgtcgagacttagacatcgccgtaccgggctcctacgcgcctggccaa 2100
 R  L  L  Q  C  R  D  L  D  I  A  V  P  G  S  Y  A  P  G  Q  700
cccgtcatctgcatcagccaggtgcagtcctcgctccaggtgctcacctccaaacagcgg 2160
 P  V  I  C  I  S  Q  V  Q  S  S  L  Q  V  L  T  S  K  Q  R  720
ccyaggaagttatgtatccgcggcagcaatggcaggaacttcgtgttcttactgaagggc 2220
 P  R  K  L  C  I  R  G  S  N  G  R  N  F  V  F  L  L  K  G  740
Cacgaggacctgcgtcaggacgagcgcgtgatgcagctgttcgggctggtcaacacgctg 2280
 H  E  D  L  R  Q  D  E  R  V  M  Q  L  F  G  L  V  N  T  L  760
ctcatcagtaacccagacactttccgccgcaacccgaccatccagcggttcgccgtcatt 2340
 L  I  S  N  P  D  T  F  R  R  N  P  T  I  Q  R  F  A  V  I  780
ccgctgtctaccaactcgggcctgattgggtgggtgccgcactgcgacacgctgcacgcc 2400
 P  L  S  T  N  S  G  L  I  G  W  V  P  H  C  D  T  L  H  A  800
ctcatccgggactggcgcgagaagaagaagatcctgctgaacatcgagcaccgcatcatg 2460
 L  I  R  D  W  R  E  K  K  K  I  L  L  N  I  E  H  R  I  M  820
ctgcggatggcccaggacttggaccatctcactctcatgcagaaggtggaggtgttcgag 2520
 L  R  M  A  Q  D  L  D  H  L  T  L  M  Q  K  V  E  V  F  E  840
cacgcgctggagcacacgcatggcgatgatctgtcgcggctgctgtggttcaagagtccc 2580
 H  A  L  E  H  T  H  G  D  D  L  S  R  L  L  W  F  K  S  P  860
tcctccgaggtgtggtttgaccggcgcaccaactactcccgctcgttggccgtcatgtcc 2640
 S  S  E  V  W  F  D  R  R  T  N  Y  S  R  S  L  A  V  M  S  880
atggtgggctatgtgcttggcctcggcgaccgccacccctccaacctcatgctagaccag 2700
 M  V  G  Y  V  L  G  L  G  D  R  H  P  S  N  L  M  L  D  Q  900
ctctccggcaagatcatccacatcgacttcggtgactgcttcgaagtggcgatgatgcgc 2760
 L  S  G  K  I  I  H  I  D  F  G  D  C  F  E  V  A  M  M  R  920
gagaaattccctgagaagatcccgttccggttgacgcgcatgttgatccacgccatggaa 2820
 E  K  F  P  E  K  I  P  F  R  L  T  R  M  L  I  H  A  M  E  940
gtgacgggcatcgacggcacgtaccgcatgacctgcgagtccgtcatggccctgatccgc 2880
 V  T  G  I  D  G  T  Y  R  M  T  C  E  S  V  M  A  L  I  R  960
cgcaacaaggactccctcatggccatgctggaggcctttgtgcccaacctgctgttctat 2940
 R  N  K  D  S  L  M  A  M  L  E  A  F  V  P  N  L  L  F  Y  980
tggggccacagggaaaataaacattctaaagggaaggggtctgtgggggccgacggggag 3000
 W  G  H  R  E  N  K  H  S  K  G  K  G  S  V  G  A  D  G  E  1000
acggggccgtccgcgccggtctctacctctgccattgccccggacccctctttggacccc 3060
 T  G  P  S  A  P  V  S  T  S  A  I  A  P  D  P  S  L  D  P  1020
gctccggcacacaccctcaccccgacctccgtggggcctcacagccaggcacgggaggac 3120
 A  P  A  H  T  L  T  P  T  S  V  G  P  H  S  Q  A  R  E  D  1040
ggcggcgtgtcagaagccctcaacaagaaggcagtggccatcgtgcatcgcgtgcgagat 3180
 G  G  V  S  E  A  L  N  K  K  A  V  A  I  V  H  R  V  R  D  1060
aaactgactggccgggacttctgcaccgaggagtcgctggacgttcatcgccaagtggag 3240
 K  L  T  G  R  D  F  C  T  E  E  S  L  D  V  H  R  Q  V  E  1080
ctgctcatcgctcatgccaccttacacgagaacctctgccagtgctacatcggctggtgt 3300
 L  L  I  A  H  A  T  L  H  E  N  L  C  Q  C  Y  I  G  W  C  1100
cccttctggtgaacacactacttcataaccgcttgcactaaccacagccgccccgaccat 3360
 P  F  W  *                                                   1103
gctctacacactacttcataaccgcttgcactaaccacagccgccccgaccatgctcttc 3420
taaggtgtagagtgtggaaaggaacattgctgagggttggtggtagcgtgacacaccctg 3480
ttgcggcgggagtgttgttgtatgttgtttgttgtttgttgttcttgttgttacagtgtt 3540
Cgctgcgccgcagggattccggtaaaatctggaggaaggtcggtctgcgtgtgtggtgta 3600
ttgacagaagaggaggagcgggggggaggggcagctaaaaccacctcaggccatattaaaa 3660
aacacacacacacggggacactagctaaactaattcaacttcagcccccgaaaaggaatc 3720
cgtcaaaggggaggagagagagagagggggggagagtg                       3758
```

Figure 2. 2. Nucleotide and deduced amino acid sequences of cDNA encoding Gl-mTOR. The cDNA encoded the 3' end of the ORF and the incomplete 3'-UTR. Asterisk indicates stop codon. The font colors correspond to the colors of the domains in Fig. 2. 1.

```
gacataccagagattacacagacgctcctcaacttggcagagttcatggagcattgtgac 60
 D  I  P  E  I  T  Q  T  L  L  N  L  A  E  F  M  E  H  C  D  20
aagggtccgttgcccttggagctgcagctactcggggaaaaggccatggagtgccgggca 120
 K  G  P  L  P  L  E  L  Q  L  L  G  E  K  A  M  E  C  R  A  40
tatgccaaggctctgcactacaaggaggaggagttccacaaggggcctacctctgaggtc 180
 Y  A  K  A  L  H  Y  K  E  E  E  F  H  K  G  P  T  S  E  V  60
ttggagcacctcatctccatcaacaacaaactgggacagaaggaggcagctgctggtttg 240
 L  E  H  L  I  S  I  N  N  K  L  G  Q  K  E  A  A  A  G  L  80
ttggaatatgcacgcaagaacaaccgtacagacatgaaggtccaggaacggtggcatgag 300
 L  E  Y  A  R  K  N  N  R  T  D  M  K  V  Q  E  R  W  H  E  100
aagctgcacgactgggatcaggcactccaagcttactctaccaagctggagactcaacct 360
 K  L  H  D  W  D  Q  A  L  Q  A  Y  S  T  K  L  E  T  Q  P  120
gatgaccttgccctcgtactgggtcaaatgaggtgtctagaggctctgggagaatggggt 420
 D  D  L  A  L  V  L  G  Q  M  R  C  L  E  A  L  G  E  W  G  140
gagttatacagcgtggcttgtgaccgctggatgggcacaatggctgaggatgtgcgtgct 480
 E  L  Y  S  V  A  C  D  R  W  M  G  T  M  A  E  D  V  R  A  160
cagatggctcgcgtggcctcagcatctgcctgggccatgggggagtggagtatgatggag 540
 Q  M  A  R  V  A  S  A  S  A  W  A  M  G  E  W  S  M  M  E  180
gagtacagtcgatgcatcccaagagacaccaatgagggggctttctaccgtgctgtgctc 600
 E  Y  S  R  C  I  P  R  D  T  N  E  G  A  F  Y  R  A  V  L  200
tctgtacataaggatcaacatcacatggcccagcagtacatcgacacagcaagagattta 660
 S  V  H  K  D  Q  H  H  M  A  Q  Q  Y  I  D  T  A  R  D  L  220
ctagacacggagctcacagctatggttggggagagctaccagcgtgcctacaactccatg 720
 L  D  T  E  L  T  A  M  V  G  E  S  Y  Q  R  A  Y  N  S  M  240
gtggcggtgcagatgttggctgagctggaggaggtgattcagtacaagctggtgccagag 780
 V  A  V  Q  M  L  A  E  L  E  E  V  I  Q  Y  K  L  V  P  E  260
agaaggcgacccatcactcatatctggtgggagaggctgcaggggtgccagcgagtggtg 840
 R  R  R  P  I  T  H  I  W  W  E  R  L  Q  G  C  Q  R  V  V  280
gaagactggcagaagatcctacaggtgcgctccctggtgctgtcccctcaggaagacatg 900
 E  D  W  Q  K  I  L  Q  V  R  S  L  V  L  S  P  Q  E  D  M  300
cggccttggctcaagtttgcctcgctgtgtcgcaagtctggtcgcctggccctgtcccac 960
 R  P  W  L  K  F  A  S  L  C  R  K  S  G  R  L  A  L  S  H  320
aagaccctggtgcggctactgggatgcgacccttctctcagccccacccagccactccca 1020
 K  T  L  V  R  L  L  G  C  D  P  S  L  S  P  T  Q  P  L  P  340
gtcagtcacccccacgtcacttaccagtactgcaagcatatctacacctacccagacaga 1080
 V  S  H  P  H  V  T  Y  Q  Y  C  K  H  I  Y  T  Y  P  D  R  360
cggcaggaggcctatggtcggctgcagaagttcctccagttcttggcaccggcagtggtg 1140
 R  Q  E  A  Y  G  R  L  Q  K  F  L  Q  F  L  A  P  A  V  V  380
gtggtgggcggagggaaccaaaacggggacaacaagctgcgcaaactggtgtcccgtgtg 1200
 V  V  G  G  G  N  Q  N  G  D  N  K  L  R  K  L  V  S  R  V  400
tacctcaagctgggtgaatggtacgagcagctacatggattgaacgaggagaacattgcc 1260
 Y  L  K  L  G  E  W  Y  E  Q  L  H  G  L  N  E  E  N  I  A  420
aatatcctcacctactacacccacgccaaggatacagacgagagctgctacaaggcttgg 1320
 N  I  L  T  Y  Y  T  H  A  K  D  T  D  E  S  C  Y  K  A  W  440
cacgcatacgcttatatgaactttgaggcaatactcttctataagaagggcttcatccgt 1380
 H  A  Y  A  Y  M  N  F  E  A  I  L  F  Y  K  K  G  F  I  R  460
tcaatctccctgagtgacgggtacagcctgcaggacacccttcgccttctcaccgtctgg 1440
 S  I  S  L  S  D  G  Y  S  L  Q  D  T  L  R  L  L  T  V  W  480
ttcgaacacggccatcagtctggagtgtacgaggcgctggtggacggactcagaccatca 1500
 F  E  H  G  H  Q  S  G  V  Y  E  A  L  V  D  G  L  R  P  S  500
gatatcgacacttggcttcaggtcattcctcagctcatcgcgcgcattgacacccctcgc 1560
 D  I  D  T  W  L  Q  V  I  P  Q  L  I  A  R  I  D  T  P  R  520
tccctcgtgtccaagctcatccaccagctgctcatggacattgggaaacaccacccacag 1620
 S  L  V  S  K  L  I  H  Q  L  L  M  D  I  G  K  H  H  P  Q  540
gcactcatctaccctctcaccgtggcagccaagtcctcggtgccggcgcgctcccaggca 1680
 A  L  I  Y  P  L  T  V  A  A  K  S  S  V  P  A  R  S  Q  A  560
gccgagaagatcctgaagaacatgagggagcactcggccaacctcgtccagcaggccatg 1740
 A  E  K  I  L  K  N  M  R  E  H  S  A  N  L  V  Q  Q  A  M  580
atggtctccgaggaactgatccgagtggctattctgtggcacgagacttggcatgagggg 1800
 M  V  S  E  E  L  I  R  V  A  I  L  W  H  E  T  W  H  E  G  600
ttggaggaggccagtcgtttatactttggggaacgtaatgagtcaggcatgttccgcacc 1860
 L  E  E  A  S  R  L  Y  F  G  E  R  N  E  S  G  M  F  R  T  620
cttgacccactacacgctatgatggctcggggaccgcagaccctcaaagaaatgtccttc 1920
```

```
 L  D  P  L  H  A  M  M  A  R  G  P  Q  T  L  K  E  M  S  F  640
aaccaggcttacgggcgtgacctgaacgaggcgcaggagtggtgccgccgctaccaacgt 1980
 N  Q  A  Y  G  R  D  L  N  E  A  Q  E  W  C  R  R  Y  Q  R  660
tcaggtaatgtacgggagctgaaccaagcctgggatctctactaccacgtgttccgccgc 2040
 S  G  N  V  R  E  L  N  Q  A  W  D  L  Y  Y  H  V  F  R  R  680
atctccagaacactaccgcagctcacctccctcgaactgcagagtgtgtccccgcgcctc 2100
 I  S  R  T  L  P  Q  L  T  S  L  E  L  Q  S  V  S  P  R  L  700
ctcaaatgcccgagatctggacatcgcagtaccgggttcctatgctcccggtatcccagt 2160
 L  K  C  P  R  S  G  H  R  S  T  G  F  L  C  S  R  Y  P  S  720
tatttgtattcatcaggtgcagtcctcgttacaggtcttgacttcaaacagcgacctagg 2220
 Y  L  Y  S  S  G  A  V  L  V  T  G  L  D  F  K  Q  R  P  R  740
aaactctgcatcaagggtagtaatgggagagactttgtgtttctgctcaagggccacgag 2280
 K  L  C  I  K  G  S  N  G  R  D  F  V  F  L  L  K  G  H  E  760
gacttgaggcaggatgaacgggtgatgcagctcttcgggttagtcaatactctgctcatt 2340
 D  L  R  Q  D  E  R  V  M  Q  L  F  G  L  V  N  T  L  L  I  780
agtaaccctgacaccttcagacgtaatcttaccattcagaggttcgccgtcatcccgctg 2400
 S  N  P  D  T  F  R  R  N  L  T  I  Q  R  F  A  V  I  P  L  800
tccactaactcgggtctcattgggtggatgcctcactgcgacactctacacgcactcatc 2460
 S  T  N  S  G  L  I  G  W  M  P  H  C  D  T  L  H  A  L  I  820
agagactggcgtgagaagaagaaaatcctcctcaacatcgagcacaggattatgttgagg 2520
 R  D  W  R  E  K  K  K  I  L  L  N  I  E  H  R  I  M  L  R  840
atggctcaggatttggaccatctaaccctcatgcagaaggtggaggtgtttgagcacgcc 2580
 M  A  Q  D  L  D  H  L  T  L  M  Q  K  V  E  V  F  E  H  A  860
ctggagcacacacaaggggatgacttagctcggttgctgtggtttaagagtccttcgtct 2640
 L  E  H  T  Q  G  D  D  L  A  R  L  L  W  F  K  S  P  S  S  880
gaggtgtggtttgatcgccggacgaattactcccgttccctggctgtcatgtccatggta 2700
 E  V  W  F  D  R  R  T  N  Y  S  R  S  L  A  V  M  S  M  V  900
ggctacgtactgggactcggtgaccggcatccctcaaacctcatgctggatcaactgtct 2760
 G  Y  V  L  G  L  G  D  R  H  P  S  N  L  M  L  D  Q  L  S  920
gggaagatcatacacattgacttcggtgactgcttcgaagtggccatgatgcgtgaaaag 2820
 G  K  I  I  H  I  D  F  G  D  C  F  E  V  A  M  M  R  E  K  940
ttcccggagaagattccattccggctgacgcgtatgttgatccacgccatggaggtcacc 2880
 F  P  E  K  I  P  F  R  L  T  R  M  L  I  H  A  M  E  V  T  960
gggattgacggcacgtatcgcatgacctgtgagagtgtcatggcactgatccgccgtaac 2940
 G  I  D  G  T  Y  R  M  T  C  E  S  V  M  A  L  I  R  R  N  980
aaggactccctcatggccatgctggaagccttcgtgcatgacccactgctcaactggcgc 3000
 K  D  S  L  M  A  M  L  E  A  F  V  H  D  P  L  L  N  W  R  1000
ctcatggacaacacgcagccaaagggaaagcgttctgtggtgggtgagggcgaggcagga 3060
 L  M  D  N  T  Q  P  K  G  K  R  S  V  V  G  E  G  E  A  G  1020
ccttcagctccagcctccacttctacaatcgctcctgaccctgctattgacactgccccg 3120
 P  S  A  P  A  S  T  S  T  I  A  P  D  P  A  I  D  T  A  P  1040
gccatcacgccagcctcggtagggccacagagccagtcacgggaggacggtggggtgtcg 3180
 A  I  T  P  A  S  V  G  P  Q  S  Q  S  R  E  D  G  G  V  S  1060
gaagccctaaacaagaaagcagtcgccatcgtccaccgcgtcagggacaaactcacaggc 3240
 E  A  L  N  K  K  A  V  A  I  V  H  R  V  R  D  K  L  T  G  1080
cgggacttctgcactgaggaacctcttgatgtgcaccgccaagtagagcttctcatcgca 3300
 R  D  F  C  T  E  E  P  L  D  V  H  R  Q  V  E  L  L  I  A  1100
caggcaacatcacatgagaacctgtgtcagtgttacattggttggtgccccttctggtaa 3360
 Q  A  T  S  H  E  N  L  C  Q  C  Y  I  G  W  C  P  F  W  *  1119
caaccatacccaaacacacccacattcaccacactgcagggtaaagtgtggccaggactt 3420
gtgaagctgaggtgccaagtttactcgtgtcttcgtgttgcgacagggttgttattcttg 3480
ttgttgttttcaccatgtaggaattccggtgtaatggtggtaaagagagaagcttgggca 3540
ttgtttggtatcgatggagggaaggaggagaaggagaagggggtgttacgagagaagctt 3600
aggcattgttttgtatcgatggaggagaaggagggaaggataaacatgaaggagcaggac 3660
atcggtaatgagagaatcaccccatcccccacacatacatacaccataacaatgactac 3720
ttttcaacatcgccattagataaatcaaacgaccagtgagtgaggcaggacaaggcaaaa 3780
attcaaccaccatcacctcctgcagaatatctcgtaagtaatctgtctgtgagtaatgtt 3840
gtgggaacttgtacattgttttataaagttacnattangcagaagaggaagaggagagga 3900
tggtgatcatttcggtgttttagaaaggagggagtgtgtgaggtcaagtgcaactgatag 3960
tttagtttanatttgggttattctgtanattaattaataaaaatanagttgagtgattgt 4020
aaaaaaaaaaa                                                   4031
```

Figure 2. 3. Figure 2. 3. Nucleotide and deduced amino acid sequences of cDNA encoding Cm-mTOR. The cDNA encoded the 3' end of the ORF and the complete 3'-UTR. Asterisk indicates stop codon. The polyadenylation signal in the 3'-UTR is underlined. The font colors correspond to the colors of the domains in Fig. 2. 1.

HEAT repeats

```
Cm-mTOR : -------------------------DIPEITQTLLNLAEFMEHCDKGPLPLELQLLGEKA :   35
Dm-mTOR : SCWTELSPDLKNELTQSLIQALQVTDMPEITQTILNLAEFMEHCDRDPIPIETKLLGTRA : 1354
Aa-mTOR : SCWTDLPDSLKEELSSSLRQALMVPDLPEITQTILNLAEFMEHCENDALRIDPKILGERA : 1339
Dp-mTOR : SCWTELSQQHQNELVKSLEQALRVPDLPEITQTILNLAEFMEHCEKELCNAELMPKHFIT : 1371

Gl-mTOR : -------------------------VLEHLISINNKLGQKEAAAGLLEY--ARKNNRTD :   32
Cm-mTOR : MECRAYAKALHYKEEEFHKGPTSE--VLEHLISINNKLGQKEAAAGLLEY--ARKNNRTD :   91
Dm-mTOR : MACRAYAKALRYKEEEFLLREDSQ--VFESLILINNKLQQREAAEGLLT---RYRNAANE : 1409
Aa-mTOR : MECRAYAKALHYKEEEFLNMKDKDQSVFESLILINNKLQQKEAAEGLLEYAMEHRSASEE : 1399
Dp-mTOR : KKPSSMSLPLLRQDRDYLQ---ILRPVLESLISINNKLQQKEAAAGLLEY--AMKKHEGE : 1426

Gl-mTOR : MKVQERWHEKLHDWDQALQAYSTKLETQPD-DLALVLGQMRCLEALGEWGELYSVSCERW :   91
Cm-mTOR : MKVQERWHEKLHDWDQALQAYSTKLETQPD-DLALVLGQMRCLEALGEWGELYSVACDRW :  150
Dm-mTOR : LNVQGRWYEKLHNWDEALEHYERNLKTDSS-DLEARLGHMRCLEALGDWSELSNVTKHEW : 1468
Aa-mTOR : MKVQVRWYEKLHSWEKALNLYQDKLESNPG-DLDSRLGQWRCLEALGEWSTLNTLTKETW : 1458
Dp-mTOR : IRVQERWHEKLHDWERALEAYRKKESNQQQQEPELVLGQMRCLEALCEWGQLHTLAETNW : 1486

Gl-mTOR : MGTVPEEVRAQMSRVAAASAWGLGEWSMMEEYSRCIPRDTNEGAFYRAVLAVHKDCHHVA :  151
Cm-mTOR : MGTVAEDVRAQMARVASASAWAMGEWSMMEEYSRCIPRDTNEGAFYRAVLSVHKDCHHMA :  210
Dm-mTOR : EN-FGTEAKSRAGPLAAVAAWGLQDWEAMREYVRCIPEDTQDGSYYRAVLAVHHDDFETA : 1527
Aa-mTOR : ES-LGTEGQSKAGRLAAAAAWGLKDWEGMQEFVKFIPEDTQDGSFYRAVLAVHHGEYELA : 1517
Dp-mTOR : KQ-VNVDVKNRFARMAAAAAWGLGKWTAMEEYVNFIPKETQDGAFYRSVLAIHREQYSQA : 1545

Gl-mTOR : QQYIDTARDLLDTELTAMVGESYQRAYNSMVAVQMLAELEEVIQYKLVPERRPPIIQIWW :  211
Cm-mTOR : QQYIDTARDLLDTELTAMVGESYQRAYNSMVAVQMLAELEEVIQYKLVPERRPITHIWW :  270
Dm-mTOR : QRLIDETRDLLDTELTSMAGESYERAYGAMVCVQMLAELEEVIQYKLIPERREPLKTMWW : 1587
Aa-mTOR : QTLIDDTRDLLDTELTAMAGESYERAYGAMVCVQMLSELEEVIQYKLIPERQETIKAMWW : 1577
Dp-mTOR : QTLIDSARDLLDTELTALSGESYQRAYGAMVLVQMLAELEEVIQYKILPERRAPIRKMWW : 1605

Gl-mTOR : ERLQGCQRVVEDWQKILQVRSLVLSPQEDMRPWLKFASLCRKSCRLALSHKTLVRLLGCD :  271
Cm-mTOR : ERLQGCQRVVEDWQKILQVRSLVLSPQEDMRPWLKFASLCRKSCRLALSHKTLVRLLGCD :  330
Dm-mTOR : KRLQGCQRLVEDWRRIIQVHSLVVKPHEDIHTWLKYASLCRKSCSLHLSHKTLVMLLGTD : 1647
Aa-mTOR : DRLLGGQRLVEDWQRILQVHTLVVHPANDVKTWLKFASLCRKSDSLKLSEKTLVMLLRYN : 1637
Dp-mTOR : QRLQGCQRIVEDWQKIIQVHSLVISPEEDMRTRLKYSSLCRKSCRLALSHKTLVTLLGTD : 1665

Gl-mTOR : PSLSPSQPLPISHPHVTYQYCKHIYTYPHRRQEAYGRLQKFLQFLAP--------AVVVV :  323
Cm-mTOR : PSLSPTQPLPVSHPHVTYQYCKHIYTYPDRRQEAYGRLQKFLQFLAP--------AVVVV :  382
Dm-mTOR : PKLNPNQPLPCNQPQVTYAYTKYMAANNQL-QEAYEQLTHFVSTYSQ--------ELSCL : 1698
Aa-mTOR : PSEYPDHPLEFMQPDISFAYAKHLWAAGEQ-EKAYNQLNRLVADMGI--------EGNFD : 1688
Dp-mTOR : PSLNPDHPLPTLHPHVTYAYSKHLWMSNQK-EQAFRQLHHFVQASLQPQSLSSISTTPVS : 1724

Gl-mTOR : GGGNQNGDNKLRKLVSRVYLKLGEWYEQLHG-LNEENIANILTYYTHAKDTDETCYKAWH :  382
Cm-mTOR : GGGNQNGDNKLRKLVSRVYLKLGEWYEQLHG-LNEENIANILTYYTHAKDTDESCYKAWH :  441
Dm-mTOR : PPEALKQQD--QRLMARCYLRMATWQNKLQDSIRPDAIQGALECFEKATSYDPNWYKAWH : 1756
Aa-mTOR : VEE--KDEN--RRLLARCYMKLGQWQNQLQG-LNEQSIKGILACYEKATKHDSNWYKAWH : 1743
Dp-mTOR : TPEEPDRHVELGKLLARCYLRLGQWQECLQG-INELSIPAVLQYYAAATEHDATWYKAWH : 1783

Gl-mTOR : AYAYMNFEAILFYKGKMDVKGEAPTTPGEDSASGAAAVVTPSKKRSAGDFAVAAVKGFIR :  442
Cm-mTOR : AYAYMNFEAILFYK-----------------------------------------KGFIR :  460
Dm-mTOR : LWAYMNFKVVQAQKSALDKQQPPGASMGMTMGSGL-----DSDLMIIQRYAVPAVQGFFR : 1811
Aa-mTOR : LWAYMNFEVVQNQKQQEDLIKNPGG---------------DKEKCMIRQYAVPAVEGFFR : 1788
Dp-mTOR : SWAYMNFEAVLFYKHQGQNTSANQTLIGENTNKG-------LTAQHVSSYTVPAVQGFFR : 1836

Gl-mTOR : SISLSDGMSLQDTLRLLTVWFEHGHQSGVYEALVDGLKTIQIDTWLQVIPQLIARIDTPR :  502
Cm-mTOR : SISLSDGYSLQDTLRLLTVWFEHGHQSGVYEALVDGLRPSDIDTWLQVIPQLIARIDTPR :  520
Dm-mTOR : SISLIKGNSLQDTLRLLTLWFDYGNHAEVYEALLSGMKLIEINTWLQVIPQLIARIDTHR : 1871
Aa-mTOR : SINLSHGNSLQDTLRLLTLWFDYGQYPKVYEALVEGMRVIEINTWLQVIPQLIARIDTPR : 1848
Dp-mTOR : SIALSHGSSLQDTLRLLTLWFDYGHWPEVYEALVEGVRTIDVNTWLQVIPQLIARIDTQR : 1896

Gl-mTOR : SLVSKLIHQLLMDIGKHHPQALIYPLTVAAKSSVARSQAAEKILKNMREHSANLVQQAM :  562
Cm-mTOR : SLVSKLIHQLLMDIGKHHPQALIYPLTVAAKSSVPARSQAAEKILKNMREHSANLVQQAM :  580
Dm-mTOR : QLVGQLIHQLLMDIGKNHPQALVYPLTVASKSASLARRNAAFKILDSMRKHSPTLVEQAV : 1931
Aa-mTOR : NLVGQLIHQLLNDIGKCHPQALVYPLTVASNSASSARRQAAHKILGSMGEHSSNLVNQAI : 1908
Dp-mTOR : QLVGRLIHQLLMDIGKAHPQALIYPLTVASKSALCARHNAANKILKNMCEHSPVLVQQAV : 1956
```

FAT Domain

FRB Domain

```
Gl-mTOR : MVSEELIRVAILWHETWHEGLEEASRLYFGERNESGMFRTLEPLHAMMARGPQTLKEMSF :  622
Cm-mTOR : MVSEELIRVAILWHETWHEGLEEASRLYFGERNESGMFRTLDPLHAMMARGPQTLKEMSF :  640
Dm-mTOR : MCSEELIRVAILWHEQWHEGLEEASRLYFGDRNVKGMFEILEPLHAMLERGPQTLKETSF : 1991
Aa-mTOR : MCSEELIRVTILWHEQWHEGLEEASRLYFGDRNIKGMFETLEPLHQMLQRGPQTLKETSF : 1968
Dp-mTOR : MVSEELIRVAILWHELWHEGLEEASRLYFGERNVTGMFATLEPLHAMLERGPQTLKETSF : 2016

Gl-mTOR : NQAFGRDLNEALEWCRRYQRSGNVRELNQAWDLYYHVFRRISRTLPQLTSLELQSVSPRL :  682
Cm-mTOR : NQAYGRDLNEAQEWCRRYQRSGNVRELNQAWDLYYHVFRRISRTLPQLTSLELQSVSPRL :  700
Dm-mTOR : SQAYGRELTEAYEWSQRYKTSAVVMDLDRAWDIYYHVFQKISRQLPQLTSLELPYVSPKL : 2051
Aa-mTOR : NQAYGRDLNEAQEWCKHYKNSGNIRDLNQAWDLYYHVFRRISRQLPQLTSLELQYVSPKL : 2028
Dp-mTOR : HQAYGRELLEAQDWCRRYKTSLNVRDLNQAWDLYYHVFRRISRQLPQLTSLELQYVSPKL : 2076
```

KD

```
Gl-mTOR : LQCRDLDIAVPGSYAPGQPVICISQVQGSLQVLTSKQRPRKLCIRGSNGRNFVFLLKGHE :  742
Cm-mTOR : LKCPRSGHRSTGFLCSRYPSYLYSSGAVLVTGLDFKQRPRKLCIKGSNGRDFVFLLKGHE :  760
Dm-mTOR : MTCKDLELAVPGSYNPGQELIRISIIKTNLQVITSKQRPRKLCIRGSNGKDYMYLLKGHE : 2111
Aa-mTOR : LACRDLELAVPGSYAPGQELIRIASIQSNLQVITSKQRPRKLCIRGSNGKEYMFLLKGHE : 2088
Dp-mTOR : LLCRDLELAIPGSYVPNQPVIRISQVNGSLQVITSKQRPRKLCITGSNGKEYMFLLKGHE : 2136

Gl-mTOR : DLRQDERVMQLFGLVNTLLISNPDTFRRNPTIQRFAVIPLSTNSGLIGWVPHCDTLHALI :  802
Cm-mTOR : DLRQDERVMQLFGLVNTLLISNPDTFRRNLTIQRFAVIPLSTNSGLIGWMPHCDTLHALI :  820
Dm-mTOR : DLRQDERVMQLFSLVNTLLLDDPDTFRRNLAIQRYAVIPLSTNSGLIGWVPHCDTLHTLI : 2171
Aa-mTOR : DLRQDERVMQLFGLVNTLLLNDPDTFRRNLTIQRYAFIPLSTNSGLIGWVPHCDTLHTLT : 2148
Dp-mTOR : DLRQDERVMQLFSLVNTLLIHDPETFRRNLTIQRYAVIPLSTNSGLIGWVPHCDTLHSLI : 2196

Gl-mTOR : RDWREKKKILLNIEHRIMLRMAQDLDHLTLMQKVEVFEHALEHTHGDDLSRLLWFKSPSS :  862
Cm-mTOR : RDWREKKKILLNIEHRIMLRMAQDLDHLTLMQKVEVFEHALEHTQGDDLARLLWFKSPSS :  880
Dm-mTOR : RDYRDKKKVPLNQEHRTMLNFAPDYDHLTLMQKVEVFEHALGQTQGDDLAKLLWLKSPSS : 2231
Aa-mTOR : RDYREKKKTMLNIEHRIMLRMATDYDHLTLMQKVEVFEYALELTKGDDLAKLLWLKSPSS : 2208
Dp-mTOR : RDYREKKKILLNIEHRIMLRMAPDYDHLSLMQKVEVFEHALEHTQGDDLAKILWLRSPSS : 2256

Gl-mTOR : EVWFDRRTNYSR---------SLAVMSMVGYVLGLGDRHPSNLMLDQLSGKIIHIDFGDC :  913
Cm-mTOR : EVWFDRRTNYSR---------SLAVMSMVGYVLGLGDRHPSNLMLDQLSGKIIHIDFGDC :  931
Dm-mTOR : ELWFERRNNYTR---------SLAVMSMVGYILGLGDRHPSNLMLDRMSGKILHIDFGDC : 2282
Aa-mTOR : EVWFDRRTNYTR---------SLAVMSMVGYILGLGDRHPSNLMLDRLSGKILHIDFGDC : 2259
Dp-mTOR : EVWFDRRTNYTRHELFFNPINLYTVMSMVGYILGLGDRHPSNLMLDRLSGKILHIDFGDC : 2316

Gl-mTOR : FEVAMMREKFPEKIPFRLTRMLIHAMEVTGIDGTYRMTCESVMALIRRNKDSLMAMLEAF :  973
Cm-mTOR : FEVAMMREKFPEKIPFRLTRMLIHAMEVTGIDGTYRMTCESVMALIRRNKDSLMAMLEAF :  991
Dm-mTOR : FEVAMTREKFPEKIPFRLTRMLIKAMEVTGIEGTYRRTCESVMLVLRRNKDSLMAVLEAF : 2342
Aa-mTOR : FEVAMTREKFPEKIPFRLTRMLINAMEVTGIEGTYRRTCESVMHVLRRNKDSLMAVLEAF : 2319
Dp-mTOR : FEVAMTREKFPEKIPFRLTRMLVNAMEVTGIEGTYRSTCESVMSVLRGNKDSLMAVLEAF : 2376

Gl-mTOR : VPNLLFYWGHRENKHSKGKGS-------VGADGETGPSAPVSTSATAPDPSLDPAPAHTL : 1026
Cm-mTOR : VHDPLLNWRLMDNTQFKGKRS-------VVGEGEAGPSAPASTSTIAPDPAIDTAPA--I : 1042
Dm-mTOR : VYDPLLNWRLLDVDK-KGNDA-------VAGAGAPGGRGGSGMQDSLSNSVEDSLPMAKS : 2394
Aa-mTOR : VYDPLLNWRLLDVDK-NRRSK-------NATDVDSTTESMEETLDLLIN--ARNLRMNEA : 2369
Dp-mTOR : VYDPLLNWRLVVDNVANTKTTRRSKSRHESSSNNSGQGDVGDSMEITANAAATSSSVLNA : 2436

Gl-mTOR : TPTSVGPH--SQAREDGGVSEALNKKAVAIVHRVRDKLTGRDFC--TEESLDVHRQVELL : 1082
Cm-mTOR : TPASVGPQ--SQSREDGGVSEALNKKAVAIVHRVRDKLTGRDFC--TEEPLDVHRQVELL : 1098
Dm-mTOR : KPYDPTLQ--QGG-LHNNVADETNSKASQVIKRVKCKLTGTDFQ--TEKSVNEQSQVELL : 2449
Aa-mTOR : NGGGDVVD--QGSNCIANPAEATNNKARAIVDRVKQKLTGKDFN--TVEPVQR--QIDLL : 2423
Dp-mTOR : AVSRSKNETVEAVVNDGFQPEILNKRALTIVSRVRDKLTGRDFPNETEGTLSIDRQVELL : 2496

Gl-mTOR : IAHATLHENLCQCYIGWCPFW : 1103
Cm-mTOR : IAQATSHENLCQCYIGWCPFW : 1119
Dm-mTOR : IQQATNNENLCQCYIGWCPFW : 2470
Aa-mTOR : IRQATNNENLCQCYIGWCPFW : 2444
Dp-mTOR : IQQATSHENLCQCYIGWCPFW : 2517
```

FATC Domain

Figure 2. 4. Multiple alignment of deduced amino acid sequences of mTOR proteins in three crustacean species and two insect species. Abbreviations: Aa, *Aedes aegypti* (AAR97336); Cm, *C. maenas* (JQ864248); Dm, *Drosophila melanogaster* (NP524891); Dp, *Daphnia pulex* (EFX69318); and Gl, *G. lateralis* (HM989973). Amino acid residues that are identical or similar in all sequences are shaded in black; gray shading indicates identical or similar amino acids in most of the sequences. Dashes indicate gaps introduced to optimize the alignment and the boxes indicate the HEAT repeat, FRB (FKBP12 rapamycin binding), KD (kinase domain) and FATC (FRAP, ATM and TRRAP C-terminal) domains. The colors of the boxes correspond to the colors of the domains in Fig. 2. 1.

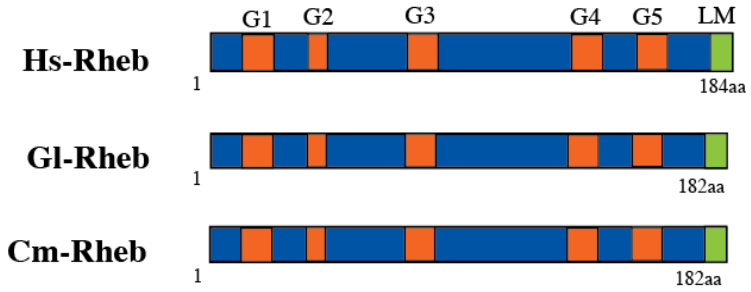

Figure 2. 5. Domain organization of Rheb. The complete Rheb protein from human (Hs-Rheb) is compared to the complete Rheb sequences from *G. lateralis* (Gl-Rheb) and *C. maenas* (Cm-Rheb). All share highly conserved G boxes (G1-G5) and lipid modification (LM) domains, indicated by orange and green shading, respectively.

```
gagagtgacgccatcaccgccaccaaaacaaacccacacctccacctgtgtttccgggca 60
cctcaggcgcacccaggggccccaggtgtgttgcgagctactcttatggaccactgagca 120
tctctccacgcagcc                                              135
atgcctcccaagacgagaaaagtggccgttatgggctacagaagcgtggggaagtcatct 195
 M  P  P  K  T  R  K  V  A  V  M  G  Y  R  S  V  G  K  S  S  20
ctatgcattcagtttgttgatggccagtttgtggacagctatgatcccaccattgaaaac 255
 L  C  I  Q  F  V  D  G  Q  F  V  D  S  Y  D  P  T  I  E  N  40
accttcacaaaaaactcaaggtgcgagggcaggaatatggcctggagctggtggacacg 315
 T  F  T  K  K  L  K  V  R  G  Q  E  Y  G  L  E  L  V  D  T  60
gcaggtcaggatgagtatagcatcttcccagcccaatactccatgaacatccacggctat 375
 A  G  Q  D  E  Y  S  I  F  P  A  Q  Y  S  M  N  I  H  G  Y  80
gtcctggtctactccatcacctcggaaaagtccttcgaggtagcccaggtcatctatgac 435
 V  L  V  Y  S  I  T  S  E  K  S  F  E  V  A  Q  V  I  Y  D  100
aagattctcgacgtgatgggcaaagtcacagttcctgtggtgttggtgggcaacaagaat 495
 K  I  L  D  V  M  G  K  V  T  V  P  V  V  L  V  G  N  K  N  120
gacttgcacctggagcgtgtggtgagcaccgaccaggggcgccgcgtggcagacaactgg 555
 D  L  H  L  E  R  V  V  S  T  D  Q  G  R  R  V  A  D  N  W  140
aaggctgtgtttcttgagacaagtgccaaggagcatgaggcagtgagtgacatcttcact 615
 K  A  V  F  L  E  T  S  A  K  E  H  E  A  V  S  D  I  F  T  160
cgagccatcctggagattgagaaggctgatgggaacctgccctccggtaacggctgtagt 675
 R  A  I  L  E  I  E  K  A  D  G  N  L  P  S  G  N  G  C  S  180
atttcatgaagcctctgtgatatagccagaacctttattgccaccacctctctgacaacc 735
 I  S  *                                                     182
agcctctgtgatatagccagaacctttattgccaccacctctctgacaaccgatttggat 795
cttgaaaacaagactttgtacatggcttattctcttcacgggcaacaggatccagaaatt 855
tgtgttttcttctgttgtatcagttctttatggccttgcctgttgtgagtatgagccagc 915
ccactggacccatgcagtaccctcctagtctgttgtgggataatggtcagtactgttggc 975
agtgggtg                                                     983
```

Figure 2. 6. Nucleotide and amino acid sequences of cDNA encoding Gl-Rheb. The cDNA encoded the 5'-UTR, complete ORF, and partial 3'-UTR. The five G boxes involved in GTP binding and the lipid modification site are indicated in bold plus underline. The font colors correspond to the colors of the domains in Fig. 2. 5. Asterisk indicates stop codon.

```
ccaccaccaccaaaacaaacccacaccttgtcctgtgtttccttcattcagagacacacc 60
caggattcccaggtgtgctgctgctgcctcgtatggaccagtaaacctgcccctagccag 120
cc                                                           122
atgcctcccaaggatagaaaagtggccgttatgggctatagaagtgttggaaagtcgtcc 182
 M  P  P  K  D  R  K  V  A  V  M  G  Y  R  S  V  G  K  S  S  20
ctgtgcattcagttcgttgacggacagtttgtggacagctacgaccctactattgaaaac 242
 L  C  I  Q  F  V  D  G  Q  F  V  D  S  Y  D  P  T  I  E  N  40
accttcaccaagaaacttaaggtgcgtggacaagagtacggccttgagctggtggacacg 302
 T  F  T  K  K  L  K  V  R  G  Q  E  Y  G  L  E  L  V  D  T  60
gccggccaggatgagtacagcatcttcccggcccagtactccatgaacattcacggctat 362
 A  G  Q  D  E  Y  S  I  F  P  A  Q  Y  S  M  N  I  H  G  Y  80
gtcctggtgtactccatcacctcggagaagtcctttgaggtggcccaggtcatctacgac 422
 V  L  V  Y  S  I  T  S  E  K  S  F  E  V  A  Q  V  I  Y  D  100
aagattctcgacatgatgggcaaagtcacagttcctgtagtgttggtgggcaacaagaat 482
 K  I  L  D  M  M  G  K  V  T  V  P  V  V  L  V  G  N  K  N  120
gatttacatttggagcgtgtggtgagcactgagcaaggccgccgcttggctgaccaatgg 542
 D  L  H  L  E  R  V  V  S  T  E  Q  G  R  R  L  A  D  Q  W  140
aaggcagcatttctggagacaagtgccaaggaacatgaggcggtgaatgacatcttcaca 602
 K  A  A  F  L  E  T  S  A  K  E  H  E  A  V  N  D  I  F  T  160
cgagccatcctggagatcgagagggccgatgggaacctgccccctggaagtagctgtcgt 662
 R  A  I  L  E  I  E  R  A  D  G  N  L  P  P  G  S  S  C  R  180
atttcatgaagactctgtgatatagccacaacctttattgccaccatcttcctgaccact 722
 I  S  *                                                     182
Gatttacattttgaaaacaggactttgtacaggcatttctctcttcatgggcaatgggac 782
Ccaggaaattatgttttgttatgttgtatcatttcttcacagccttgcctgttgtgagta 842
Tgagccagcccagtggttccctgccgggctgtccctgtgtctgacacgggggtggtcact 902
Actggagccggtgggtgtggcttgcaattcaaggctcagtatatacatagataaaaatat 962
Tagtggatatatatgttagggaacacagctcatccactgccttagatggtggatttgtac 1022
Actaaggctatttgggtctggctttgagatgaagactagagtgtgtgatttgggagtcat 1082
Agtaatcaattctagttatttctttgcaatgcaatgcaaaagactaagagtgtgtgattt 1142
Gggagtcatagtaatcaaattcctagtttatttttttgccattgcaatgcaagggaggg 1202
Aacagtttttttcaactcagtgtggttaggaaaaattgtatcagttcagtttttttttt 1262
Tttttttgttctgtctctcctttttggaagagaatttagagccatcagtctgttggataca 1322
Atgacggccatattggaattccacttacatttgtagacaatttttcacatgtgggaatg 1382
Acatttgttcatcaataacttacattttagtaagagaggaaaactacacgtggaagctga 1442
Gctaatggtgaaatagctaagcttataattactataatgtaaggcaataaattcatagaa 1502
aacagaaaaaaaaaaaaaaaaaaaaaaaaaaaaaaaaaaaaaaaa                1543
```

Figure 2. 7. Nucleotide and amino acid sequences of cDNA encoding Cm-Rheb. The cDNA encoded the 5'-UTR, complete ORF, and partial 3'-UTR. The five G boxes involved in GTP binding and the lipid modification site are indicated in bold plus underline. The font colors correspond to the colors of the domains in Fig. 2. 5. Asterisk indicates stop codon. The polyadenylation signal in the 3'-UTR is underlined.

```
            G1-Box                          G2-Box
Gl-Rheb : MPPKTRKVAVMGYRSVGKSSLCIQFVDGQFVDSYDPTIENTFTKKLKVRGQEY :  53
Cm-Rheb : MPPKDRKVAVMGYRSVGKSSLCIQFVDGQFVDSYDPTIENTFTKKLKVRGQEY :  53
Ha-Rheb : MPPKNRKVAVMGYRSVGKSSLCIQFVDGQFVDSYDPTIENTFTKKLKVRGQEY :  53
Dm-Rheb : MPTKERHIAMMGYRSVGKSSLCIQFVEGQFVDSYDPTIENTFTKIERVKSQDY :  53
Aa-Rheb : MPAKERNIAMMGYRSVGKSSLSIQFVEGQFVDSYDPTIENTFTKITRVNSTDY :  53
                    G3-Box
Gl-Rheb : GLELVDTAGQDEYSIFPAQYSMNIHGYVLVYSITSEKSFEVAQVIYDKILDVM : 106
Cm-Rheb : GLELVDTAGQDEYSIFPAQYSMNIHGYVLVYSITSEKSFEVAQVIYDKILDMM : 106
Ha-Rheb : GLELVDTAGQDEYSIFPAQYSMDIHGYVLVYSITSEKSFEVAQVIYDKILDMM : 106
Dm-Rheb : IVKLIDTAGQDEYSIFPVQYSMDYHGYVLVYSITSQKSFEVVKIIYEKLLDVM : 106
Aa-Rheb : EVKLVDTAGQDEYSIFPAQYSMDFHGYVLVYSITSQKSFEVIQIIYEKLLDVM : 106
          G4-Box                          G5-Box
Gl-Rheb : GKVTVPVVLVGNKNDLHLERVVSTDQGRRVADNWKAVFLETSAKEHEAVSDIF : 159
Cm-Rheb : GKVTVPVVLVGNKNDLHLERVVSTEQGRRLADQWKAAFLETSAKEHEAVNDIF : 159
Ha-Rheb : GKVTVPVVLVGNKNDLHMERVVSTDQARKVADTWKAVFLETSAKQHEAVSDIF : 159
Dm-Rheb : GKKYVPVVLVGNKIDLHQERTVSTEEGKKLAESWRAAFLETSAKQNESVGDIF : 159
Aa-Rheb : GKAYVPVVLVGNKTDLHQERAVSTEEGKKLAECWKAQFLETSAKQNESVADIF : 159

Gl-Rheb : TRAILEIEKADGNLPSGNGCSIS : 182
Cm-Rheb : TRAILEIERADGNLPPGSSCRIS : 182
Ha-Rheb : TRVILEIEKADGNSSPEGKCFIS : 182
Dm-Rheb : HQLLILIENENGNPQEKSGCLVS : 182
Aa-Rheb : HLLLQQIERDNGNTGEKSSCTIS : 182
```

Lipid Modification Site

Figure 2. 8. Multiple alignment of deduced amino acid sequences of Rheb proteins in three decapod crustacean species and two insect species. Abbreviations: Aa, *A. aegypti* (XP001659013); Cm, *C. maenas* (HM989970); Dm, *D. melanogaster* (NP730950); Gl, *G. lateralis* (HM989971); and Ha, *Homarus americanus* (HM989972). Amino acid residues that are identical or similar in all sequences are shaded in black; gray shading indicates identical or similar amino acids in most of the sequences. Dashes indicate gaps introduced to optimize the alignment. G boxes (G1-G5) and lipid modification (LM) site are indicated.

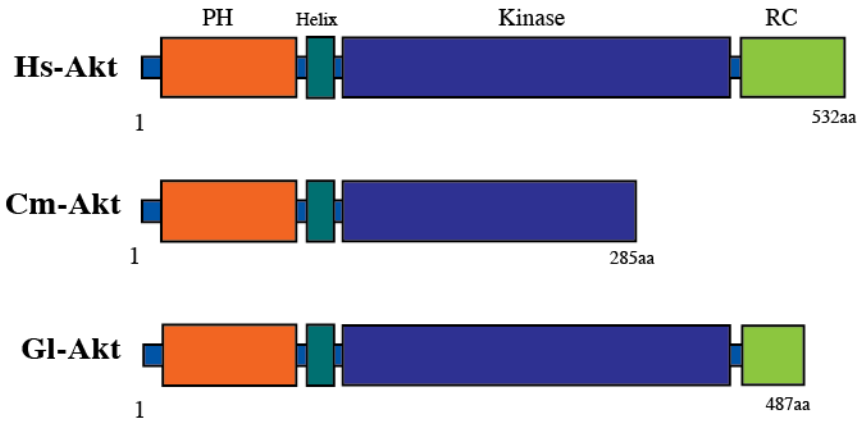

Figure 2. 9. Domain organization of Akt. The complete Akt protein from human (Hs-Akt) is compared to the partial Akt sequences from *G. lateralis* (Gl-Akt) and *C. maenas* (Cm-Akt). All have highly conserved pleckstrin homology (PH), helix, and kinase domains, indicated by orange, turquoise, and purple shading, respectively. The Gl-Akt has a portion of the regulatory C-terminal (RC) domain, indicated by green shading.

```
atggatgaggcagcaacccctcccaggcctaatattgtcaaggaaggctggctcaacaag 60
 M  D  E  A  A  T  P  P  R  P  N  I  V  K  E  G  W  L  N  K  20
cgtggggagcacatcaagaactggaggcagcgttactttttctccaggaggatggtaca 120
 R  G  E  H  I  K  N  W  R  Q  R  Y  F  F  L  Q  E  D  G  T  40
ctcttgggattcaagacaaagccagagcatggccttgaggacccactcaacaatttcaca 180
 L  L  G  F  K  T  K  P  E  H  G  L  E  D  P  L  N  N  F  T  60
gtgaagcgatgtcagatcctgaaaacagaaaggccacggccgaacacttttatcatccgt 240
 V  K  R  C  Q  I  L  K  T  E  R  P  R  P  N  T  F  I  I  R  80
ggacttcactggaccactgtcattgagagaacattcaatgctcagtcagcaagtgacagg 300
 G  L  H  W  T  T  V  I  E  R  T  F  N  A  Q  S  A  S  D  R  100
gaagaatggatggaagctatcaagcaggtgtctgagagaatatcagacaactcatcaggt 360
 E  E  W  M  E  A  I  K  Q  V  S  E  R  I  S  D  N  S  S  G  120
cgctgtgttgagatcaaggaggttgactcagtggagcacatccaactcaagtactccagc 420
 R  C  V  E  I  K  E  V  D  S  V  E  H  I  Q  L  K  Y  S  S  140
gatgatgatgatgactcacagggctcacggggcaccaagaagaagaggaaaattacactg 480
 D  D  D  D  D  S  Q  G  S  R  G  T  K  K  K  R  K  I  T  L  160
gacaactttgagttccttaaagtgttagggaaaggaacatttggtaaagttatcctctgt 540
 D  N  F  E  F  L  K  V  L  G  K  G  T  F  G  K  V  I  L  C  180
cgtgaaaagagtagcaaccatttctatgccatcaagatcttgcgtaaagatgtgatcatc 600
 R  E  K  S  S  N  H  F  Y  A  I  K  I  L  R  K  D  V  I  I  200
aagcgtgacgaggtggcccacacactcacagagaaccgggtcctgcaagtagtcgatcac 660
 K  R  D  E  V  A  H  T  L  T  E  N  R  V  L  Q  V  V  D  H  220
ccttttcttacttacctcaagtattccttccaaaccaatgaccgactctgcttcgtaatg 720
 P  F  L  T  Y  L  K  Y  S  F  Q  T  N  D  R  L  C  F  V  M  240
gagtacgtgaacggcggggaactgttcttccacctcaaccaggagcggatctttcctgag 780
 E  Y  V  N  G  G  E  L  F  F  H  L  N  Q  E  R  I  F  P  E  260
gaacgagccaggttctatggagcagaaatatgccttgcactgggttacttacacgaaaga 840
 E  R  A  R  F  Y  G  A  E  I  C  L  A  L  G  Y  L  H  E  R  280
aatattatctatcgtgatttgaagttagaaaaccttctactggatgctgatgggcacata 900
 N  I  I  Y  R  D  L  K  L  E  N  L  L  L  D  A  D  G  H  I  300
aaaattgctgactttgggctatgtaaggaagacatctcctacggctcaaccacccgaaca 960
 K  I  A  D  F  G  L  C  K  E  D  I  S  Y  G  S  T  T  R  T  320
ttctgtggcacaccagaatacttggccccagaggtgctagaagaaaatgactatgggcga 1020
 F  C  G  T  P  E  Y  L  A  P  E  V  L  E  E  N  D  Y  G  R  340
ggtgttgactggtggggctacggagtctgcttgtacgagatgatggttggccgcctcccc 1080
 G  V  D  W  W  G  Y  G  V  C  L  Y  E  M  M  V  G  R  L  P  360
ttctatgacaaggaccatgacaagttattccagctcattgtttgtgaagatgttcgcttc 1140
 F  Y  D  K  D  H  D  K  L  F  Q  L  I  V  C  E  D  V  R  F  380
ccaaggaccatctcccaggaggcccgtgaccttcttaagggtctgctgcacaaggatccc 1200
 P  R  T  I  S  Q  E  A  R  D  L  L  K  G  L  L  H  K  D  P  400
aacaagcgccttggagggggaccaggcgatgttgaagaggtccagagtcacccccttctac 1260
 N  K  R  L  G  G  G  P  G  D  V  E  E  V  Q  S  H  P  F  Y  420
attacaatcaactggaagctcttggaagagaagaagctcaccccacctttcaaaccccaa 1320
 I  T  I  N  W  K  L  L  E  E  K  K  L  T  P  P  F  K  P  Q  440
gtaacaagcgagacggacactcgctactttgaccgagagtttactggagagtctgtgcag 1380
 V  T  S  E  T  D  T  R  Y  F  D  R  E  F  T  G  E  S  V  Q  460
ctcacaccacctgatcaagtggaacacctcaattctattgctgaggaatcagaaaatgcg 1440
 L  T  P  P  D  Q  V  E  H  L  N  S  I  A  E  E  S  E  N  A  480
gctttcaatcaattttcatat                                         1461
 A  F  N  Q  F  S  Y                                          487
```

Fig. 2. 10. Nucleotide and amino acid sequences of cDNA encoding Gl-Akt. The cDNA encoded an incomplete ORF. The activation loop in the kinase domain indicated by blue. The font colors correspond to the colors of the domains in Fig. 2. 9.

```
atggatgaggcagcatcccctcccacccctgccattgttaaggaagggtggctcaacaaa 60
 M  D  E  A  A  S  P  P  T  P  A  I  V  K  E  G  W  L  N  K  20
cgtggggaacacattaaaaactggaggcagcgctacttctttcttcaagaagatggcacc 120
 R  G  E  H  I  K  N  W  R  Q  R  Y  F  F  L  Q  E  D  G  T  40
cttctgggatttaagacaaaaccagagcatggtcttgaagatccacttaacaattttaca 180
 L  L  G  F  K  T  K  P  E  H  G  L  E  D  P  L  N  N  F  T  60
gtgaagcaatgccagatcctgaaaacagaaagaccgcggccgaacactttcattatccga 240
 V  K  Q  C  Q  I  L  K  T  E  R  P  R  P  N  T  F  I  I  R  80
ggacttcattggacaactatcattgaaagaacctttaatgctcaatcggctagtgacagg 300
 G  L  H  W  T  T  I  I  E  R  T  F  N  A  Q  S  A  S  D  R  100
gaatcatggatggaagccatcaaacaggtgtctgagagaatatcagatactcaatcagat 360
 E  S  W  M  E  A  I  K  Q  V  S  E  R  I  S  D  T  Q  S  D  120
gagtgttttgagatccaggaggcgagtagaatgaaacaattacaactcaactactccagc 420
 E  C  F  E  I  Q  E  A  S  R  M  K  Q  L  Q  L  N  Y  S  S  140
gatgatgatgatacacccggtttgcgaggcaccaagaagaaaaggaaaattactttagat 480
 D  D  D  D  T  P  G  L  R  G  T  K  K  K  R  K  I  T  L  D  160
aactttgaatttcttaaagtgcttgggaaagggacgtttggaaaagttatcctgtgtcga 540
 N  F  E  F  L  K  V  L  G  K  G  T  F  G  K  V  I  L  C  R  180
gaaaaggtcagcaaccatttttacgctattaagatcctgcgtaaagatgtgattattgag 600
 E  K  V  S  N  H  F  Y  A  I  K  I  L  R  K  D  V  I  I  E  200
cgtgatgaggtggtccacacactcacagagaaccgggttctgcaggttgtagatcatccc 660
 R  D  E  V  V  H  T  L  T  E  N  R  V  L  Q  V  V  D  H  P  220
ttccttacttacctcaagtattccttccaaaccaacgatcgcctctgtttcgtgatggag 720
 F  L  T  Y  L  K  Y  S  F  Q  T  N  D  R  L  C  F  V  M  E  240
tatgtcaatggtggagaactatttttcatctcaccagggagcgcttcttccctgaagaa 780
 Y  V  N  G  G  E  L  F  F  H  L  T  R  E  R  F  F  P  E  E  260
cgagccagattttatggagcagaaatatgtcttgcattaggttatttacatgaaaaaaa 840
 R  A  R  F  Y  G  A  E  I  C  L  A  L  G  Y  L  H  E  K  K  280
aaaacctatagtgag                                              855
 K  T  Y  S  E                                               285
```

Figure 2. 11. Nucleotide and amino acid sequences of cDNA encoding Cm-Akt. The cDNA encoded an incomplete ORF. The font colors correspond to the colors of the domains in Fig. 2. 9.

```
                                                                  PHD
Cm-Akt :                    MDEAASPPTPAIVKEGWLNKRGEHIKNWRQRYFFLQEDGTLLGF :  44
Gl-Akt :                    MDEAATPPRPNIVKEGWLNKRGEHIKNWRQRYFFLQEDGTLLGF :  44
Dm-Akt :   MSINTTFDLSSPSVTSGHALTEQTQVVKEGWLMKRGEHIKNWRQRYFVLHSDGRLMGY :  58
Aa-Akt : MSSSDTTQPPAVPVTQPARVIQPSAALIVKEGWLYKRGEHIKNWRSRYFILRDDGTLVGY :  60
Dp-Akt :                   MAESVVPAKSPAIIKEGWLLKRGEHIKNWRQRYFVLQDDGSLLGF :  45

Cm-Akt : KTKP--EHGLEDP---LNNFTVKQCQILKTERPRPNTFIIRGLHWTTIIERTFNAQSASD :  99
Gl-Akt : KTKP--EHGLEDP---LNNFTVKRCQILKTERPRPNTFIIRGLHWTTVIERTFNAQSASD :  99
Dm-Akt : RSKP-ADSASTPSDFLLNNFTVRGCQIMTVDRPKPFTFIIRGLQWTTVIERTFAVESELE : 117
Aa-Akt : KNRPDASFQAEPS----NNFTVRGCQIMSVDRPRPFTFIIRGLQWTTVIERMFHVEEERE : 116
Dp-Akt : KHKPEPSIGLAEP---LNNFTVKGCQIMKADRPKPFTFHIRGLQWTTVIERTFHVESEKE : 102
                                                                  Helix
Cm-Akt : RESWMEAIKQVSERISDTQSD---ECFEIQEASRMKQLQLNYSSDDDD------------ : 144
Gl-Akt : REEWMEAIKQVSERISDNSSG---RCVEIKEVDSVEHIQLKYSSDDDDD----------- : 145
Dm-Akt : RQQWTEAIRNVSSRLIDVGE----VAMTPSEQTDMTDVDMATIAEDELS----------- : 162
Aa-Akt : RQEWVEAIRSVANRLTEA------EAYQGSQSNGDGDVEMASIAEDELLT---------- : 160
Dp-Akt : REEWMVAIEHVAARLHTDTDSTDVDMPAVSEENDLKNSSSPSSLSNKMVSSPMDSGNDEF : 162
                                                                  KD
Cm-Akt : --TPGLRGTK------KKRKITLDNFEFLKVLGKGTFGKVILCREKVSNHFYAIKILRKD : 196
Gl-Akt : --SQGSRGTK------KKRKITLDNFEFLKVLGKGTFGKVILCREKSSNHFYAIKILRKD : 197
Dm-Akt : -EQFSVQGT--TCNSSGVKKVTLENFEFLKVLGKGTFGKVILCREKATAKLYAIKILKKE : 219
Aa-Akt : -EKFSVQGTS-TGKISGRKKVTLENFEFLKVLGKGTFGKVILCREKTTAKLYAIKILKKE : 218
Dp-Akt : QMKFLITGTSNRPHHSGKKKVTLENFEFIKMLGKGTFGKVILCREKGTGHLFAIKILKKE : 222

Cm-Akt : VIIERDEVVHTLTENRVLQVVDHPFLTYLKYSFQTNDRLCFVMEYVNGGELFFHLTRERF : 256
Gl-Akt : VIIKRDEVAHTLTENRVLQVVDHPFLTYLKYSFQTNDRLCFVMEYVNGGELFFHLNQERI : 257
Dm-Akt : VIIQKDEVAHTLTESRVLKSTNHPFLISLKYSFQTNDRLCFVMQYVNGGELFWHLSHERI : 279
Aa-Akt : VIVQKDEVAHTMAENRVLKKTNHPFLISLKYSFQTVDRLCFVMQYVNGGELFFHLSRERV : 278
Dp-Akt : VIIAKDEVAHTLTENRVLQTTNHPFLIALKYSFQTAERLCFVMEYVNGGELFFHLSRERI : 282
                                                Activation Loop
Cm-Akt : FPEERARFYGAEICLALGYLHEKKKTYSE                                 : 285
Gl-Akt : FPEERARFYGAEICLALGYLHERNIIYRDLKLENLLLDADGHIKIADFGLCKEDISYGST : 317
Dm-Akt : FTEDRTRFYGAEIISALGYLHSQGIIYRDLKLENLLLDKDGHIKVADFGLCKEDITYGRT : 339
Aa-Akt : FSEDRTRFYGAEIISALGYLHSHEIVYRDLKLENLLLDKDGHIKIADFGLCKEQITYGRT : 338
Dp-Akt : FSEDRTRFYGAEIVSALGYLHEQGIIYRDLKLENLLLDKDGHIKIADFGLCKEDITYGRT : 342

Gl-Akt : TRTFCGTPEYLAPEVLEENDYGRGVDWWGYGVCLYEMMVGRLPFYDKDHDKLFQLIVCED : 377
Dm-Akt : TKTFCGTPEYLAPEVLDDNDYGQAVDWWGTGVVMYEMICGRLPFYNRDHDVLFTLILVEE : 399
Aa-Akt : TKTFCGTPEYLAPEVLEDNDYGLAVDWWGTGVVMYEMMCGRLPFYNRDHDILFTLILMEE : 398
Dp-Akt : TKTFCGTPEYLAPEVLEDNDYGRAVDWWGLGVVMYELMCGRLPFYDRDHDVLFERILLEE : 402

Gl-Akt : VRFPRTISQEARDLLKGLLHKDPNKRLGGGPGDVEEVQSHPFYITINWKLLEEKKLTPPF : 437
Dm-Akt : VKFPRNITDEAKNLLAGLLAKDPKKRLGGGKDDVKEIQAHPFFASINWTDLVLKKIPPPF : 459
Aa-Akt : VKFPRSISANARDLLAGLLMKQPRDRLGGGPNDVKEIMVHPFFSSINWTDLVQKRIAPPF : 458
Dp-Akt : VRFPRTLSQEAKELLGGLLAKDPQKRLGGGPEDYKEITQHPFFLPISWTDLEQRKIPPPF : 462
                                                                  RCD
Gl-Akt : K                                                             : 438
Dm-Akt : KPQVTSDTDTRYFDKEFTGESVELTPPDPTGPLGSIAEEP----LFPQFSYQGDMASTLG : 515
Aa-Akt : KPQVTSDTDTRYFDSEFTGESVELTPPDNNGPLGAVQEEP----HFSQFSYQ-DMASTLN : 513
Dp-Akt : KPQVVSETDTRYFESEFTGESVELTPPDP-GPLHSISEEVEPPCYFEKFSYCPEASSTLG : 521

Dm-Akt : TSSHISTSTSLASMQ : 530
Aa-Akt : TPSFINNPNSYVSMQ : 528
Dp-Akt : S----NTSLTHAALG : 532
```

Figure 2. 12. Multiple alignment of deduced amino acid sequences of Akt proteins in three crustacean species and two insect species. Abbreviations: Aa, *A. aegypti* (AAP37655); Cm, *C. maenas* (JQ864249); Dm, *D. melanogaster* (NP732114); Dp, *D. pulex* (EFX86288); and Gl, *G. lateralis* (HM989974). Amino acid residues that are identical or similar in all sequences are shaded in black; gray shading indicates identical or similar amino acids in most of the sequences. Dashes indicate gaps introduced to optimize the alignment and the boxes indicate highly conserved domains, including pleckstrin homology (PH) domain and activation loop in the kinase domain. The colors of the boxes correspond to the colors of the domains in Fig. 2. 9.

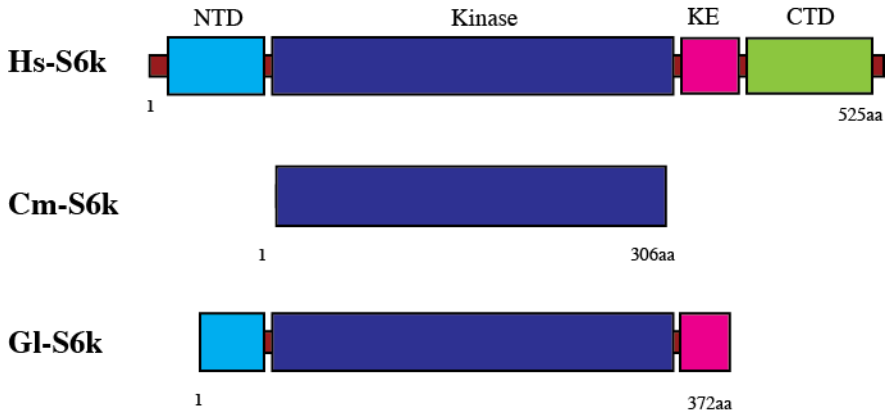

Figure 2. 13. Domain organization of S6k. The complete S6k protein from human (Hs-S6k) is compared to the partial S6k sequences from *G. lateralis* (Gl-S6k) and *C. maenas* (Cm-S6k). Both had the N-terminal domain (NTD) and kinase domain (KD), indicated by light blue and dark blue shading, respectively. The Gl-S6k had the kinase extension (KE) domain and a portion of the C-terminal domain (CTD), indicated by magenta and green shading. The Cm-S6k was shorter and contained a portion of the KE domain.

```
tatgaacaaggcccagatatgattgagaccttacagttgtcggacagtacagtcaaccca 60
 Y  E  Q  G  P  D  M  I  E  T  L  Q  L  S  D  S  T  V  N  P  20
ggcagggagaaggtgcgtccatcagactttcagctactgaaggttcttggaaagggcggt 120
 G  R  E  K  V  R  P  S  D  F  Q  L  L  K  V  L  G  K  G  G  40
tatggcaaggtctttcaggttagaaaaatgacaggaggtaggggaggagggaaaattttt 180
 Y  G  K  V  F  Q  V  R  K  M  T  G  G  R  G  G  G  K  I  F  60
gcaatgaaggtcctgaaaaaagctacaatagtacgtaaccagaaggacacagcgcacaca 240
 A  M  K  V  L  K  K  A  T  I  V  R  N  Q  K  D  T  A  H  T  80
aaggcagaaagaaacatccttgaagctgttaagcaccccttcattctggatttagtgtat 300
 K  A  E  R  N  I  L  E  A  V  K  H  P  F  I  L  D  L  V  Y  100
gctttccaaacgggtggtaagctatatctcatcctggagtacctctcaggtggggagctc 360
 A  F  Q  T  G  G  K  L  Y  L  I  L  E  Y  L  S  G  G  E  L  120
ttcatgcatctggaaagagagggaatattcatggaggacacagcttgtttttacatatct 420
 F  M  H  L  E  R  E  G  I  F  M  E  D  T  A  C  F  Y  I  S  140
gagattatactggctctggaacatcttcactctgagggcatcatctacagagacctgaag 480
 E  I  I  L  A  L  E  H  L  H  S  E  G  I  I  Y  R  D  L  K  160
cctgaaaatattctattagatgcttttggacatgtgaagctcacagactttggattatgc 540
 P  E  N  I  L  L  D  A  F  G  H  V  K  L  T  D  F  G  L  C  180
aaagaaaaaattcaggatgactctgtgacacacacattctgtggtaccattgagtacatg 600
 K  E  K  I  Q  D  D  S  V  T  H  T  F  C  G  T  I  E  Y  M  200
gcaccagagatactcacccgcacaggccatggtaaggcagtggactggtggtccctcgga 660
 A  P  E  I  L  T  R  T  G  H  G  K  A  V  D  W  W  S  L  G  220
gcactcatgtacgacatgttgacgggtgcgccgcctttcacagctgagaatcgcaagaag 720
 A  L  M  Y  D  M  L  T  G  A  P  P  F  T  A  E  N  R  K  K  240
accatagagaagatcctgaaggggaagctgaaccttccaccctacctgactcctgatgca 780
 T  I  E  K  I  L  K  G  K  L  N  L  P  P  Y  L  T  P  D  A  260
cgagacctcatccgcaaactgctcaagcgtcaagtcagccagcgattgggcagtgggcca 840
 R  D  L  I  R  K  L  L  K  R  Q  V  S  Q  R  L  G  S  G  P  280
gatgatggggagcccattaagaggcatcttttcttcaagctcattaactgggatgttatc 900
 D  D  G  E  P  I  K  R  H  L  F  F  K  L  I  N  W  D  V  I  300
aacagaaagctggacccccattcaagcctgttttgagtggtgatgatgatgtgagccaa 960
 N  R  K  L  D  P  P  F  K  P  V  L  S  G  D  D  D  V  S  Q  320
ttcgacagcaagttcaccaagcagacgccagttgactctcctgatgaccacatgctcagc 1020
 F  D  S  K  F  T  K  Q  T  P  V  D  S  P  D  D  H  M  L  S  340
gagagtgccaacatggtctttgaggggttcacatatgtggcaccatcagtgttagaggaa 1080
 E  S  A  N  M  V  F  E  G  F  T  Y  V  A  P  S  V  L  E  E  360
atggctcggccaagtgtggtgaaagcagaatctcca                         1116
 M  A  R  P  S  V  V  K  A  E  S  P                          372
```

Figure 2. 14. Nucleotide and amino acid sequences of cDNA encoding Gl-S6k. The activation loop in the kinase domain indicated by underlined orange. The font colors correspond to the colors of the domains in Fig. 2. 13.

```
cagaaaatgacaggaggcagaggaggtggcagtatctttgccatgaaggtcctgaaaaag 60
 Q  K  M  T  G  G  R  G  G  G  S  I  F  A  M  K  V  L  K  K  20
gctaccatagtacgtaaccaaaaggacacagcacacacaaaagctgaaagaaatatcctg 120
 A  T  I  V  R  N  Q  K  D  T  A  H  T  K  A  E  R  N  I  L  40
gaagctgtgaagcatccattcattgtggatctggtgtatgcatttcaaacgggtggcaag 180
 E  A  V  K  H  P  F  I  V  D  L  V  Y  A  F  Q  T  G  G  K  60
ttgtacctcatcttggagtacctgtccggtggtgagcttttcatgcacctggagagagag 240
 L  Y  L  I  L  E  Y  L  S  G  G  E  L  F  M  H  L  E  R  E  80
ggaatattcatggaggacacagcttgtttttacatatcggaaatcatactggctctggaa 300
 G  I  F  M  E  D  T  A  C  F  Y  I  S  E  I  I  L  A  L  E  100
catcttcattctgagggcatcatctacagagacttgaagccagaaaatatacttctggat 360
 H  L  H  S  E  G  I  I  Y  R  D  L  K  P  E  N  I  L  L  D  120
tcttatgggcatgtgaagctcacagattttggattatgcaaagaaaagattcaggatgac 420
 S  Y  G  H  V  K  L  T  D  F  G  L  C  K  E  K  I  Q  D  D  140
tcagtgactcataccttctgtggcaccattgagtacatggcacccgagatcctgacccgc 480
 S  V  T  H  T  F  C  G  T  I  E  Y  M  A  P  E  I  L  T  R  160
accggccatggcaaggcagtggactggtggtctcttggagcactcatgtatgacgtgttg 540
 T  G  H  G  K  A  V  D  W  W  S  L  G  A  L  M  Y  D  V  L  180
acgggggcgcctccatttacagctgaaaatcgaaagaagacaatagagaagattctaaag 600
 T  G  A  P  P  F  T  A  E  N  R  K  K  T  I  E  K  I  L  K  200
gggaagctgaacctgccaccttacttgacacctgattcacgagaccttatccgcaaactg 660
 G  K  L  N  L  P  P  Y  L  T  P  D  S  R  D  L  I  R  K  L  220
ctcaagcgtcaagttagtcaacgattgggcagcggctcagatgacggagaacccatcaag 720
 L  K  R  Q  V  S  Q  R  L  G  S  G  S  D  D  G  E  P  I  K  240
aggcatctgttcttcaaactcattaactgggatgaagttattaatcgcaagttggatcct 780
 R  H  L  F  F  K  L  I  N  W  D  E  V  I  N  R  K  L  D  P  260
ccattcaagccagtattgagtggtgatgatgatgtgagccagtttgacagcaagttcacc 840
 P  F  K  P  V  L  S  G  D  D  D  V  S  Q  F  D  S  K  F  T  280
aaacagacaccagtggactcccctgatgaccacacgctcagtgaaagtgccaatatcttg 900
 K  Q  T  P  V  D  S  P  D  D  H  T  L  S  E  S  A  N  I  L  300
ctgaaaaactcgagccat                                           918
 L  K  N  S  S  H                                            306
```

Figure 2. 15. **Nucleotide and amino acid sequences of cDNA encoding Cm-S6k.** The activation loop in the kinase domain indicated by underlined orange. The font colors correspond to the colors of the domains in Fig. 2. 13.

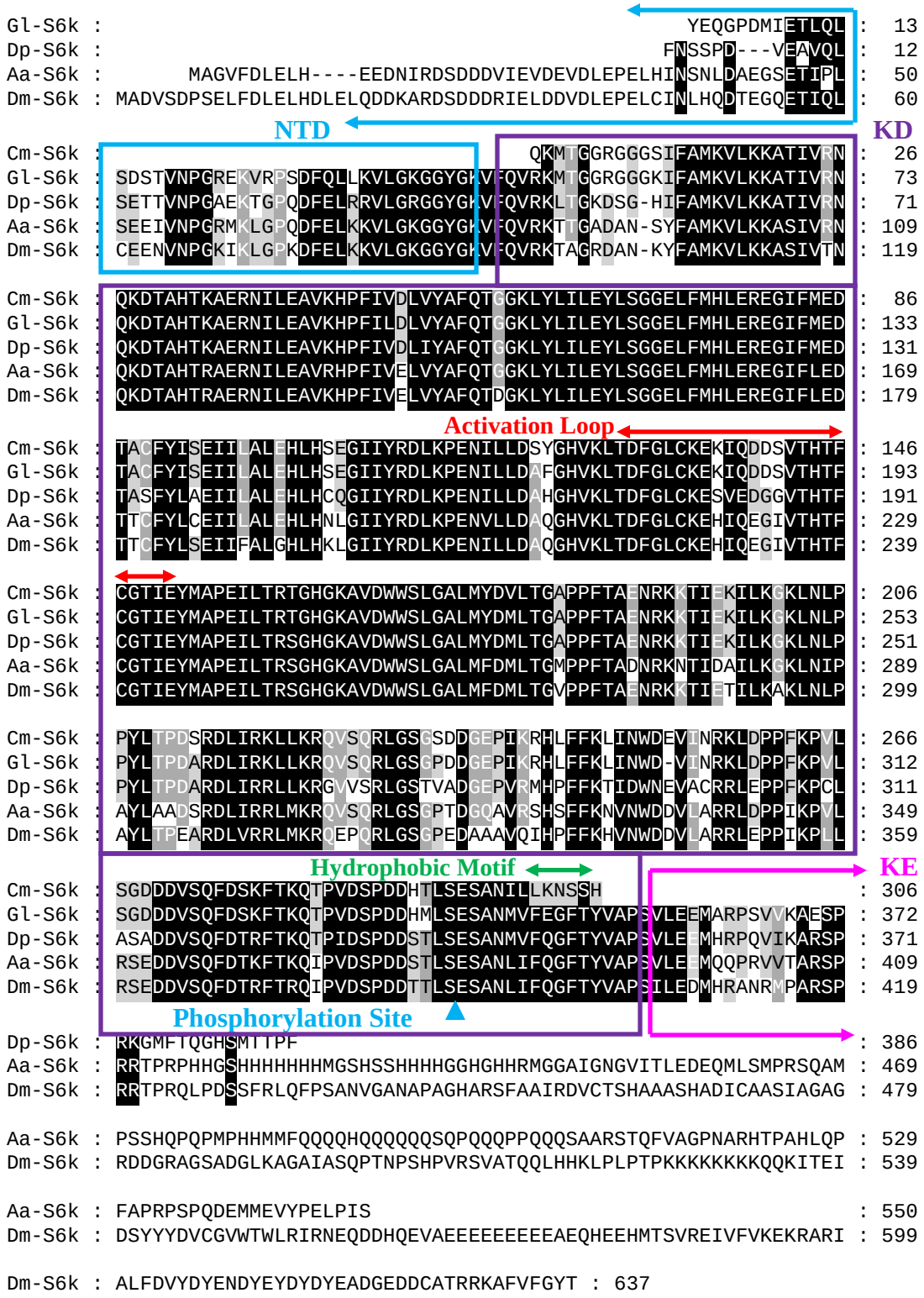

Figure 2. 16. Multiple alignment of deduced amino acid sequences of S6k proteins in three crustacean species and two insect species. Abbreviations: Aa, *A. aegypti* (XP001650653); Cm, *C. maenas* (JQ864250); Dm, *D. melanogaster* (AAC47429); Dp,. *D. pulxe* (EFX86042); and Gl,

G. lateralis (HM989975). Amino acid residues that are identical or similar in all sequences are shaded in black; gray shading indicates identical or similar amino acids in most of the sequences. Dashes indicate gaps introduced to optimize the alignment. The boxes indicate highly conserved domains including activation loop in the kinase domain and hydrophobic motif. The blue triangle indicates the phosphorylation site. The colors of the boxes correspond to the colors of the domains in Fig. 2. 13.

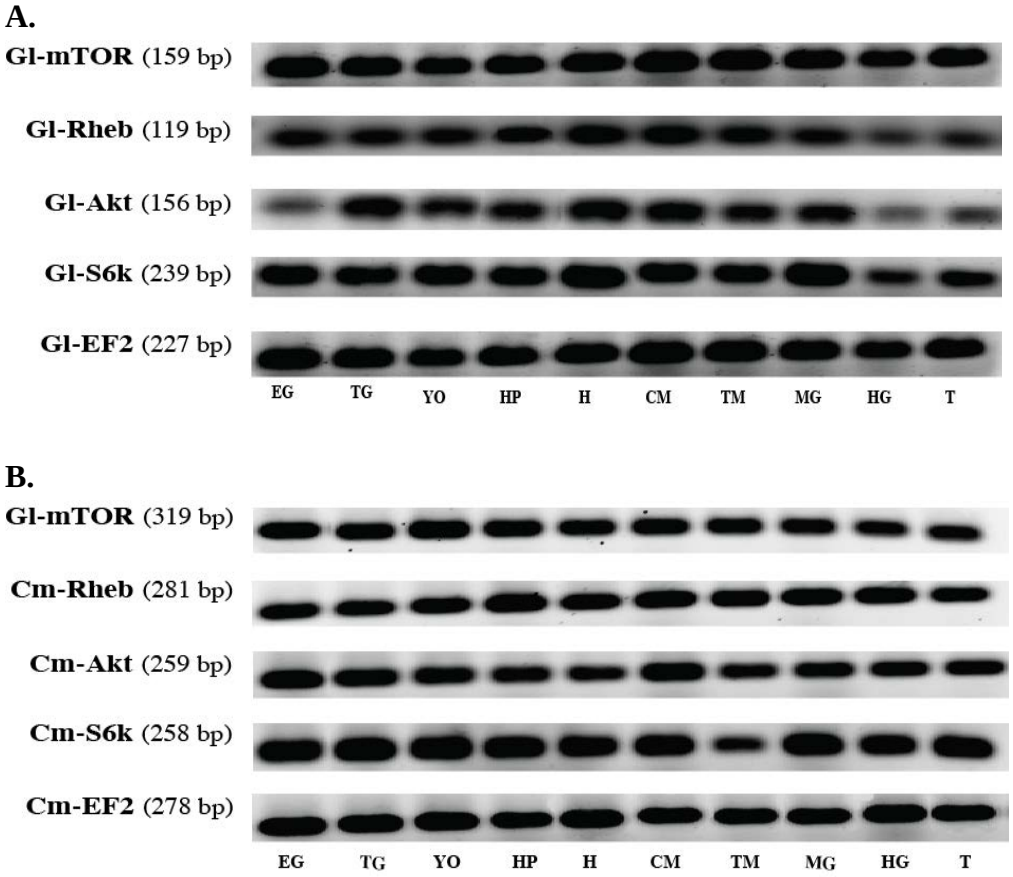

Figure 2. 17. Expression of EF2 and mTOR signaling components in *G. lateralis* (A) and *C. maenas* (B) tissues using endpoint RT-PCR. Elongation factor 2 (EF2) is a constitutively expressed gene that served as a control for RNA isolation and cDNA synthesis. PCR products after 30 cycles (EF2) or 35 cycles (mTOR, Rheb, Akt, and S6k) were resolved by agarose gel electrophoresis. Inverted images of ethidium bromide-stained gels are shown. Sizes of expected PCR products are indicated at left. All five genes were expressed in all tissues. Abbreviations, from left to right: EG, eyestalk ganglia; TG, thoracic ganglia; YO, Y-organ; HP, hepatopancreas; H, heart; CM, claw muscle; TM, thoracic muscle; MG, midgut; HG, hindgut; and T, testis.

CHAPTER THREE

ROLE OF MECHANISTIC TARGET OF RAPAMYCIN (mTOR) AND TGFB SIGNALING IN THE CRUSTACEAN Y-ORGAN DURING THE MOLT CYCLE

SUMMARY

Molting in decapod crustaceans is controlled by molt-inhibiting hormone (MIH), an eyestalk neuropeptide that suppresses production of ecdysteroids by a pair of molting glands (Y-organs or YOs). In the blackback land crab, *G. lateralis*, molting is induced by eyestalk ablation (ESA) or autotomy of 5 or more walking legs (multiple limb autotomy or MLA). The green crab *C. maenus* (both color morphs) were refractory to ESA and MLA, remaining in intermolt. The YO transitions through four physiological states during the molting cycle: "basal" state at postmolt and intermolt; "activated" state at early premolt (D_0); "committed" state at mid premolt ($D_{1, 2}$); and "repressed" state at late premolt ($D_{3,4}$). The basal to activated state transition is triggered by a transient reduction in MIH; the YOs hypertrophy, but remain sensitive to MIH, as premolt is suspended by MIH injection or by limb bud autotomy (LBA). Mechanistic Target of Rapamycin (mTOR), which controls global translation of mRNA into protein, appears to be involved in YO activation in early premolt. Rapamycin (1 μM) inhibited *C. maenas* and *G., lateralis* YO ecdysteroidogenesis *in vitro*. Injection of rapamycin (10 μM final) lowered hemolymph ecdysteroid titer in ES-ablated *G. lateralis*. At the activated to committed state transition, the animal becomes committed to molt, as the YO is less sensitive to MIH and premolt is not suspended by LBA. YO commitment involves a putative transforming growth factor-beta (TGFβ)-like factor. Injection of SB431542 (10 μM final), a TGFβ receptor antagonist, lowered

hemolymph ecdysteroid titers in 7 and 14 day post-ESA *G. lateralis*, but had no effect on ecdysteroid titers at 1 and 3 days post-ESA. Quantitative PCR data indicated that up-regulation of Gl-EF2 and mTOR may reflect an increase in protein synthetic capacity in the premolt YO. These data are consistent with the hypothesis that the activated YO synthesizes a required TGFβ-like factor for the mid-premolt transition and a sustained constitutive increase in ecdysteroid synthesis. MLA experiment showed upregulation of Gl-mTOR and Gl-EF2 activity that important for increasing translation of mRNA into protein. This increase in protein synthesis is necessary for increased ecdysteroid levels in circulating hemolymph

INTRODUCTION

Control of molting in crustaceans involves a complex interaction between the eyestalk neurosecretory center, which produces inhibitory neuropeptides (e.g., MIH), and a pair of molting glands (Y-organs or YOs) in the anterior cephalothorax. The YO goes through four physiological states during the molt cycle that are mediated by endocrine and autocrine factors. A reduction in MIH triggers the transition from the basal state in intermolt (C_4) to the activated state in early premolt (D_0); a putative TGFβ factor triggers the transition from the activated state to the committed state in mid premolt (D_{1-2}); and high ecdysteroids trigger the transition from the committed state to the repressed state in late premolt (D_{3-4}). In most decapods, including *G. lateralis*, molting is induced by ESA or MLA. YO ecdysteroidogenesis is inhibited by cycloheximide, an inhibitor of translation, but not actinomycin D, an inhibitor of transcription (Mattson and Spaziani, 1986).

The YO is a dynamic organ that changes over the molt cycle. MIH suppresses ecdysteroidogenesis by the YO during intermolt, but the YO becomes refractory to MIH by late premolt (Covi et al., 2010; Chang and Mykles, 2011). There is no reduction in MIH receptors

during intermolt or premolt (Webster, 1993), which suggests that the desensitization of MIH signaling is downstream from the receptor, possibly through changes in the levels and activities of phosphodiesterases (PDEs) and NO/cGMP signaling components. Increased PDE activity contributes to the reduced response to MIH by keeping intracellular cyclic nucleotides low (Nakatsuji et al., 2009; Chang and Mykles, 2011). In *G. lateralis* and *Carcinus maenas* YOs, expression of NOS and GC-Iβ is up-regulated in response to an acute and chronic withdrawal of MIH and other neuropeptides by ESA (Lee et al., 2007; McDonald et al., 2011). At the end of premolt there is a precipitous drop in hemolymph ecdysteroids within a few days of ecdysis (Skinner, 1985; Mykles, 2011). This drop appears to determine the timing of ecdysis, as artificially elevated ecdysteroid during late premolt delays ecdysis (Chang and Mykles, 2011). It is the result of two processes: an increase in ecdysteroid excretion and a decrease in YO ecdysteroid production. 20E inhibits YO ecdysteroidogenesis when injected into crayfish (Dell et al., 1999). RH-5849, a non-steroidal ecdysteroid agonist, inhibits ecdysteroid secretion by crayfish YOs *in vitro*. Both treatments produce significant reductions in ecdysteroidogenesis within 1 h, suggesting a non-genomic response mediated by G protein-coupled and/or membrane-associated ecdysteroid receptors (Srivastava et al., 2005; Schlattner et al., 2006). This inhibition lasts at least 24 h after a single 20E injection (Dell et al., 1999), which suggests that ecdysteroid may also affect gene expression.

mTOR is a protein kinase highly conserved among all metazoans; that controls protein synthesis. It functions as the major sensor for cellular growth regulation by nutrients, cellular energy status, oxygen level, and growth factors (Proud, 2009; Laplante and Sabatini, 2012). mTOR is crucial for cell growth, aging, development, reproduction, and metamorphosis in insects (Layalle et al., 2008; Maestro et al., 2009; Montagne et al., 2010). mTOR increases the

ecdysteroid biosynthetic capacity of the insect molting gland (prothoracic gland or PG). Nutrients and insulin-like peptides (ILPs) activate mTOR, which phosphorylates components of the protein synthetic machinery, such as p70-S6 kinase (S6k) and eIF4E-binding protein (4E-BP1) to increase translation of mRNA (Proud, 2009; Teleman, 2010). FK506-binding protein (FKBP12), complexes with rapamycin to inhibit mTOR (Camargo et al., 2012; Laplante and Sabatini, 2012). Binding of ILP to an insulin receptor activates a signal transduction cascade involving PI3K, PDK1, and Akt protein kinases (Teleman, 2010). mTORC1 is activated by the Rheb GTP. Rheb-GAP (TSC1/2) is inhibited when phosphorylated by Akt. ILP signaling prevents the hydrolysis of GTP by Rheb through the inhibition of Rheb-GAP, thus keeping mTOR in the active state (Teleman, 2010). The ILP/mTOR pathway controls PG size and ecdysteroidogenic capacity (Mirth and Shingleton, 2012). Over-expressing Rheb-GAP inhibits PG growth, and over-expressing PI3K, an upstream activator of Akt, stimulates PG growth (Mirth et al., 2005). In addition, PI3K and mTOR inhibitors block PTTH-induced increases in ecdysteroid secretion in the PG (Gu et al., 2011; Gu et al., 2012). mTOR, FKBP12, Rheb, Akt, and S6K are expressed in crustacean tissues, including YO and skeletal muscle (MacLea et al., 2012).

The transforming growth factor-β (TGFβ) superfamily of cytokines is mediated by Smad transcription factors that regulate genes through transcriptional activation or repression (Heldin and Moustakas, 2012; Xu et al., 2012). Our hypothesis indicates that the TGFβ-like factor activated YO synthesizes, which is required for the mid-premolt transition and a sustained constitutive increase in ecdysteroid synthesis. At mid premolt animals become committed to molt, which coincides with reduced sensitivity of the YO to MIH. We hypothesize that YO commitment requires a TGFβ factor acting through Activin receptor/Smad signaling, resulting in

sustained mTOR activation, up-regulation of ecdysteroid biosynthetic enzymes, and down-regulation of MIH signaling.

In this present study, the central hypothesis is that YO ecdysteroidogenesis requires up-regulation of mTOR signaling. MIH suppresses the mTOR pathway. YO commitment requires a TGFβ factor acting through Activin receptor/Smad signaling, resulting in sustained mTOR activation, up-regulation of ecdysteroid biosynthetic enzymes, and down-regulation of MIH signaling. We determined the effects molt induction by MLA and ESA on expression of EF2, mTOR, Rheb, Akt, and S6k in *G. lateralis* YO using qPCR. The effects of rapamycin, an inhibitor of mTOR, on YO ecdysteroidogenesis *in vivo* and *in vitro*, as well as on the expression of mTOR signaling components were determined. The effects of Activin receptor antagonist SB431542 on hemolymph ecdysteroid levels and expression of mTOR signaling components in *G. lateralis* YO. We also quantified effects of ESA and molt stage on the expression of mTOR components in the *C. maenus* YO.

MATERIALS AND METHODS

Animals and molt induction

Adult land crabs *G. lateralis* were collected in the Dominican Republic and shipped via commercial air cargo to Colorado, USA. Animals were maintained at 27 ºC in 75-90% relative humidity with intermolt individuals kept in communal plastic cages lined with aspen bedding wetted with 5 p.p.t. Instant Ocean (Aquarium Systems, Mentor, OH). The crab environmental chamber was maintained in 12 h:12 h light:dark cycle with twice-weekly animal feedings of carrots, iceberg lettuce, and raisins (Covi et al. 2010). These crabs molt approximately once a year. Green shore crabs *C. maenas* were collected from the harbor at Bodega Bay, California.

They were maintained under ambient conditions in the facilities of Bodega Marine laboratory or were shipped to Colorado. In Colorado, animals were kept in aerated 30 ppt Instant Ocean at 20 °C and fed cooked chicken liver twice a week. Instant Ocean was changed twice a week (or more if water became cloudy or there was a death in the cage) (Lee et al., 2007).

Molting is easily manipulated in *G. lateralis*. Experiments used two methods to induce molting: ES ablation (ESA) and multiple leg autotomy (MLA). MLA resembles "natural" molting, as animals take 3-6 weeks to form basal regenerates before entering premolt and successfully completing ecdysis. ESA is an effective and convenient method, as the XO/SG complex is the sole source of MIH (Skinner, 1985). It also is the primary source of other neuropeptides that may directly or indirectly affect the YO (Lacombe et al., 1999; Chang, 2001). The major advantage is that ESA provides a precise reference point for YO activation. In *G. lateralis*, hemolymph titers increase by 1 day post-ESA (Lee et al., 2007). Animals enter premolt immediately, but do not successfully complete ecdysis (Covi et al. 2010). Regenerating limbs provide an external measure of the progress of premolt events in *G. lateralis*. This measure is defined as the R index (calculated as the length of the regenerate x 100/carapace width), which increases from 0 to ~23 prior to ecdysis (Skinner and Graham, 1972; Yu et al., 2002). Limb regeneration occurs in two phases: (1) basal growth, which forms a small differentiated LB (R index 8-10), occurs during intermolt and requires low levels of ecdysteroids; (2) proecdysial growth occurs during premolt and requires high levels of ecdysteroids (Hopkins, 2001; Yu et al., 2002). Molt stage is determined by a combination of hemolymph ecdysteroid titer, R index, and integumentary structure (membranous layer and setal development in maxillae) (Moriyasu and Mallet, 1986).

Effects of molting on mTOR signaling expression in the YO

Molting was induced by MLA in *G. lateralis*. Animals were divided into three premolt stages (early premolt, R ~10; mid-premolt, R ~15; and late premolt, R ~22) and two postmolt stages (2 days and 10 days postmolt). Hemolymph samples were collected for ecdysteroid titers using ELISA (Nimitkul et al., 2010; see Chapter 4) and YOs were harvested for qPCR. *C. maenus* were refractory to MLA (see Chapter 4). Instead, animals at various molt stages (intermolt, early premolt, late premolt and postmolt) were collected during the spring molting season in Bodega harbor. Hemolymph samples were collected for measuring ecdysteroid titers and YOs were harvested for qPCR.

Effects of ESA, SB431542, and rapamycin on YO ecdysteroidogenesis and gene expression

The effects of SB431542 were determined *in vivo*. Intact intermolt and ES-ablated *G. lateralis* were injected with SB431542 (~10 µM estimated final hemolymph concentration) or vehicle (DMSO, ~1% final concentration) at Day 0 (mass ×0.3µl= amount to inject). Hemolymph samples were taken and YOs were harvested at 0, 1, 3, 7, and 14 days post-injection. Hemolymph ecdysteroid was quantified by ELISA.

The effects of rapamycin were determined *in vivo* and *in vitro*. *G. lateralis* were ES-ablated and injected with vehicle (~1% DMSO final concentration) or rapamycin (~10 µM final concentration) at Day 0 (mass ×0.3µl= amount to inject). Hemolymph samples were taken and YOs were harvested at 0, 1, 3, 7, and 14 days post-injection. For the *in vitro* study, paired YOs from 3 day post-ESA *G. lateralis* and *C. maenas* were incubated with rapamycin or 1% DMSO for 4.5 h. As the paired YOs from the same animal have similar rates of secretion, one YO serves as the control and the other as the experimental treatment. Ecdysteroids secreted into the culture medium were quantified by ELISA (Nimitkul et al., 2010).

Adult intermolt *C. maenus* (both red and green color morphs) were ES-ablated. Hemolymph samples were taken and YOs were harvested at 0, 7, and 14 days post-ESA.

RNA purification, cDNA synthesis and quantitative real-time RT-PCR

Tissues were flash-frozen in liquid nitrogen and stored at -80 ˚C. Total RNA was isolated from crab tissues using TRIzol reagent (Life Technologies, Carlsbad, CA) as described previously (Covi et al., 2010). Briefly, tissues (YOs) (50-200 mg) were homogenized in 1 ml TRIzol and centrifuged at 12,000 xg for 15 min at 4 ºC. Supernatants were phenol-chloroform extracted and RNA in the aqueous phase was precipitated using isopropanol (0.75 ml per 1 ml TRIzol reagent). RNA was treated with DNase I (Life Technologies), extracted twice with phenol:chloroform:isoamyl alcohol (25:24:1), precipitated with isopropanol, washed twice with 70% ethanol in DEPC water, and resuspended in nuclease-free water. First-strand cDNA was synthesized using 2 µg total RNA in a 20 µl total reaction with SuperScript III reverse transcriptase (Life Technologies) and oligo-dT(20)VN primer (50 µmol/l; IDT, Coralville, IA) as described (Covi et al., 2010). RNA was treated with RNase H (Fisher Scientific, Pittsburgh, PA) and stored at -80 ºC.

A LightCycler 480 thermal cycler (Roche Applied Science, Indianapolis, IN) was used to quantify levels of EF2, mTOR, Rheb, Akt and S6k mRNAs for *G. lateralis* and *C. maenas*. Reactions consisted of 1 µl first strand cDNA or standard, 5 µl 2× SYBR Green I Master mix (Roche Applied Science), 0.5 µl each of 10 mM forward and reverse primers (Table 1), and 3 µl nuclease-free water. PCR conditions were as follows: an initial denaturation at 95 ºC for 5 min, followed by 45 cycles of denaturation at 95 ºC for 10 s, annealing at 62 ºC for 20 s, and extensions at 72 ºC for 20 s, followed by melting curve analysis of the PCR product. Transcript concentrations were determined with the LightCycler 480 software (Roche, version 1.5) using a

series of dsDNA gene standards produced by serial dilutions of PCR product for each gene (10 ag/μl^{-1} to 10 ng/μl^{-1}). The absolute amounts of transcript in copy numbers per µg of total RNA in the cDNA synthesis reaction were calculated based on the standard curve and the calculated molecular weight of dsDNA products.

Statistical analyses and software

Statistical analysis was performed using JMP 5.1.2, 6.0.0, or 8.0.2 (SAS Institute, Cary, NC). Group variances were analyzed using a Brown-Forsythe test and found to be equal ($P < 0.05$). Means for different developmental stages and treatments were compared using analysis of variance (ANOVA). All data not plotted as individual points are represented as mean ± 1 S.E. and the level of significance for the all the data analyses was set at $\alpha = 0.05$. All qPCR data was log transformed to reduce the variance of the mean. The data were performed using Excel 2010 (Microsoft, Redmond, WA) and JMP. Excel 2010 (Microsoft, Redmond, WA) was used for constructing/annotating graphs and figures.

RESULTS

Effects of molting on expression of mTOR signaling components

G. lateralis were multiple leg autotomized and entered premolt a few weeks later. Molt stage was monitored by measuring the R index. The ecdysteroid titers in the hemolymph were low during early premolt; titers increased in mid-premolt and reached a peak in late premolt (Fig. 3. 1A). Ecdysteroid titers were lowest at 2 days and 10 days postmolt, indicating that the YOs had returned to the basal state (Fig. 3. 1A).

There were significant effects of molting on *Gl-EF2*, *Gl-mTOR*, and *Gl-Akt* expression in the *G. lateralis* YO. Gl-EF2 mRNA level increased during premolt, with the mean at late premolt

(R ~22) significantly higher than the mean at early premolt (R ~10) (Fig. 3. 1B). There was a significant decrease in Gl-EF2 mRNA levels at 2 and 10 days postmolt to levels that were not significantly different from the Gl-EF2 level at early premolt (Fig. 3. 1B). Gl-mTOR expression was elevated during premolt, with the means at early, mid, and late premolt not significantly different from each other (Fig. 3. 1C). Gl-mTOR mRNA levels decreased during postmolt, with the mean at 10 days postmolt significantly different from the means at mid and late premolt (Fig. 3. 1C). Gl-Akt mRNA levels increased during premolt, with the means at mid and late premolt significantly higher than the mean at early premolt (Fig. 3. 1E). There was a significant decrease at 2 days postmolt, with the means at 2 and 10 days postmolt not significantly different from the mean at early premolt (Fig. 3. 1E). There was no significant effect of molting on the expression of *Gl-Rheb* (Fig. 3. 1 D) and *Gl- S6k* (Fig. 3. 1 F).

As adult *C. maenas* are refractory to molt induction by ESA or MLA (see Chapter 4), gene expression in the YOs of animals (green morphs) undergoing natural molts was quantified. Crabs were collected during the spring molting season in Bodega harbor. The hemolymph ecdysteroid titers showed the characteristic pattern over the molt cycle: low levels during intermolt, increasing levels during premolt, and lowest levels during postmolt (Fig. 3. 2A). The YOs from these same animals were used to quantify *Cm-mTOR*, *Cm-Rheb*, *Cm-Akt*, *Cm-S6k*, and *Cm-EF2* expression. The postmolt stage was not quantified, as the RNA concentrations obtained from YOs from postmolt animals were too low for cDNA synthesis. Unlike *G. lateralis*, there was no effect of molting on the expression of *Cm-EF2* and mTOR signaling components. There were no significant differences in the means of the five mRNAs between intermolt, early premolt, and late premolt stages (Fig. 3. 2B).

Effects SB431542 on YO ecdysteroidgenesis and gene expression in G. lateralis in vivo

Intermolt intact and ES-ablated animals were injected with SB431542 dissolved in DMSO or DMSO alone at Day 0. ES-ablated animals injected with DMSO at Day 0 showed a significant increase in hemolymph ecdysteroid titers (Fig. 3. 3A). Intact animals injected with vehicle alone (DMSO) or SB431542 had no effect (Fig. 3. 3A). ESA animals injected with SB431542 showed a significant increase in hemolymph ecdysteroid titer that paralleled the control animals at Day 1 and Day 3 post-ESA. However SB431542 significantly decreased the hemolymph ecdysteroid titers at Day 7 and Day 14 post-ESA. ESA animals transition from the activated to the committed state around Day 7 (Covi et al., 2010).

SB431542 blunted the effects of ESA on the expression of *Gl-EF2*, *Gl-mTOR*, and *Gl-Akt*, but not *Gl-Rheb* and *Gl-S6k*. In controls, there were significant increases in the expression of *Gl-EF2*, *Gl-mTOR*, *Gl-Rheb*, *Gl-Akt*, and *Gl-S6k* by 3 days post-ESA and decreases by 14 days post-ESA (Fig. 3. 3B-F). By contrast, gene expression in YOs from SB431542-injected animals either did not change (*Gl-EF2*, *Gl-Rheb*, and *Gl-S6k*) or decreased (*Gl-mTOR* and *Gl-Akt*) by 3 days post-ESA (Fig. 3. 3B-F). The expression levels between control and experimental treatments converged at 14 days post-ESA for all five genes (Fig. 3. 3B-F). *Gl-EF2* mRNA level showed a significant increase from 1 day post-ESA to 3 and 7 days post-ESA in control animals, while the *Gl-EF2* mRNA level did not increase in the experimental animals (Fig. 3. 3B). The means of the control animals were significantly greater than the means of the experimental animals at 3 and 7 days post-ESA (Fig. 3. 3B).

Expression of *Gl-mTOR* mRNA increased significantly at 3 and 7 days post-ESA in controls, when compared with day 0 (Fig. 3. 3C). The *Gl-mTOR* mRNA level decreased significantly from 7 days to 14 days post-ESA in controls (Fig. 3. 3C). The means of the control

and experimental treatments were significantly different at 3 and 7 days post-ESA (Fig. 3. 3C). *Gl-Rheb* mRNA level in control animals increased significantly at 3 days post-ESA and decreased significantly by 14 days post-ESA (Fig. 3. 3D). However, there were no significant differences in the means between control and experimental treatments, indicating that SB431542 had no effect on Gl-Rheb expression (Fig. 3. 3D). There was as small, but significant, increase in *Gl-Akt* expression in control animals at 3 days post-ESA (Fig. 3. 3E). In the experimental treatment, there were significant decreases in *Gl-Akt* mRNA levels at 3 and 7 days post-ESA and the difference of the means between control and experimental treatments at Day 3 were statistically significant (Fig. 3. 3E). *Gl-S6k* mRNA level in control animals increased significantly from 0 to 3 days post-ESA, which decreased to Day 0 levels at 7 and 14 days post-ESA (Fig. 3. 3F). There were no significant differences between the means of the control and experimental treatments at all time points, indicating that SB431542 had no effect on *Gl-S6k* expression in the YO (Fig. 3. 3F).

Effects of rapamycin on YO ecdysteroidgenesis in vitro and in vivo

Rapamycin, an mTOR inhibitor, is a potent inhibitor of YO ecdysteroidogenesis *in vivo* and *in vitro*. Injection of rapamycin into ES-ablated *G. lateralis* significantly lowered hemolymph ecdysteroid titers 1 through 14 days post-injection (Fig. 3. 4A). *In vitro*, YOs from *G. lateralis* and *C. maenas* showed a dose-dependent inhibiton by rapamycin, with maximum inhibition of ecdysteroid secretion (70% and 85%, respectively) at 1 μM (Fig. 3. 4B).

Effects of ESA on hemolymph ecdysteroid levels and gene expression in C. maenas

In *C. maenas*, ESA had little effect on hemolymph ecdysteroid titer and no effect on expression of mTOR signaling components. There were no differences between green and red morphs (Fig. 3. 5). Hemolymph ecdysteroid levels remained low, although there was a

significant decrease in hemolymph ecdysteroid level at 7 days and 14 days post-ESA in both color morphs (Fig. 3. 5A). There was no significant effect of ESA on the expression of Cm-mTOR, Cm-Rheb, Cm-Akt, Cm-S6k and Cm-EF2 in red morphs (Fig. 3. 5B) and green morphs (Fig. 3. 5C).

DISCUSSION

The highly conserved insulin/IGF/mTOR signaling pathway is found in all metazoans and has an important role as a nutrient sensor (Proud, 2009) critical for growth and development in insects (Hietakangas and Cohen, 2009; Layalle et al., 2008; Maestro et al., 2009; Montagne et al., 2009; Walkiewicz and Stern, 2009) and other invertebrates (Soulard et al., 2009). Before undertaking this project, it was not clear whether components of this pathway would be regulated during the molt cycle of crustaceans as is the case in insects (Song and Gilbert, 1994), although study of *Artemia* spp. did demonstrate the increased expression of p70S6 kinase in emergence from quiescence (Santiago and Sturgill, 2001; Malarkey et al., 1998).

Induction of molting by multiple limb autotomy showed increase in hemolymph ecdysteroids (Fig. 3. 1A). In this experiment, the expression of *Gl-EF2*, *Gl-mTOR* and *Gl-Akt* mRNA (Fig. 3. 1B, C, E) increased during premolt and peaked at late premolt, followed by a return to intact levels in postmolt. The expression patterns of *Gl-Rheb* and *Gl-S6k* (Fig. 3. 1D, F) were similar to each other. There was a trend in an increase in the expression of each gene by $R = 22$, but the changes were not significant. We conclude that molting induced by MLA increases the expression of Gl-EF2, Gl-mTOR, and Gl-Akt, but has no effect on the expression of Gl-Rheb and Gl-S6k.

This observed up-regulation of mTOR activity and its well understood downstream effectors of p70 S6 kinase and 4E-BP1, are important for increasing translation of mRNA into protein

(Proud, 2009). Our data indicate that we have identified at least part of the mechanism by which this overall (non-specific) increase in protein synthesis occurs (Covi et al., 2010). This increase in protein synthesis is necessary for increased ecdysteroid levels in circulating hemolymph (Mykles and Skinner, 1982a; Mykles, 1999). How exactly ecdysteroid titers are mediating this process is a key area of investigation. The previous analysis (Covi et al., 2010) and these data, taken together, allow us to correlate levels of ecdysteroid with expression of mTOR components.

The changes observed in mTOR signaling components in YOs may be only one important aspect of mTOR regulation during molting. Development of *Drosophila* larvae is mediated by mTOR signaling in the prothoracic gland (PG), a gland in insects that secretes ecdysone and is homologous to the YO in crustaceans (McNeill et al., 2008; Layalle et al., 2008). The mTOR-dependent ecdysone secretion of the PG in fruit flies in response to nutrient/energy-dependent signals is important for the transition from larva to pupa (Layalle, et al., 2008). Similarly, caste development of the honeybee, *Apis mellifera*, is also dependent on mTOR signaling, as royal jelly is unable to cause development of queen bees in its absence (Patel et al., 2007). In crustacean YO, induction of molting by methods including MLA result in activation of the gland and increased ecdysteroid levels (Fig. 3. 1A). The activation of the YO involves up-regulation of ecdysteroid synthetic genes (Mykles, 2010), and also affects synthesis of other genes such as nitric oxide synthase and guanylyl cyclases (McDonald et al., 2011).

Eyestalk ablation (ESA) was used to examine the mTOR pathway transcriptional response of land crab *G. lateralis* in the intermolt phase of the molt cycle to activation of the YOs. We observed that ESA resulted in large increases in hemolymph ecdysteroid concentrations (Fig. 3. 3A). Injecting ES-ablated land crabs with SB431542, an antagonist of the Activin RII receptor, caused a ~65% decrease in hemolymph ecdysteroid titers at 7 days post-injection (Fig. 3. 3A).

The Day 7 time point is especially significant, as this is the time when ESA animals transition from D_0 to D_1 and become committed to molt (Covi et al., 2010). The TGFβ superfamily is not necessary for YO activation, as the titers in ESA animals ± SB431542 were the same at 1 and 3 days post-injection. The expression of *Gl-EF2*, *Gl-mTOR* and *Gl-Akt* in the group that were eyestalk ablated and injected with SB431542 showed a significant decrease with respect to control animals at 3 and 7 days post-injection for *Gl-EF2* and *Gl-mTOR* and at 3 days post-injection for *Gl-Akt* (Fig. 3. 3B, C, D). As EF2 is a constitutively expressed gene essential for mRNA translation, the up-regulation of *Gl-EF2* may reflect a large increase in protein synthetic capacity in the premolt YO.

Taken together, the data are consistent with the model presented in Chapter 1 (Figs. 4-6). mTOR-dependent protein synthesis is required for activation of the YO at the onset of premolt, as rapamycin inhibited YO ecdysteroidogenesis *in vivo* and *in vitro*. Moreover, molt induction by MLA and ESA up-regulates components of the mTOR signaling pathway. Once activated, the YO synthesizes and secretes a TGFβ-like factor, which is required for the mid-premolt transition to the committed state and a sustained mTOR-dependent constitutive increase in ecdysteroid synthesis. This is supported by the prolonged effect of a rapamycin injection (Fig.3. 4A) and the delayed effect of SB431542 injection into ES-ablated animals (Fig. 3. 3A). These results are highly significant, as they provide the first evidence that an Activin-like TGFβ factor is involved in regulating YO ecdysteroidogenesis in crustaceans.

Recent work indicates that a similar mechanism operates in the insect PG. Loss of Activin signaling by RNAi knockdown of Type I receptor, Type II receptor, Co-Smad, or R-Smad prevents the PTTH-induced ecdysteroid peak that triggers metamorphosis in *Drosophila* (Gibbens, 2011). Over-expression of ligand or Activin I receptor causes precocious pupariation

(Gibbens, 2011). mRNA levels of PTTH receptor, insulin receptor, and Halloween genes are decreased in the PG of dSmad2 RNAi larvae (Gibbens, 2011), indicating that TGFβ/Smad signaling is required for PTTH-dependent stimulation of PG ecdysteroidogenesis.

Green crab *C. maenas* and land crab *G. lateralis* differed in their response to ESA. *G. lateralis* soon entered premolt and proceed to ecdysis, although most do not successfully molt; this corresponds to increasing ecdysteroid level that reached a peak by the end of late premolt (Fig. 3. 3A) (Covi et al., 2010). ESA did not have any effect on *C. maenus* mTOR signaling components expression nor was there any increase in hemolymph ecdysteroid levels (Fig. 3. 5). These data suggest that both red and green morphs are resistant to ESA. This is examined in Chapter 4.

Adult green crabs (green morphs) captured during late winter and early spring underwent spontaneous molting. YOs were harvested from animals at intermolt, early premolt, late premolt and postmolt stages. Molt stage had no significant effect on the expression of *Cm-mTOR*, *Cm-Rheb*, *Cm-Akt*, *Cm-S6k* and *Cm-EF2* (Fig. 3. 2B), suggesting that increased expression of mTOR signaling components is not required for YO ecdysteroidogenesis in *C. maenas*.

CONCLUSIONS

In the blackback land crabs *G. lateralis*, molting is induced by eyestalk ablation (ESA) or autotomy of 5 or more walking legs (multiple leg autotomy, MLA). mTOR, which controls translation of mRNA into protein, appears to be involved in YO activation in early premolt, as rapamycin inhibits YO ecdysteroidogenesis *in vitro* and *in vivo*. At the activated to committed state transition, the animal becomes committed to molt, as the YO is less sensitive to MIH and premolt is not suspended by LBA. YO commitment involves a putative TGFβ-like factor.

Activin receptor antagonist SB431542 causes a delayed decrease in hemolymph titer in ESA animals at the time animals transition from D_0 to D_1. This suggests that the transition to molt commitment requires activation of Activin/Smad signaling by a TGFβ factor, which up-regulates mTOR and Halloween genes (e.g., Phm) and down-regulates MIH signaling. Quantitative PCR data indicated up-regulation of Gl-EF2 and mTOR that may reflect an increase in protein synthetic capacity in the premolt YO. These data are consistent with the hypothesis that the activated YO synthesizes a TGFβ-like factor for the mid-premolt transition and a sustained constitutive increase in ecdysteroid synthesis that is mTOR-dependent. These results provide the first evidence that an Activin-like TGFβ is involved in regulating YO ecdysteroidogenesis. Unlike *G. lateralis*, molting had no effect on expression of *Cm-mTOR*, *Cm-Rheb*, *Cm-Akt*, and *Cm-S6k*, suggesting that up-regulation of mTOR signaling is not necessary for YO ecdysteroidogenesis in *C. maenas*. Experiments are planned to determine the effects of rapamycin and SB431542 injection on hemolymph ecdysteroid titers in molting green crabs.

Table 3. 1. Oligonucleotide primers used in the expression analysis (qPCR) of mTOR signaling components from *G. lateralis* (Gl) and *C. maenas* (Cm). Abbreviations: F, forward; R, reverse; EF2, elongation factor 2; mTOR, mechanistic Target of Rapamycin; Rheb, Ras homolog expressed in brain; Akt, protein kinase B; S6k, p70 S6 kinase.

Primer	Sequence (5'-3')	Product Size (bp)	Annealing Temperature
Gl-EF2 F1	TTCTATGCCTTTGGCCGTGTCTTCTC	227	62ºC
Gl-EF2 R1	ATGGTGCCCGTCTTAACCA		62ºC
Gl-mTOR F2	AGAAGATCCTGCTGAACATCGAG	159	62ºC
Gl-mTOR R2	AGGAGGGACTCTTGAACCACAG		62ºC
Gl-Rheb F1	TTTGTGGACAGCTATGATCCC	119	62ºC
Gl-Rheb R1	AAGATGCTATACTCATCCTGACC		62ºC
Gl-Akt F2	AACTCAAGTACTCCAGCGATGATG	156	62ºC
Gl-Akt R1	GGTTGCTACTCTTTTCACGACAGA		62ºC
Gl-s6k F2	GGACATGTGAAGCTCACAGACTTT	239	62ºC
Gl-s6k R1	TTCCCCTTCAGGATCTTCTCTATG		62ºC
Cm-EF2 F1	CCATCAAGAGCTCCGACAATGAGCG	278	62ºC
Cm-EF2 R1	CATTTCGGCACGGTACTTCTGAGCG		62ºC
Cm-mTOR F2	CATCCCTCAAACCTCATGCT	319	62ºC
Cm-mTOR R2	CACCCACCACAGAACGCTTT		62ºC
Cm-Rheb F2	ATGGGCAAAGTCACAGTTCC	281	62ºC
Cm-Rheb R2	GTCAGGAAGATGGTGGCAAT		62ºC
Cm-Akt F1	GTGAAGCAATGCCAGATCCT	259	62ºC
Cm-Akt R2	CGGGTGTATCATCATCATCG		62ºC
Cm-s6k F2	TCTCCGTCATCTGAGCCGCT	258	62ºC
Cm-s6k R2	GTACATGGCACCCGAGATCC		62ºC

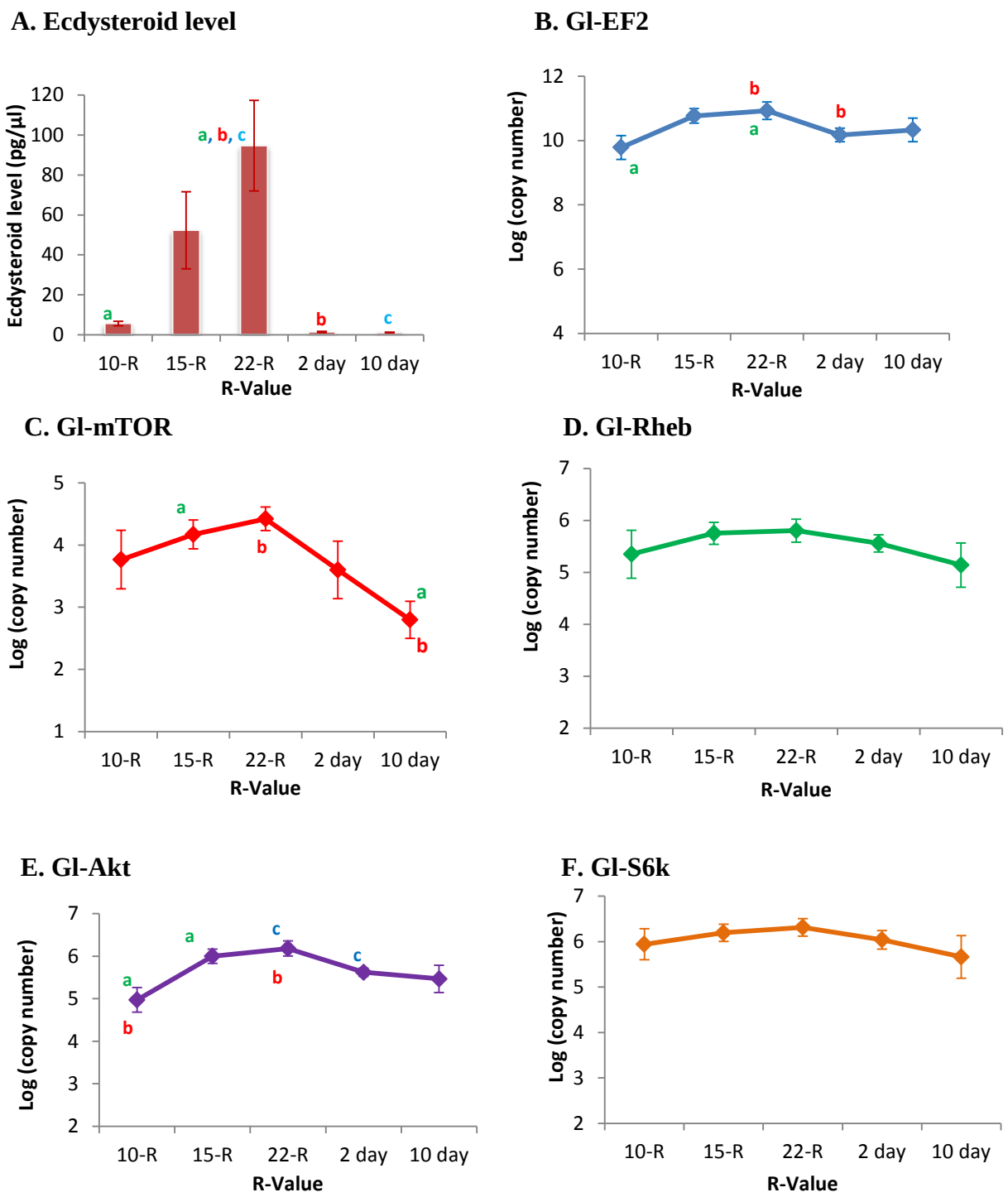

Figure 3. 1. Effects of molt induction by MLA on hemolyph ecdysteroid titers (A) and YO expression of *Gl-EF2* and mTOR components (B-F) in *G. lateralis.* Hemolymph ecdysteroid levels were quantified by ELISA. *Gl-mTOR*, *Gl-Rheb*, *Gl-Akt*, *Gl-S6k*, and *Gl-EF2* mRNA levels at early premolt (10-R), mid premolt (15-R), late premolt (22-R), 2 days postmolt, and 10 days postmolt were quantified by real-time PCR (see Materials and methods). Data are presented as

mean ± 1 S.E. (n = 6 for 10-R, 13 for 15-R, 6 for 22-R, 9 for 2 days postmolt, and 4 for 10 days posmolt. Means that are significantly different from each other have the same the same letter (A, B, C, and E). There were no significant differences in the means for *Gl-Rheb* (D) and *Gl-S6k* (F).

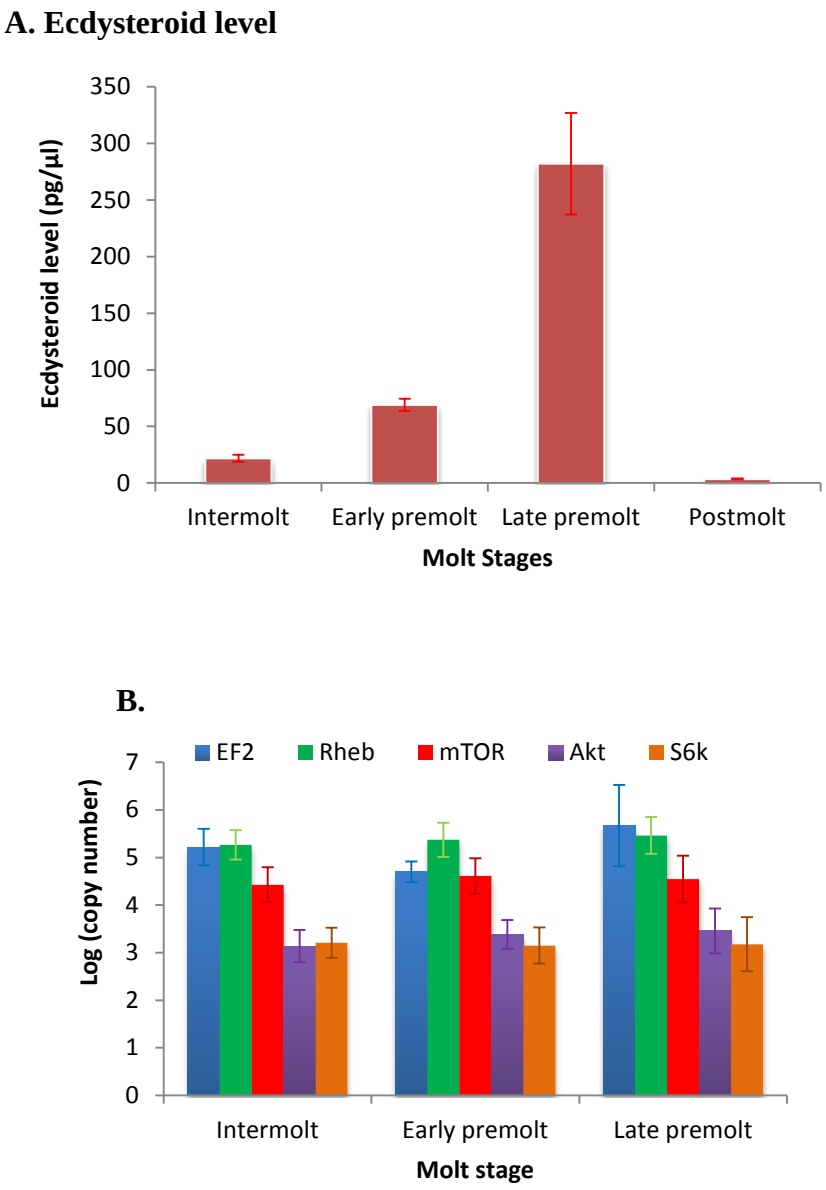

Figure 3. 2. Effects of molting on hemolymph ecdysteroid titers (A) and YO expression of *Cm-EF2* and mTOR components (B) in *C. maenas*. Hemolymph ecdysteroid levels were quantified by ELISA. *Cm-mTOR*, *Cm-Rheb*, *Cm-Akt*, *Cm-S6k*, and *Cm-EF2* mRNA levels at intermolt, early premolt, and late premolt stages were quantified by real-time PCR (see Materials and methods). Data are presented as mean ± 1 S.E. (intermolt, n = 6; early premolt, n = 12; late premolt, n = 6; and postmolt, n = 8). There were no significant differences in the means for all five genes at all the molt stages.

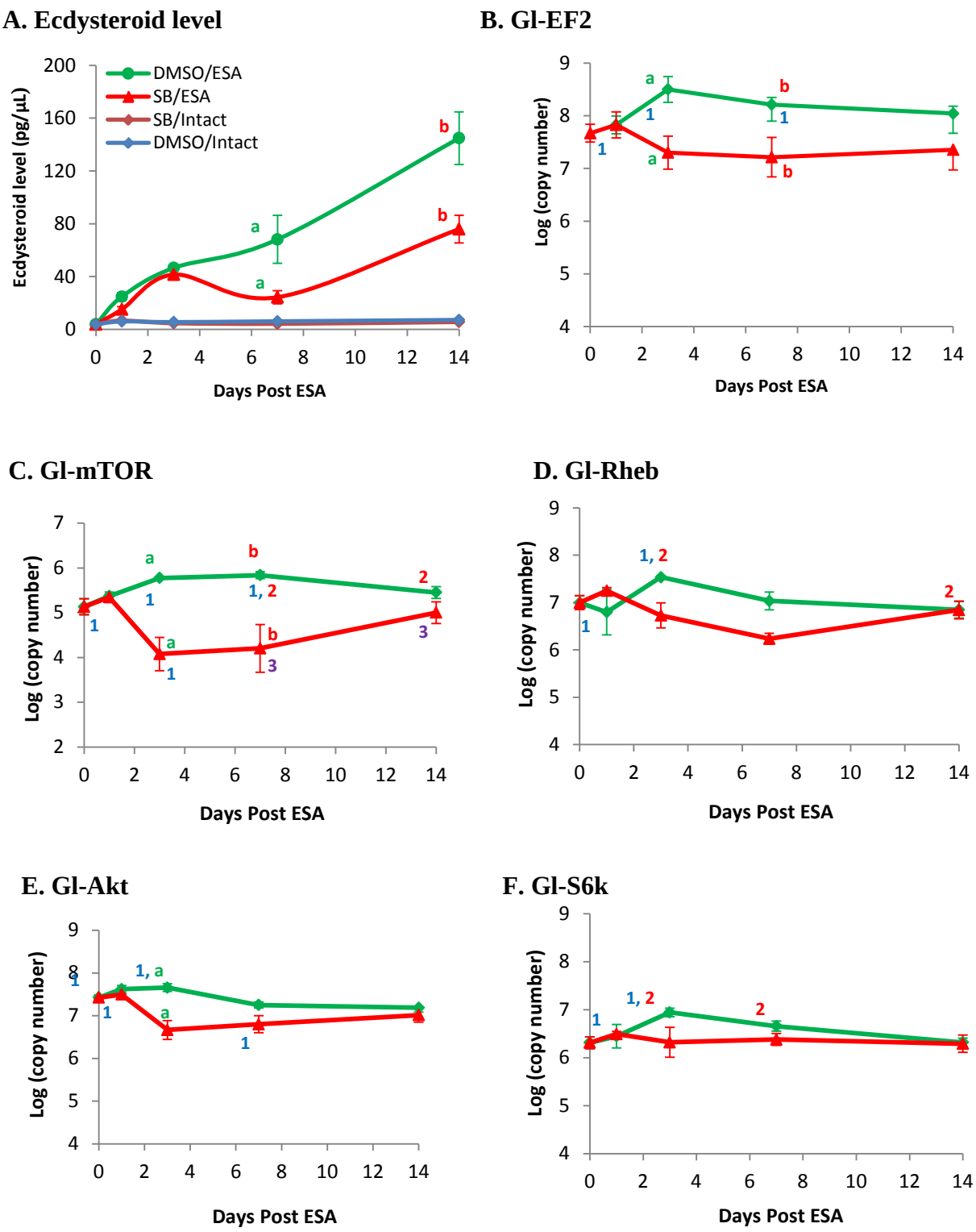

Figure 3. 3. Effects of Activin receptor antagonist SB431542 on hemolymph ecdysteroid titers (A) and YO expression of *Gl-EF2* and mTOR signaling components (B-F) in *G. lateralis in vivo*. Intact and ES-ablated animals were injected with a single dose of DMSO (~1%) final hemolymph concentration or SB431542 in DMSO (~10 µM final hemolymph

concentration) at Day 0. Data are presented as mean ± 1 S.E. (sample size for each treatment: Day 0, n = 8; Days 1, 3, and 7, n = 5; Day 14, n = 7). Means within treatments that were significantly different from each other have the same number for the SB/ESA treatment and the same letter for the DMSO/ESA treatment. Same letters indicate means that were significantly different between treatments at the same time point. Same numbers indicate the means were significantly different between each time point. YO expression in intact animals was not measured (see Materials and methods).

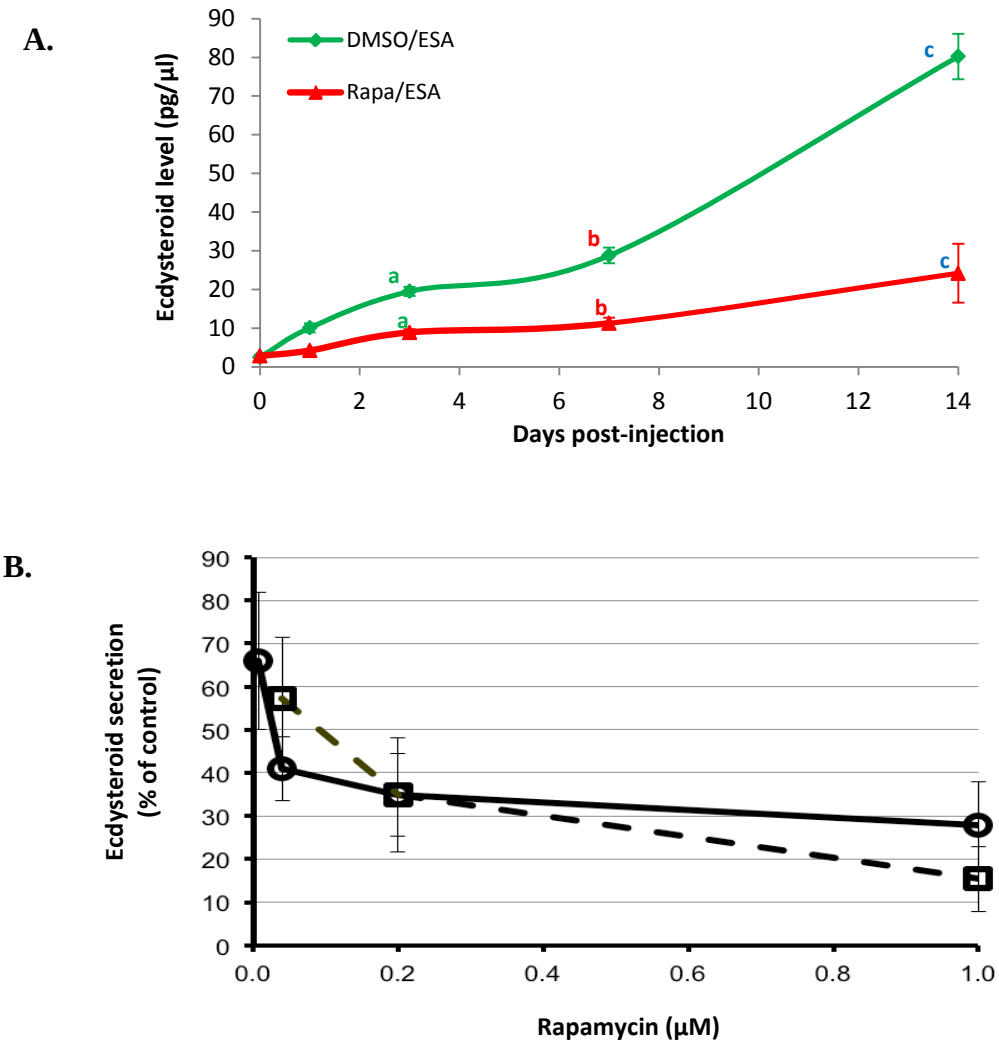

Figure 3. 4. Effects of mTOR inhibitor rapamycin inhibits on YO ecdysteroidogenesis in *G. lateralis in vivo* (A) and *in vitro* (B). (A) Animals were ES-ablated at Day 0 and injected with a single dose of rapamycin (~10 µM final hemolymph concentration) or equal volume DMSO. (~1% final hemolymph volume). Same letters indicate means that were significantly different between control and rapamycin at the same time point. (B) Paired YOs from 3 day post-ESA *G. lateralis* (**O**) and *C. maenas* (□) were incubated with 5-fold dilutions of rapamycin (1, 0.2, 0.04, and 0.008 µM) or 1% DMSO for 4.5 h and ecdysteroids secreted into the medium were quantified by ELISA. The secretion with rapamycin was expressed as the % of the control secretion of the same pair. Data presented as mean ± 1 S.E. (n = 5-8).

A. Ecdysteroid level

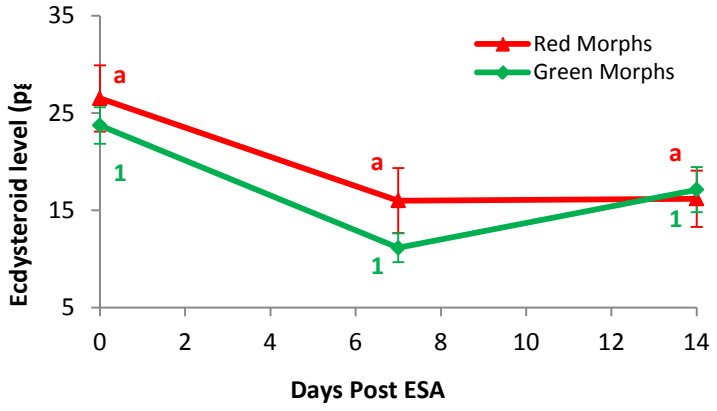

B. Red Morphs

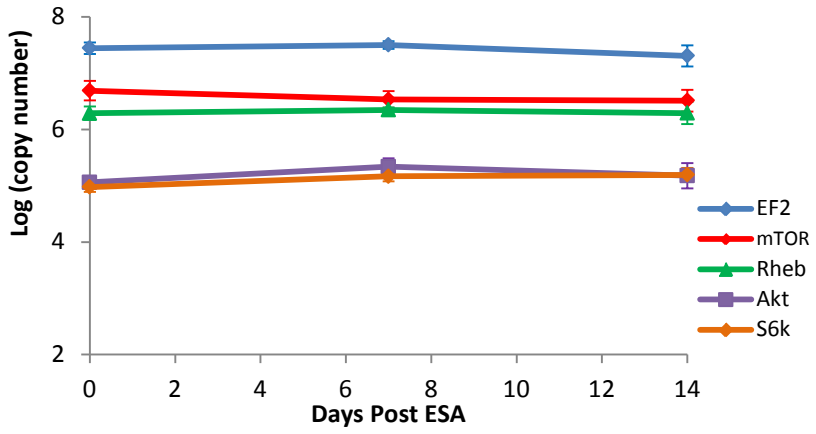

C. Green Morphs

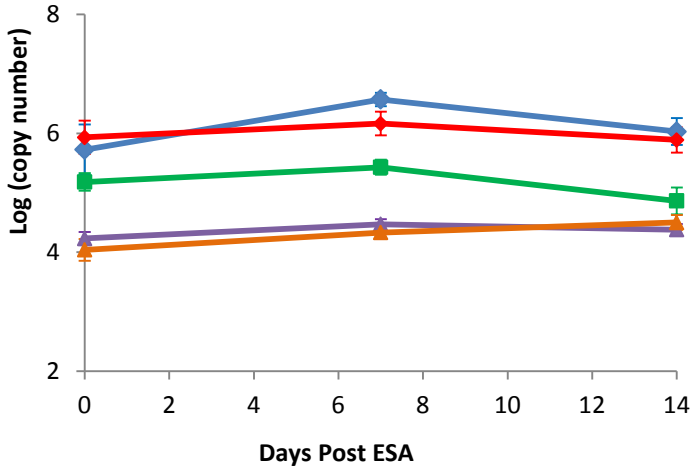

Figure 3. 5. Effects of ESA on hemolymph ecdysteroid titer (A) and YO expression of *Cm-EF2* and mTOR components in *C. maenas*. Intermolt red (B) and green (C) morphs were ES-ablated at Day 0. Hemolymph and YOs tissues were collected from intact (Day 0) and at 7 days and 14 days post-ESA (see Materials and methods). Means of ESA animals that were significantly different from intact control (Day 0) are indicated by "1" for green morphs and "a" for red morphs (A). There was no significant effect of ESA on expression of the five genes.

CHAPTER FOUR

ADULT GREEN SHORE CRAB, *CARCINUS MAENAS*, IS REFRACTORY TO MOLT INDUCTION BY EYESTALK ABLATION AND MULTIPLE LEG AUTOTOMY: EXPRESSION OF NO SYNTHASE AND GUANYLYL CYCLASES IN MOLTING GLAND (Y-ORGAN) AND MOLT-INHIBITING HORMONE IN EXTRA-EYESTALK TISSUES

SUMMARY

Regulation of the molt cycle in decapod crustaceans is controlled by the X-organ/sinus gland complex in the eyestalks (ES). The complex secretes molt-inhibiting hormone (MIH) that suppresses production of molting hormone (ecdysteroids) by molting glands (Y-organs or YOs). MIH signaling involves NO and cyclic nucleotides in the YO, which expresses NO synthase (NOS) and NO-sensitive guanylyl cyclase (GC-I). During premolt the YO becomes refractory to MIH, which is due, at least in part, to a down-regulation of MIH signaling. In most decapods, precocious molting is induced by eyestalk ablation (ESA), which removes the primary source of MIH, and by multiple leg autotomy (MLA), which stimulates limb regeneration. However, ESA of the green shore crab (*Carcinus maenas*) has limited effects on hemolymph ecdysteroid titers and *Cm-NOS* expression, and animals do not initiate premolt processes by 7 days post treatment. The purpose of this study was to determine the effects of ESA and MLA on molting and YO gene expression at intermediate (16 and 24 days) and long-term (~90 days) intervals in the "green" and "red" color morphs of adult *C. maenas*. The two color morphs differ in physiological traits: green morphs invest more energy to growth and molt more frequently, while red morphs invest more energy to reproduction and molt less frequently. Partial cDNAs encoding

the catalytic subunit of GC-I (*Cm-GC-Iβ*, a receptor GC (*Cm-GC-II*), and a soluble NO-insensitive GC (*Cm-GC-III*) were cloned. In intermediate-interval experiments, ESA of intermolt animals caused transient increases in hemolymph ecdysteroid titers in both color morphs during the first 2 weeks. In long-term experiments on intermolt red and green morphs, ESA increased hemolymph ecdysteroid titers, compared to intact and MLA animals, by 30 days post treatment, but there was no late premolt peak (>600 pg/µl) characteristic of molting animals. ESA accelerated the transition of green to the red phenotype, which was due to a decrease in the ratio of green to red color in the exoskeleton. Not surprisingly, there was no significant effect of intermediate and long-term ESA and MLA treatments on the expression of *Cm-NOS*, *Cm-GC-Iβ*, *Cm-GC-II*, *Cm-GC-III* in the YO from either color morph. In green morphs that were in premolt at the time of treatment, ESA appeared to delay molting, whereas intact and MLA animals molted by 30 days post treatment. Surprisingly, there was no effect of molt stage on expression of *Cm-NOS*, *Cm-GC-Iβ*, *Cm-GC-II*, and *Cm-GC-III* in the YO. This indicated that reduced sensitivity to MIH during premolt was not due to transcriptional down-regulation of *Cm-NOS* and *Cm-GC-Iβ*. The ineffectiveness of ESA to stimulate molting suggested that there was a secondary source of MIH. Using nested reverse transcription-polymerase chain reaction (RT-PCR), *Cm-MIH* transcripts were detected in eyestalk ganglia, brain, and thoracic ganglion from intermolt animals. ESA had no significant effect on the expression of *Cm-MIH* in brain and thoracic ganglion. The expression of *Cm-MIH* sustained to intact levels in red and green morphs. We conclude the MIH expression was similar between the color morphs and ESA had little effect on MIH transcript levels, indicating that the MIH gene was not regulated transcriptionally by the loss of the eyestalks. The data suggest that MIH secreted by neurons in the brain and

thoracic ganglion (serve as secondary sources of MIH) is sufficient to prevent molt induction when the primary source of MIH is removed by ESA.

INTRODUCTION

The European green shore crab, *Carcinus maenas*, has invaded sheltered coastal and estuarine habitats worldwide (Grosholz and Ruiz, 1996; Hanfling et al., 2011). *C. maenas* were first reported at Bodega Bay, California in 1993 and now the harbor sustains a large resident population (de Rivera et al., 2011; Grosholz and Ruiz, 1995). Genetic analysis indicates that the populations at Bodega Bay and other western North America coastal locations are derived from a small number of individuals introduced to San Francisco Bay, California from the east coast of North America (Grosholz and Ruiz, 1995; Tepolt et al., 2009). Adults occur as two color morphs that are distinguished by the pigmentation of the ventral surface of the thoracic segments and the arthrodial membrane articulating the basal segments of each of the legs. “Green” morphs have a light green ventral surface and leg joints and “red” morphs have red pigmentation in the leg joints that spreads to the ventral surface as the animal ages (McGaw et al., 1992; McGaw and Naylor, 1992a). In the Bodega harbor population, green morphs are more common during the winter months and molt frequently during February to April. The green morphs transition to red morphs during the summer and are most common in fall. The color morphs in United Kingdom populations differ in ecophysiological traits. Red morphs occur primarily in the subtidal zone and cannot tolerate low salinity for extended periods (McGaw et al., 1992; McGaw and Naylor, 1992a, b). Green morphs are more prevalent in the high intertidal zone and salt marshes and can tolerate greater ranges in salinity (McGaw et al., 1992; McGaw and Naylor, 1992a, b). Green color morphs direct more energy into molting and growth, while red morphs molt less frequently and direct more energy to reproduction (Reid et al., 1997). As a consequence of the longer

intermolt period, red morphs have a thicker exoskeleton and stronger claws (Reid et al., 1997; Taylor et al., 2009).

The process of ecdysis, or molting, in crustaceans requires precise coordination of physiological processes occurring in various organs and tissues, such as the degradation of the old exoskeleton, synthesis of a new exoskeleton, regeneration of lost appendages, and atrophy of skeletal muscle in the claws (Chang and Mykles, 2011; Mykles, 1997; Skinner, 1985). The molt cycle is divided into four major stages: intermolt, premolt, ecdysis, and postmolt (Skinner, 1985). Steroid molting hormones, or ecdysteroids, which are synthesized and secreted by a pair of molting glands, or Y-organs (YOs), initiate and coordinate these processes (Lachaise et al., 1993; Skinner, 1985). Thus, the YOs, located in the anterior cephalothorax, are activated to initiate the transition from the intermolt stage to the premolt stage (Chang and Mykles, 2011). Hemolymph ecdysteroid levels are low during postmolt and intermolt stages, and increase during premolt, reaching a peak at the end of premolt (Chang, 1989; Mykles, 2011). There is a large drop in ecdysteroid level a few days before ecdysis, which serves as a trigger for actual shedding of the exoskeleton (ecdysis), as well as the growth of the claw muscles and the synthesis and calcification of the exoskeleton during the postmolt stage (Chang and Mykles, 2011; Skinner, 1985).

The YOs are controlled by inhibitory neuropeptides produced by the X-organ/sinus gland (XO/SG) complex located in the eyestalks of decapod crustaceans (Chang and Mykles, 2011; Hopkins, 2012; Skinner, 1985; Webster et al., 2012). These neuropeptides, molt-inhibiting hormone (MIH) and crustacean hyperglycemic hormone (CHH), inhibit ecdysteroidogenesis in the YO (Chang and Mykles, 2011; Covi et al., 2012; Nakatsuji et al., 2009; Webster et al., 2012). MIH is expressed primarily in the XO/SG complex, but there are a few reports of MIH

expression in extra-eyestalk tissues (Lu et al., 2001; Tiu and Chan, 2007; Zhu et al., 2011). By contrast CHH is expressed in a wide variety of tissues including the XO/SG complex (Webster et al., 2012). Both neuropeptides share similar highly conserved motifs (Nakatsuji et al., 2009; Webster et al., 2012) and inhibit ecdysteroid synthesis via cGMP-dependent signaling pathways (Covi et al., 2009; Mykles et al., 2010). CHH is a pleiotropic neuropeptide that regulates glucose utilization, molting, osmoregulation, and metabolism (Chung et al., 2010; Fanjul-Moles, 2006; Webster et al., 2012). The eyestalk CHH isoform inhibits the YO through a membrane receptor guanylyl cyclase, or GC-II (Chung et al., 2010). MIH signaling pathway may involve a calmodulin (CaM)-dependent NO synthase (NOS) and NO-dependent guanylyl cyclase (GC-I) (Chang and Mykles, 2011; Covi et al., 2012). Thus, CHH and MIH inhibit YO ecdysteroid biosynthesis through two distinct signaling pathways involving membrane receptor and NO-dependent GCs, respectively.

The YO expresses NOS, the catalytic subunit of GC-I (GC-I*β*, a receptor GC (GC-II), and a soluble NO-insensitive GC (GC-III) (Chang and Mykles, 2011; Mykles et al., 2010; Webster et al., 2012). cDNAs encoding NOS, GC-I*β*, GC-II, and GC-III have been cloned from the blackback land crab, *Gecarcinus lateralis* (Kim et al., 2004; Lee et al., 2007b). cDNAs encoding GC-II have also been cloned from crayfish, *Procambarus clarkii*, and blue crab, *Callinectes sapidus* (Liu et al., 2004; Zheng et al., 2006). In addition, a cDNAs encoding NOS in *C. maenas*, *Marsupenaeus japonicus*, *Panulirus argus*, *Litopenaeus vannamei*, *Scylla paramamosain*, and the water flea, *Daphnia magna*, have been cloned and characterized (Inada et al., 2010; Labbe et al., 2009; Li et al., 2012; McDonald et al., 2011; Rodriguez-Ramos et al., 2010; Yao et al., 2010). Crustacean NOS has an N-terminal oxygenase domain and a C-terminal reductase domain linked by a CaM-binding domain, which is characteristic of CaM-dependent NOS genes in other

species (Daff, 2010; Kim et al., 2004; McDonald et al., 2011). GC-I is a heterodimer; the catalytic, or β subunit has heme/NO-binding and heme/NO-binding-associated domains, which are characteristic of β subunits of NO-sensitive GCs in other species (Lee et al., 2007b; Potter, 2011). The GC-II has extracellular ligand-binding, transmembrane, cytosolic kinase homology, dimerization, and catalytic domains (Lee et al., 2007b; Liu et al., 2004; Potter, 2011; Zheng et al., 2006). The GC-III resembles GC-II; it is truncated in the kinase homology domain and thus it may be constitutively active (Lee et al., 2007b).

In most decapod crustaceans molting can be induced by eyestalk ablation (ESA) or by autotomy of at least 5 walking legs (multiple leg autotomy or MLA) (Chang and Mykles, 2011; Mykles, 2001; Skinner, 1985). ESA removes the primary source of MIH and results in an immediate activation of the YO and an increase in hemolymph ecdysteroid titers within 1 day (Covi et al., 2010; Lee et al., 2004; Lee et al., 2007b; Lee and Mykles, 2006). In *G. lateralis*, ESA increases *Gl-NOS*, *Gl-GC-Iβ* and *Gl-GC-III* expression ~6-fold, ~10-fold, and ~4-fold, respectively, in the YO by 7 days post-ESA, which indicates that YOs are responsive to acute withdrawal of eyestalk neuropeptides (Lee et al., 2007b; McDonald et al., 2011). In green morphs of *C. maenas*, hemolymph ecdysteroid titer and YO *Cm-NOS* mRNA increases about 2-fold and 4-fold, respectively, by 3 days post-ESA, with little or no further increases by 7 days post-ESA; expression of GCs was not measured, as cDNAs were not available (McDonald et al., 2011). These data suggest that *G. lateralis* and *C. maenas* differ in responsiveness to ESA.

The purpose of this study was to determine the effects of ESA and MLA on molting and YO gene expression in the two color morphs at intermediate and long-term time intervals. As red morphs molt less frequently than green morphs, we hypothesized that red morphs would be less responsive to molt induction than green morphs. Partial cDNAs encoding three guanylyl cyclases

from *C. maenas*, designated *Cm-GC-Iβ*, *Cm-GC-II*, and *Cm-GC-III*, were cloned to assess responsiveness to molt induction. The effects of ESA and MLA on the color morphs were determined by measuring hemolymph ecdysteroid levels and YO gene expression of *Cm-NOS*, *Cm-GC-Iβ*, *Cm-GC-II*, and *Cm-GC-III* using quantitative polymerase chain reaction (qPCR). The expression of *GCs* and *NOS* was also quantified in YOs from green morphs undergoing spontaneous molts. The expression of MIH in brain and thoracic ganglion in intact and ESA green and red morphs was determined by nested PCR and qPCR. The results showed that both color morphs are refractory to ESA and MLA and that the brain and thoracic ganglion serve as secondary sources of MIH.

MATERIALS AND METHODS

Animals and experimental treatments

Adult male green shore crabs (*Carcinus maenas*) were collected from the harbor at Bodega Bay, California. They were maintained under ambient conditions at approximately 13 ˚C in the facilities of Bodega Marine Laboratory and fed squid twice per week. Some crabs were shipped to Colorado. In Colorado, animals were kept in aerated 30 parts per thousand Instant Ocean (Aquarium Systems, Mentor, OH, USA) at 20 °C on a 12 h:12 h dark:light cycle. They were fed cooked chicken liver once a week and water was changed after feeding. ESA and MLA used the same procedures as those described for *G. lateralis* (Lee et al., 2007a; Skinner and Graham, 1972).

Animals (green morphs) undergoing natural molts were collected in February to April, 2010 and 2011. YOs were harvested from intermolt, premolt, and postmolt animals, frozen in liquid

nitrogen, and stored at -80 ˚C. Hemolymph samples (100 µl) were taken at the time of tissue harvest and combined with 300 µl methanol for ELISA (see below).

Intermediate-interval experiments determined the effects of ESA in green and red morphs for up to 24 days. YOs were harvested from intact (Day 0) animals and from ESA animals at various intervals post-ESA. Hemolymph samples (100 µl) were taken at the time of harvest and combined with 300 µl methanol for ELISA (see below).

Long-term experiments determined the effects of ESA and MLA after about 3 months in green and red morphs. Green morph animals from the winter molting season were divided into three treatment groups: intact control (n = 10), ESA (n = 9), and MLA (n = 18). All 8 walking legs were autotomized in the MLA group. Digital images of the ventral area of each crab were acquired every two weeks. Photographs were analyzed with Photoshop CS software using the "Info" tab to quantify the intensities of red, green, and blue from the center of first thoracic sternum on the crab's left side. Results were analyzed by one-way analysis of variance (ANOVA) using Sigmastat version 3.00 (SPSS, Inc.). Red morph animals from the late spring season were divided into four treatment groups: intact control (n = 3), ESA (n = 4), MLA (n = 4), and ESA + MLA (n = 4). Every week, hemolymph samples (50 µl) were combined with 350 µl methanol for ELISA (see below). After about 90 days, the YOs were harvested, frozen in liquid nitrogen, and stored at -80 ˚C.

Ecdysteroid ELISA

The ecdysteroid ELISA was modified from (Kingan, 1989) and (Tamone et al., 2007). Plates (96-well, Costar 3366, Corning, NY, USA) were coated with AffiniPure goat anti-rabbit IgG Fc fragment antiserum (Jackson ImmunoResearch Labs 111-005-008, West Grove, PA, USA; 0.5 µg in 90 µl per well) in phosphate-buffered saline (PBS; 10 mM sodium phosphate,

0.15 M NaCl, pH 7.5) for 2 h at 23 ˚C. The wells were incubated (300 µl per well) with assay buffer (AB; 25 mM sodium phosphate, pH 7.5; 150 mM NaCl; and 1 mM EDTA disodium dihydrate) containing 0.1% bovine serum albumin (BSA, Fraction V; Sigma A-9647, St. Louis, MO, USA) for 2 h at 23 ˚C. The wells were washed 3 times with PBS containing 0.05% Tween 20 (PBS-T; Sigma, P-5927). All samples were run in duplicate. Nonspecific binding (NSB) was determined by loading wells with AB containing 0.1% BSA (100 µl per well). Standards ranged from 0 to 120 pg 20-hydroxyecdysone (20E) in AB containing 0.1% BSA (50 µl per well). Hemolymph samples in methanol were centrifuged for 10 min at 20,000 xg at 4 ˚C to remove precipitated protein. Supernatant aliquots (10 µl) were dried under vacuum in a Speed Vac centrifuge (Savant, West Palm Beach, FL, USA) and dissolved in 150 µl AB containing 0.1% BSA. Samples (50 µl), in duplicate, were loaded into each well. An internal standard consisting of lobster (*Homarus americanus*) hemolymph was included to assess inter-assay variation. 20E conjugated to horseradish peroxidase (HRP) reagent (1:64,000 dilution in AB with 0.1% BSA; 50 µl) was added to all wells and incubated for 5 min at 23 ˚C. A rabbit anti-ecdysteroid primary antibody (50 µl; 1:100,000 dilution in AB with 0.1% BSA) was added to all wells, except for the first two wells containing NSB. The 20E/HRP conjugate and 20E antibody were obtained from Dr. Timothy Kingan. The plates were sealed with Parafilm and incubated overnight at 4 ˚C. Equal volumes of Solutions A and B of a tetramethylbenzidine-peroxidase (TMB) kit (KPL, catalog 50-76-03, Gaithersburg, MD, USA) were combined and 100 µl were added to each well. The plates were incubated for 15 min at 23 ˚C in the dark. The reaction was stopped by the addition of 100 µl 1 M phosphoric acid and read with a Genios plate reader (Tecan, San Jose, CA, USA) at 450 nm. The data were archived with Magellan 6 (Tecan) and analyzed with Microplate Manager (Bio-Rad) software.

Cloning of Cm-Guanylyl cyclases (Cm-GCs)

RT-PCR and RACE were used to clone partial cDNAs encoding *Cm-GCIβ, Cm-GCII,* and *Cm-GCIII*. An initial partial cDNA sequence for *Cm-GCIβ*, *Cm-GCII,* and *Cm-GCIII* was obtained by designing nested degenerate primers to two highly-conserved sequences in the catalytic domain of *G. lateralis* guanylyl cyclases (Lee et al., 2007b). Mixed tissue cDNA from YO, claw muscle, and thoracic ganglion was used for the initial PCR (RNA isolation and cDNA synthesis are described below). The PCR conditions were an initial denaturation at 96 °C for 4 min followed by 35 cycles of denaturation for 30 s at 96 °C, annealing for 30 s at the appropriate melting temperature for the specific primer set (Table 4. 1), and extension for 30-90 s at 72 °C. Extension time varied with expected product size allowing 30 s for every 500 bp. PCR consisted of 1 µl cDNA template, 0.5 µl each forward and reverse primers (Table 4. 1), 5 µl GoTaq Green Master Mix (Promega Corp., Madison, WI, USA), and 3 µl sterile deionized water (Integrated DNA Technology). Reactions were performed using a Veriti 96 Well Thermal Cycler (Applied Biosystems Inc., Foster City, CA, USA).

5’ RACE and 3’ RACE used the FirstChoice RLM-RACE kits (Applied Biosystems/Ambion, Austin, TX, USA) as described by (McDonald et al., 2011). Nested primers were used to amplify products from the RACE templates. Outer reactions contained 1 µl 3’ or 5’ RACE template, 2 µl 3’ or 5’ RACE outer primer, 2 µl specific outer primer (Table 4. 1), 14.25 µl GoTaq Green mix (Promega), and 30.75 µl nuclease free water (Integrated DNA Technology). Inner reactions contained 1 µl outer 3’ or 5’ RACE reaction, 1 µl specific inner primer (Table 4. 1), 1 µl 3’ or 5’ RACE inner primer, 5 µl GoTaq Green mix (Promega), and 2 µl nuclease free water. PCR conditions were 3 min denaturation at 94 °C, followed by 35 cycles of 30 s at 94 °C, 30 s at 60 °C, 1 min 30 s at 72 °C, and a final extension of 7 min at 72 °C. PCR products were separated by 1.0% agarose gel electrophoresis and stained with ethidium bromide. The gel slices

were purified using Qiaex II Gel Extraction kit (Qiagen, Inc., Valencia, CA, USA) and DNA was ligated into pJet 1.2 (Fermentas, Glen Burnie, MD, USA) vector, which was transformed into CH3 Blue *E. coli* cells (Bioline USA Ins., Taunton, MA, USA). Plasmids were purified using QAIprep Spin Miniprep kit (Qiagen) and sequenced using pJET sequence-specific primers (Davis Sequencing, Davis, CA, USA).

RNA isolation and RT-PCR

The RNA isolation protocol is described in (Covi et al., 2010). Animals were anesthetized with ice for 5 min prior to dissection of the YO and other tissues. Hemolymph samples (100 µl) were combined with 300 µl methanol for quantification of ecdysteroids by radioimmunoassay (Medler et al., 2005) or ELISA (see above). Tissues were frozen in liquid nitrogen and stored at -80 °C. Total RNA was isolated using TRIzol reagent (Invitrogen, Carlsbad, CA, USA) using manufacturer's protocol. Total RNA was treated with DNAase I for 30 min, extracted with phenol:chloroform:isoamyl alcohol (25:24:1), precipitated with 1 volume of isopropanol, and dissolved in 30 µl nuclease-free water (Integrated DNA Technology). RNA concentration was determined by absorbance at 260 nm using a NanoDrop ND-1000 Spectrophotometer (Thermo Fisher Scientific, Inc). cDNA was synthesized in reactions (20 µl) containing 1 µg RNA, 4 µl Transcriptor RT reaction buffer (Roche, Nutley, NJ, USA), 0.5 µl Ribolock RNase Inhibitor (40 u/µl; Fermentas), 0.5 µl Reverse Transcriptase (Roche), 2.0 µl dNTP (10 mM), and 5 µl nuclease-free water. Complementary RNA was removed with RNase H (New England Biolabs, Ipswich, MA, USA).

The tissue distribution of *C. maenas* guanylyl cyclases (*Cm-GCIβ, Cm-GCII*, and *Cm-GCIII*), *Cm-MIH* (GenBank accession # X75995; (Klein et al., 1993)), and *Cm-Elongation Factor-2* (*Cm-EF-2*; #GU808334) was determined by end-point PCR. Reactions contained 1 µl

template cDNA and 5 pmol each of the appropriate expression primers (Table 2) in master mix 2 (Thermo scientific). After denaturation at 94 ºC for 3 min, 30 or 35 cycles of 94 ºC for 30 s, lowest annealing temperature of a primer pair for 30 s, and 72 ºC for 30 s, were completed. Final extension was for 7 min at 72 ºC. After PCR was terminated, products were separated on a 1% agarose gel containing TAE (40 mM Tris acetate and 2 mM EDTA, pH 8.5). The gels were stained with ethidium bromide and visualized with a UV light source. *Cm-EF-2* is a "housekeeping" gene that is constitutively expressed and served as the control for RNA isolation and cDNA synthesis.

A Light Cycler Fast Start DNA Master Plus SYBR GREEN I reaction mix (Roche Applied Science) and a Light Cycler 480 thermal cycler (Roche) was used for quantitative analysis of *Cm-GCIβ, Cm-GCII, Cm-GCIII,* and *Cm-NOS* (GenBank accession #GQ862349*), Cm-MIH*, and *Cm-EF-2*. qPCR reactions contained 1 µl cDNA, 5 µl 2x SYBR Green Master Mix, 0.5 µl (10 mM) each of forward and reverse gene-specific primers (Table 4. 2), and 3 µl of PCR-grade water. The primers for *Cm-GCII* were targeted to the kinase homology domain (Table 4. 3). The PCR conditions were an initial 95 °C for 5 min, followed by 45 cycles of 95 °C for 5 s (denaturation), 62 °C for 5 s (annealing), and 72 °C for 20 s (extension). Melting temperature analysis of the PCR products and the concentrations of the PCR transcripts used Roche version 1.2 Light cycler 480 software. Standard curves were prepared by serial dilutions of purified PCR products (10^{-8} ng/µl to 10^{-16} ng/µl) for *Cm-GCIβ, Cm-GCII, Cm-GCIII, Cm-NOS, Cm-MIH*, and *Cm-EF-2*. The PCR reactions contained 1 µl template cDNA and 5 pmol each of the appropriate expression primers (Table 4. 2) in Master Mix 2 (Thermo scientific). After denaturation at 94 ºC for 3 min, 35 cycles of 94 ºC for 30 s, lowest annealing temperature of a primer pair for 30 s, and 72 ºC for 30 s, were completed. Final extension was for 7 min at 72 ºC. After PCR was

terminated, products were separated on a 1% agarose gel containing TAE (40 mM Tris acetate and 2 mM EDTA, pH 8.5). The gels were stained with ethidium bromide and visualized with a UV light source. PCR products were purified using Qiaex II Gel Extraction kit (Qiagen).

Statistical analysis was performed using JMP 5.1.2 software (SAS institute, Inc., Cary, NC, USA). All qPCR data was log transformed to reduce the variance of the mean. Means for transcript abundance were compared using an analysis of variance (ANOVA) for days post-ESA verses log copy number. An ANOVA was also used to compare the means of naturally molting animals in various molting stages verses log copy numbers. A paired t-test was used to compare the means for transcript abundance between red and green morph hemolymph ecdysteroid concentration verses log copy number. A Grubb's test was used to detect outliers. The level of significance for the all the data analyses was set at $\alpha = 0.05$.

RESULTS

Cloning and characterization of cDNAs encoding green shore crab guanylyl cyclases

cDNAs encoding *GC-Iβ*, *GC-II*, and *GC-III* were cloned to assess the response of the YO to ESA and MLA. An initial PCR product (~230 bp) amplified using degenerate primers was ligated into a plasmid vector and used to transform *E. coli* cells. Plasmids were purified from each clone and sequenced. Three distinct sequences were obtained that corresponded to *G. lateralis GC-Iβ*, *GC-II*, and *GC-III* (Lee et al., 2007b) (Fig. 4. 1). Nested 3' RACE using sequence-specific primers (Table 4. 1) directed toward each of the three initial sequences yielded the remainder of the 3' open reading frame (ORF) and the 3' untranslated region (UTR) of *Cm-GC-Iβ* and *Cm-GC-III* (Table 3). 3' RACE failed to amplify the complete 3' sequence of the *Cm-GC-II*. However, a second sequence was obtained when the RLM-RACE kit reverse primer

apparently annealed to an A-rich sequence in the kinase homology (KH) domain 5' to the guanylyl cyclase (GC) domain in the ORF (Table 4. 3). An additional 5' sequence of *Cm-GC-III* was amplified using sequence-specific *Cm-GC-II* gap bridging primers (Table 4. 1). The *Cm-GC-II* primer sequences and *Cm-GC-III* cDNA sequence apparently were similar enough to allow annealing of the primers to the *Cm-GC-III* cDNA. Nested 5' RACE failed to obtain the 5' UTR of *Cm-GC-II* and *Cm-GC-Iβ*, which was most likely due to the predicted length (~2100 bp and ~1600 bp, respectively), based on the *G. lateralis* GC sequences. The DNA and translated amino acids sequences of *GC-Iβ, Cm-GC-II*, and *Cm-GC-III* are presented in Figures 4. 2, 4. 4, and 4. 6 respectively. Multiple sequence alignments showed that the deduced amino acid sequences of *Cm-GC-Iβ, Cm-GC-II*, and *Cm-GC-III* were similar to those of other decapod crustacean and insect guanylyl cyclases (Figs. 4. 3, 4. 5, and 4. 7, respectively). Cm-GC-Iβ shared 93% amino acid identity with Gl-GCIβ (Fig. 4. 3), Cm-CII shared 54% identity with Gl-GCII (Fig. 4. 5), and Cm-GC-III shared 78% identity with Gl-GC-III (Fig. 4. 7).

The tissue distribution of *Cm-GC-Iβ*, *Cm-GC-II*, and *Cm-GC-III* was determined using endpoint RT-PCR (Fig. 4. 8). Sequence-specific primers were targeted to the ORF and 3' UTR of *Cm-GC-Iβ*, the KH sequence of *Cm-GC-II*, and the 3' UTR of *Cm-GC-III* (Table 4. 2). Each primer set generated a single PCR product, as determined by qPCR melting temperature analysis (see Materials and methods). The identities of the PCR products were confirmed by direct sequencing. All three GCs were expressed in all the tissues examined; Cm-GC-III appeared to show a greater variation in expression level (Fig. 4. 8).

Intermediate-interval experiment: effects of ESA and MLA on hemolymph ecdysteroid and gene expression in YOs from red and green morphs

The effects of ESA on hemolymph ecdysteroid levels and NOS and GC expression was determined in green morphs over a 16-day interval and red morphs over a 24-day interval. ESA resulted in a transient increase in ecdysteroid titers, but the magnitude and timing differed between the color morphs (Fig. 4. 9A). In red morphs, there was a 4.2-fold increase to 48.9 pg/µl ($P < 0.0001$) in the ecdysteroid concentration at 14 days post-ESA, which was followed by a 3.8-fold decrease ($P < 0.0001$) at 21 days post-ESA (Fig. 4. 9A). In green morphs, there was a 2-fold increase to 20.5 pg/µl ($P < 0.012$) in hemolymph ecdysteroid at 3 days post-ESA, which returned to pre-ESA levels at 14 and 21 days post-ESA (Fig. 4. 9A).

ESA had no significant effect on the expression of *Cm-EF2*, which served as a constitutively expressed control, in green and red morphs (Fig. 4. 9B). Moreover, *Cm-EF2* mRNA levels were not significantly correlated with hemolymph ecdysteroid concentration in either color morph (data not shown). ESA had no significant effect on the expression of *Cm-NOS* in either the red or green morph (Fig. 4. 9C). In addition, there were no significant correlations between *Cm-NOS* mRNA levels and hemolymph ecdysteroid concentrations in either morph (data not shown).

ESA had a small, but significant, effect on *Cm-GC-Iβ* expression in red morphs, but not in green morphs. There was a decrease in *Cm-GC-Iβ* mRNA level ($P < 0.022$) that coincided with the peak in hemolymph ecdysteroid at 14 days post-ESA. *Cm-GC-Iβ* mRNA levels were negatively correlated ($P < 0.014$) with hemolymph ecdysteroid concentration in the red morphs, but not in the green morphs (data not shown). There was no significant effect of ESA on the expression of *Cm-GC-II* and *Cm-GC-III* in either color morph (Fig. 4. 9E, F). Moreover, mRNA

levels of *Cm-GC-II* and *Cm-GC-III* were not significantly correlated with hemolymph ecdysteroid concentrations in either red or green morph (data not shown).

Long-term experiment: effects of ESA and MLA on hemolymph ecdysteroid and gene expression in YOs from red and green morphs

The long-term effects of ESA and MLA were determined on red and green morphs. Red morphs were divided into four treatment groups: intact (control), ESA, MLA, and combined ESA+MLA. The experiment was conducted during the summer, after the winter/spring molting season. All the red morphs were in the intermolt stage and remained in the intermolt stage; none of the animals molted during the 90-day duration of the experiment. ESA, either singly or in combination with MLA, significantly increased hemolymph ecdysteroid level at Day 28 and later time intervals, although the means never exceeded 30 pg/µl (Day 45; Fig. 4. 10). There was no significant difference between the intact and MLA animals, except at Day 52 (Fig. 4. 10).

Green morphs were divided into three treatment groups: intact (control), ESA, and MLA. The experiment was initiated in February at the beginning of the molting season. Hemolymph samples were taken at weekly intervals and ecdysteroid titers were determined at the end of the experiment. Eight of the 30 animals were in premolt, as indicated by elevated ecdysteroid (between 72.0 and 196.0 pg/µl), at Day 0: 2 in the control group, 3 in the MLA group, and 3 in the ESA group. MLA had no effect on molting of the premolt crabs; ecdysteroid levels in the premolt intact and MLA animals continued to increase and all 5 crabs molted within 4 weeks (Fig. 4. 11; compare A and B). By contrast, ESA delayed molting of premolt animals. The increase in hemolymph ecdysteroid was delayed in 2 animals, which molted at Day 40 and Day 90; in the third animal, ecdysteroid titer decreased and the animal did not molt during the experiment (Fig. 4. 11C). The other 22 animals that were in intermolt at Day 0 did not molt for

the duration of the experiment. MLA had no effect on hemolymph ecdysteroid levels, as there were no significant differences between the means of the intact and MLA animals at all-time intervals, except at Day 63 (Fig. 4. 11D). By contrast, ESA significantly increased hemolymph ecdysteroid levels at Day 21 and later time intervals, although the means never exceeded 53 pg/µl (Day 70; Fig. 4. 11D).

While conducting the intermediate-interval experiments on the green morphs, we observed that ESA accelerated the transition from the green to red color morph pigmentation. This transition was documented in the long-term experiment by capturing digital images of the ventral surface of the cephalothorax of intact, MLA and ESA animals at 2-week intervals. Fig. 4. 12A shows images of representative animals from each group. MLA resulted in the reddening of the arthrodial membranes of the basi-ischial joints, compared to those of the intact animals, which was noticeable by 4 weeks post-MLA (12 March 2010; Fig. 4. 12A). There was also a slight reddening of the ventral cephalothorax 6 to 12 weeks post-MLA (Fig. 4. 12A). ESA resulted in the accumulation of red pigment in the basi-ischial joints and ventral cephalothorax within 2 weeks and the red color became more intense at later time intervals (Fig. 4. 12A). The images from all the animals were analyzed for changes in red, blue, and green colors of the ventral exoskeleton (see Materials and methods). The results are presented as the ratio of green to red intensities, as green color was affected by treatment, while red and blue colors were relatively constant (data not shown). ESA significantly decreased the green to red color ratio (Fig. 4. 12B). There was also a decrease in the green: red ratio in MLA animals, but the means were not significantly different from those of intact animals. We conclude that ESA caused a loss of green color, which revealed the red pigment present in the exoskeleton. Experiment showed changes over the molt cycle for all the mTOR pathway components examined.

At the conclusion of the long-term experiments, YOs were harvested and the expression of three guanylyl cyclases and EF2 were quantified by real-time PCR (Fig. 4. 13). ESA and MLA experiments showed little change for all the *Cm-GCIβ, Cm-GCII, Cm-GCIII* and *Cm-EF2* examined in red and green morph. There were no significant changes in three guanylyl cyclases and EF2 copy numbers expressed in YOs tissue in red or green morph.

Effects of molting on hemolymph ecdysteroid and YO expression of NOS, GC-Iβ, GC-II, GC-III, and EF2

The hemolymph ecdysteroid levels were collected during the natural molt cycle stages (intermolt premolt and postmolt). The hemolymph ecdysteroid levels (Fig. 4. 14A), increased in early premolt followed by greater peak compared with intermolt animals, the levels observed in postmolt animals immediately following molt were very low.

As intermolt green and red morphs were refractory to ESA and MLA, the expression of NOS, three guanylyl cyclases and EF2 were quantified in YOs from naturally molting green morphs at 3 molt stages: intermolt, premolt and posmolt for qPCR. Green crabs during the natural molt showed little changes over the molt cycle for all the three guanylyl cyclases, NOS and EF2 examined (Fig. 4. 14B). There are no significant changes in *NOS, GC-Iβ, GC-II, GC-III* and *EF2* copy numbers expressed in YOs tissue in green morphs at molt stages: intermolt, premolt and posmolt (Fig. 4. 14B).

Tissue expression of Cm-MIH and effects of ESA on expression of Cm-MIH and Cm-EF2 in brain and thoracic ganglion from green and red morphs

The XO/SG complex in the eyestalks is the primary site of MIH synthesis in decapod crustaceans. As ESA did not induce molting in intermolt animals, the brain and thoracic ganglion were investigated at secondary sources of MIH. Nested endpoint PCR indicated that MIH was

expressed in brain and thoracic ganglion from intact intermolt animals (Fig. 4. 15). The identity of the PCR product as *Cm-MIH* was verified by direct sequencing. cDNAs from claw and thoracic muscles were also tested under the same conditions as negative controls. Nested PCR yielded no *Cm-MIH* product (Fig. 4. 15).

C. maenas brain and thoracic ganglion were harvested from intact, 7-day and 14-day ESA red and green morphs to quantify the expression of MIH and EF2 (Fig. 4. 16B, C). ESA had no significant effect on the expression of *Cm-MIH* and *Cm-EF2* in brain and thoracic ganglion. The expression of *Cm-MIH* sustained to intact levels in red and green morphs (Fig. 4. 16C). We conclude the brain and thoracic ganglion serve as secondary sources of MIH, which can compensate for the loss of the eyestalks and prevent precocious molting.

DISCUSSION

A model of the MIH signaling pathway is arranged in two phases. The "triggering" phase produces a rapid, transient increase in cAMP, influx of Ca^{2+}, and binding of Ca^{2+} to CaM; the "summation" phase follows when Ca^{2+}/CaM activates NOS, which, in turn, activates GC-I and produces a large sustained increase in cGMP (Chang and Mykles, 2011; Covi et al., 2012; Webster et al., 2012). YOs express a CaM-dependent NOS and an NO-sensitive GC, the expression of which is up-regulated by acute withdrawal of MIH by ESA (Kim et al., 2004; Lee et al., 2007a; Lee et al., 2007b; McDonald et al., 2011). Moreover, it appears that inactivation of NOS by phosphorylation is required for increased YO ecdysteroidogenesis (Lee and Mykles, 2006). CHH represses YO ecdysteroidogenesis by activating a membrane receptor GC. Thus, both neuropeptides inhibit YO ecdysteroidogenesis by increasing cGMP by way of two distinct guanylyl cyclases.

Partial cDNAs encoding three guanylyl cyclases were cloned and used as markers for YO activation in *C. maenas*. Four types of GCs have been characterized in arthropods (Morton, 2004, 2011; Morton and Hudson, 2002). GC-I is an NO-sensitive soluble GC that forms a heterodimer of α and β subunits (Lee et al., 2007b; Morton and Hudson, 2002). The catalytic subunit, GC-Iβ, has heme/NO-binding and heme/NO-binding-associated domains (Lee et al., 2007b; Morton and Hudson, 2002). A membrane receptor GC, *Gl-GC-II*, has signal peptide, N-terminal extracellular ligand-binding, transmembrane, kinase homology, dimerization, and catalytic domains (Lee et al., 2007b; Morton and Hudson, 2002). GC-III is a soluble NO-insensitive GC that resembles GC-II, but lacks the signal peptide, ligand-binding, transmembrane, and most of the kinase homology domain (Lee et al., 2007b; Morton and Hudson, 2002). A GC-IV has also been identified in insects that are involved in the hypoxia escape response (Morton, 2004, 2011; Morton and Hudson, 2002). Full-length cDNAs encoding *GC-Iβ* and *GC-III* have been cloned in *G. lateralis* and *GC-II* has been cloned in *G. lateralis*, *Callinectes sapidus* (blue crab), and *Procambarus clarkii* (crayfish) (Lee et al., 2007b; Liu et al., 2004; Zheng et al., 2006). The partial cDNA sequences obtained from initial PCR using degenerate nested primers directed to the catalytic domain were grouped into three major classes based on sequence identities with crustacean and insect guanylyl cyclases in the GenBank database. *Cm-GC-Iβ, Cm-GC-II*, and *Cm-GC-III* are orthologs of *Gl-GCIβ, Gl-GCII*, and *Gl-GCIII*, respectively, based on at least a 60% amino acid sequence identity between each class using sequence alignments (Figs 4. 3, 4. 5, 4. 7; Table 4. 3).

There was little effect of ESA and MLA and molt stage on NOS and GC expression in the *C. maenas* YO. McDonald et al. (2011) found that NOS expression increases in both *G. lateralis* and *C. maenas* YOs by 32-fold for *Gl-NOS* at day 24 and by 5-fold for Cm-NOS by day 7 after

ESA. *Gl-NOS* and *Cm-NOS* transcript numbers were correlated with hemolymph ecdysteroid levels (McDonald et al., 2011). In land crab, *Gl-NOS* and *Gl-GC-Iβ* transcript numbers are correlated with hemolymph ecdysteroid levels, suggesting that expression of these genes is associated with YO activation. *Gl-GC-Iβ* mRNA transcript number increases ~10-fold by 7 days post-ESA (Lee et al., 2007b). Here we report that *Cm-NOS* transcript levels and hemolymph ecdysteroid concentrations were non-responsive, which did not confirm the results of McDonald et al. (2011). Both Lee et al. (2007b) and McDonald et al. (2011) showed that ESA increases *Gl-GC-1β* expression in land crab YOs. By contrast, ESA did not have an effect on *C. maenus* green morph *GC-Iβ* mRNA expression levels nor was there any correlation with hemolymph ecdysteroid levels. The means were not significantly different between the various days post-ESA animals for *Gl-GC-II* mRNA (McDonald et al., 2011). In addition, there was no significant correlation between *Gl-GC-II* mRNA and hemolymph ecdysteroid concentration (McDonald et al., 2011). Similarly, ESA did not have an effect on *Cm-GC-II* mRNA expression (Fig 4. 9E). Both color morphs are resistant to ESA, as ESA caused only a small, transient increase in hemolymph ecdysteroid titers. ESA did not have any effect on *Cm-NOS, Cm-GC-II,* and *Cm-GC-III* transcript copy numbers in either red or green morph (Fig. 4. 9 A-F).

Color change in crustaceans has long been known to be dependent on eyestalk factors (Pouchet, 1872; Shibley, 1968). The body of the most crabs blanches after eyestalk removal as a result of concentration of pigment in chromatophores (Shibley, 1968). Injection of eyestalk extracts into the animal temporarily reverses the condition (Abramowitz, 1937; Carlson, 1936; Fingerman, 1965; Kleinholz, 1961; Shibley, 1968). Also, eyestalk ablation can abolish daily rhythmic color changes in the fiddler crab *Uca* and the crayfish, *Astacus* (Brown, 1961). In 1951, Lenel and Veillet (Lenel and Veillet, 1951) reported the changes in color after removing the

eyestalks of *C. maenas*. The pigmentary layer of the new cuticle is affected first and then the epidermal chromatophores (Goodwin, 1960; Lenel and Veillet, 1951). This change in color was not due to increased accumulation of the carotenoid astaxanthin, but rather to the dissociation of the brown and green astaxanthin-protein complex (Lenel and Veillet, 1951). Our results were consistent with those of Lenel and Veillet (Lenel and Veillet, 1951). The ESA treatment group showed a strong decline in the green:red ratio from the first two weeks until the end of the experiment (Fig. 4. 12). There was no change in red color intensity, which presumably measured the amount of astaxanthin, in ESA and MLA animals. The color change was not strictly linked to molting, as green morphs remained in intermolt (indicated by low hemolymph ecdysteroid titers and presence of the membranous layer at the end of the experiment) and did not molt. The green:red ratio of MLA animals showed a decreasing trend, but it was not significantly different from intact animals (Fig. 4. 12). This suggests that MLA can alter the synthesis and/or release of eyestalk neuroendocrine factor(s) regulating green to red transformation. The identity of this factor(s) and its mode of action require further investigation.

The XO/SG complex is the primary source of MIH in decapod crustaceans. However, there are several reports of MIH being expressed in other tissues. Me-MIH-A is expressed only in eyestalk, but Me-MIH-B is expressed in eyestalk, brain, thoracic ganglion, and ventral nerve cord (Tiu and Chan, 2007). In the swimming crab, *Portunus trituberculatus*, MIH is expressed in eyestalk ganglia, brain, thoracic ganglion, and gonadal tissues (Zhu et al., 2011). In *Cancer pagurus*, MIH expressed in the nervous tissues (optic nerve, ventral nerve cord and thoracic/abdominal ganglion). The results of the nested PCR analysis (Fig. 4. 15) clearly show the presence of PCR products the expected size of MIH (199 bp) in brain and thoracic ganglion. However, we considered the possibility of cross-contamination of PCR reactions of thoracic

ganglion and brain preps with MIH mRNA or cDNA. Although we can't completely rule out this possibility, this is less likely, since the muscle cDNAs along with water control did not yield PCR products (Fig. 4. 15).

CONCLUSIONS

The shift from the green to red morphotype is regulated by eyestalk neuroendocrine factor(s), as change in pigmentation was accelerated by ESA. MIH does not appear to be involved, as the transition occurs in intermolt animals. What is interesting is that the change in color is not due to an increase in red pigment. Instead, there is a decrease in green color, which unmasks the red pigment and makes it more apparent. Three partiral sequences reported for Cm*GCIβ, Cm-GCII,* and *Cm-GCIII and* diposited in the GeneBank. ESA and MLA experiments had no effect in the three guanylyl cyclase and NOS. There were no significant effect on expression of guanylyl cyclase and NOS by long-term experiments ESA and MLA. Moreover, naturally molting green morphs showed little changes over the molt cycle for all the three guanylyl cyclases and NOS. There are no significant changes in *NOS, GC-Iβ, GC-II, GC-III* expression. Adult green shore crab, *C. maenas* is refractory to ESA. Nested endpoint RT-PCR showed that MIH transcript is present in brain and thoracic ganglion of intermolt crabs. MIH expression was similar between the color morphs and ESA had little effect on MIH transcript levels, indicating that the MIH gene was not regulated transcriptionally by the loss of the eyestalks. The data suggest that MIH secreted by neurons in the brain and thoracic ganglion is sufficient to prevent molt induction when the primary source of MIH is removed by ESA.

Table 4. 1. Primers used for cloning cDNAs encoding *C. maenas* guanylyl cyclases Iβ, II, and III. Abbreviations: Cm, *C. maenas*; deg, degenerate; F, forward; GC, guanylyl cyclase; IF, inner forward; IR, inner reverse; OF, outer forward; OR, outer reverse.

Primer	Use	Sequence (5' to 3')	Annealing Temperature
Cm-GC-deg OF3	Nested PCR	TAYAARGTGGAGACHRTVGG	52.˚C
Cm-GC-degOR3	Nested PCR	GGAAASAGRCARTADCMHGGC	56.4 ˚C
Cm-GC-degIF4	Nested PCR	AARTGGAGACHRTVGGSGA	58.1 ˚C
Cm-GC-degIR4	Nested PCR	AASAGRCARTADCMHGGCAT	54.6 ˚C
F1 GCII 3'RACE	3' RACE	CTGTTGGACGCCATCAAC	54.1 ˚C
F2 GCII 3'RACE	3' RACE	CTACCTATCCGTAACGAGGAGC	56.2 ˚C
F13 GCII	PCR	CCCAACATCTTCGACAACATGCTG	58.5 ˚C
R7 GCII	PCR	GTTACGGATAGGTAGCCCGCTTAC	58.8 ˚C
F1 GCIβ	3' RACE	CACCATCGGCATCCACAC	56.5 ˚C
F2 GCIβ	3' RACE	CACGCCAAGTGCATCGGC	60.3 ˚C
F1 GCIII	3' RACE	CTTCACCATTGCTCACCGTC	56.3 ˚C
F2 GCIII	3' RACE	GACGCATACATGGTGGTATC	53.1 ˚C

Table 4. 2. Primers used for *Cm-MIH, Cm-NOS, Cm-EF2, Cm-GCIβ, Cm-GCII,* and *Cm-GCIII* qPCR. Cm, *C. maenas*; F, forward; R, reverse; GC, guanylyl cyclase.

Primer	Sequence (5' to 3')	Product Size	Annealing Temperature
Cm-NOS F4	GTGTGGAAGAAGAACAAGGACG	158 bp	55˚C
Cm-NOS R1	CCACCATCCTCTATGCCACAGA		58˚C
Cm-EF2 F1	CCATCAAGAGCTCCGACAATGAGCG	278 bp	61˚C
Cm-EF2 R1	CATTTCGGCACGGTACTTCTGAGCG		61˚C
Cm-GCIβ F8	CAAGATGATGGGTTCGCCTTCACCTACC	149 bp	62˚C
Cm-GCIβ R7	CTCTCTCTGGTCGTGTCTCTGCCTC		61˚C
Cm-GCII F3	CGGTGGGTGGTGAAGATCAG	375 bp	57˚C
Cm-GCII R3	CTCCGCCCAGCACTCCGTC		63˚C
Cm-GCIII F7	CCTCCTCACACAAAGACTCCAACGC	259 bp	60˚C
Cm-GCIII R8	GTGTGCCGTTACTAGACGAGAAATACGC		61 ˚C
Cm-MIH F1	TATCGGTGGTGGTTCTGG	281 bp	54 ˚C
Cm-MIH R1	AGCCCCAAGAATGCCAACC		58˚C
Cm-MIH F2	CGGCGAGAGTTATCAACG	199 bp	53˚C
Cm-MIH R2	TCTCTCAGCTCTTCGGACC		55˚C

Table 4. 3. Partial cDNAs encoding *C. maenas* guanylyl cyclases (GC).

Gene	Accession number	Size (bp)	Domain(s)	Identity to *G. lateralis* GC
Cm-GC-Iβ	JQ911525	1260	HNOBA, Catalytic and 3' UTR	93%
Cm-GC-II	JQ911527	1188	KH and Catalytic	54%
Cm-GC-III	JQ911526	1157	Catalytic and 3' UTR	78%

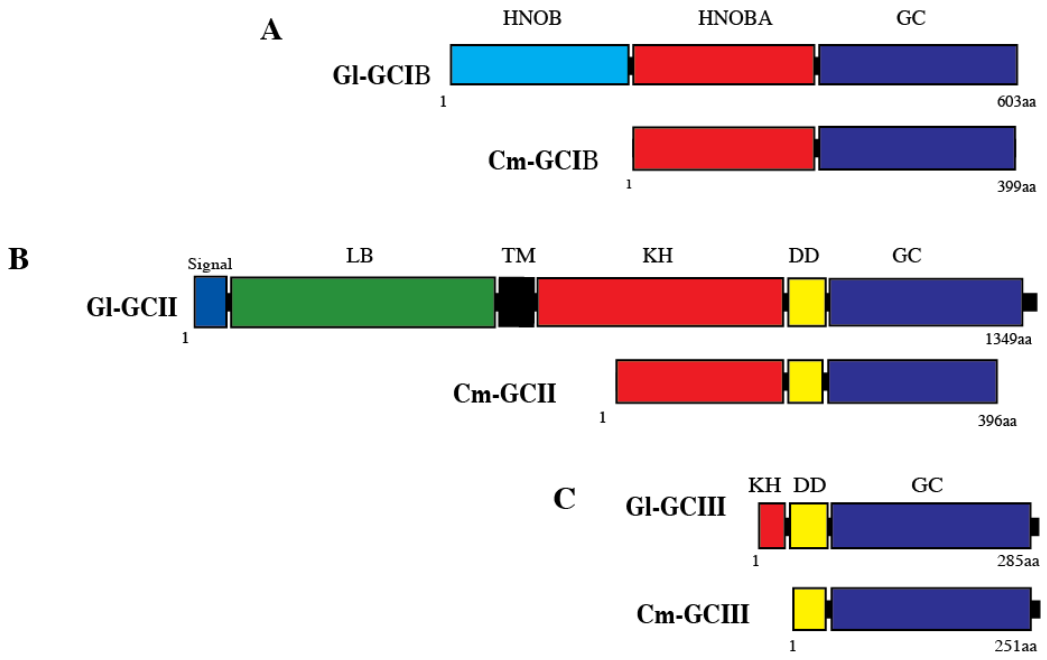

Figure 4. 1. Domain organization of three guanylyl cyclases from land crab (Gl-GC) and green crab (Cm-GC). The deduced amino acid sequences of GC-Iβ, GC-II, and GC-III from both species are depicted; all have a highly conserved catalytic (GC) domain. (A) CGIβ has heme/NO-binding (HNOB) and heme/NO-binding-associated (HNOBA) domains, which are characteristic of the β subunit of NO-sensitive GCs. (B) GC-II has signal peptide (Signal), ligand-binding (LB), transmembrane (TM), kinase homology (KH), and dimerization (DD) domains. (C) GC-III resembles the GC-II, but lacks the signal peptide, LB, TM, and most of the KH domain. Amino acid residues, numbered from the N-terminus to the C-terminus are indicated.

```
cagatcagcccgaggacgttctgccaggtgtgtcccttccacttgatgtttgaccgtgac 60
Q  I  S  P  R  T  F  C  Q  V  C  P  F  H  L  M  F  D  R  D   20
ctgcacgtgcaccaggcgggggactccatctcccgcgtgctgccctccgtctgccacccc 120
L  H  V  H  Q  A  G  D  S  I  S  R  V  L  P  S  V  C  H  P   40
ggcgcctccctcggcaaactcttccaaattgttcgtcctcacatggagctcacctttgag 180
G  A  S  L  G  K  L  F  Q  I  V  R  P  H  M  E  L  T  F  E   60
aacattctctcccacatcaacaccatctacgtccttcgggcttgcgagggactgtccacg 240
N  I  L  S  H  I  N  T  I  Y  V  L  R  A  C  E  G  L  S  T   80
gcttcccgcgatgattctaaccccgaacagcgctgcctcagattaaagggtcagatgatc 300
A  S  R  D  D  S  N  P  E  Q  R  C  L  R  L  K  G  Q  M  I   100
tacctccccgagactgacttaatgctgtacgtatgctcgccttccgttctcaacctggac 360
Y  L  P  E  T  D  L  M  L  Y  V  C  S  P  S  V  L  N  L  D   120
gacctctaccgccgcggcctctacctctcagacatgcctctccacgacgccacaagagac 420
D  L  Y  R  R  G  L  Y  L  S  D  M  P  L  H  D  A  T  R  D   140
ctcgtcctcctcagcgagaagttcgaggccgagtacgccctaaccactaacctcgagatt 480
L  V  L  L  S  E  K  F  E  A  E  Y  A  L  T  T  N  L  E  I   160
ctgacggacaagttgcagcaaacccatcgcgagctcgaaggagagagacagaaaacggac 540
L  T  D  K  L  Q  Q  T  H  R  E  L  E  G  E  R  Q  K  T  D   180
aagctgctctattcagtcctgcctatcagtattgccaatgagctgaggcacaagagacca 600
K  L  L  Y  S  V  L  P  I  S  I  A  N  E  L  R  H  K  R  P   200
gtgccgccgcggaggtacgaggtggtaacactgctctttcgggcatcgtgggcttcacc 660
V  P  P  R  R  Y  E  V  V  T  L  L  F  S  G  I  V  G  F  T   220
gactactgctcccgacacactgacatcgccggagcttccaagattgtacggatgttgaat 720
D  Y  C  S  R  H  T  D  I  A  G  A  S  K  I  V  R  M  L  N   240
gatctctacactgcctttgacgtgctcaccgacgaggtcaagaatcccaatgtttataag 780
D  L  Y  T  A  F  D  V  L  T  D  E  V  K  N  P  N  V  Y  K   260
gtggagacggtgggggacaaatacatggcggtgagtggactgcccgaagcctgtgatcac 840
V  E  T  V  G  D  K  Y  M  A  V  S  G  L  P  E  A  C  D  H   280
cacgccaagtgcatcggtaacctcgcactggatatgatggacaaggcagccggggtcatt 900
H  A  K  C  I  G  N  L  A  L  D  M  M  D  K  A  A  G  V  I   300
gtggacggccagcgtgtgcaaatcaccatcggcatccacacgggcgaagtagtgacgggt 960
V  D  G  Q  R  V  Q  I  T  I  G  I  H  T  G  E  V  V  T  G   320
gtgataggacagaggatgccgcgctactgtctatttggcaacactgtcaacatcacctcg 1020
V  I  G  Q  R  M  P  R  Y  C  L  F  G  N  T  V  N  I  T  S   340
aggacggagacgacgggcgagaagggacgagtcaacgtgtctgaagtgtcgtacaggtat 1080
R  T  E  T  T  G  E  K  G  R  V  N  V  S  E  V  S  Y  R  Y   360
ctgcagcagccggagaaccaagatgatgggttcgccttcacctaccgcggtcctgtgcct 1140
L  Q  Q  P  E  N  Q  D  D  G  F  A  F  T  Y  R  G  P  V  P   380
atgaagggaaggaaggagcccatgcaggtgtggttcctcagcaggcggaaggcagcgtga 1200
M  K  G  R  K  E  P  M  Q  V  W  F  L  S  R  R  K  A  A  *   399
ggtgaagaagcaggacaagatggaagcagagacacgaccagagagagaaaaaaaaaaaaa 1260
```

Figure 4. 2. Nucleotide and amino acid sequences of cDNA encoding *C. maenas* GC-Iβ. Initial sequence within the catalytic domain was obtained using nested degenerate primers (Table 1) directed toward conserved sequences in the catalytic domain of land crab and insect GCs. The 3' UTR sequence was obtained using 3' RACE. The glycine-rich site underlined in the KH domain. The locations of secondary structures (β2, β3, β5 and α4) that form the GTP-binding pocket in GC domain are indicated by font colors and underlines. The font colors correspond to the colors of the domains in Fig. 4. 1.

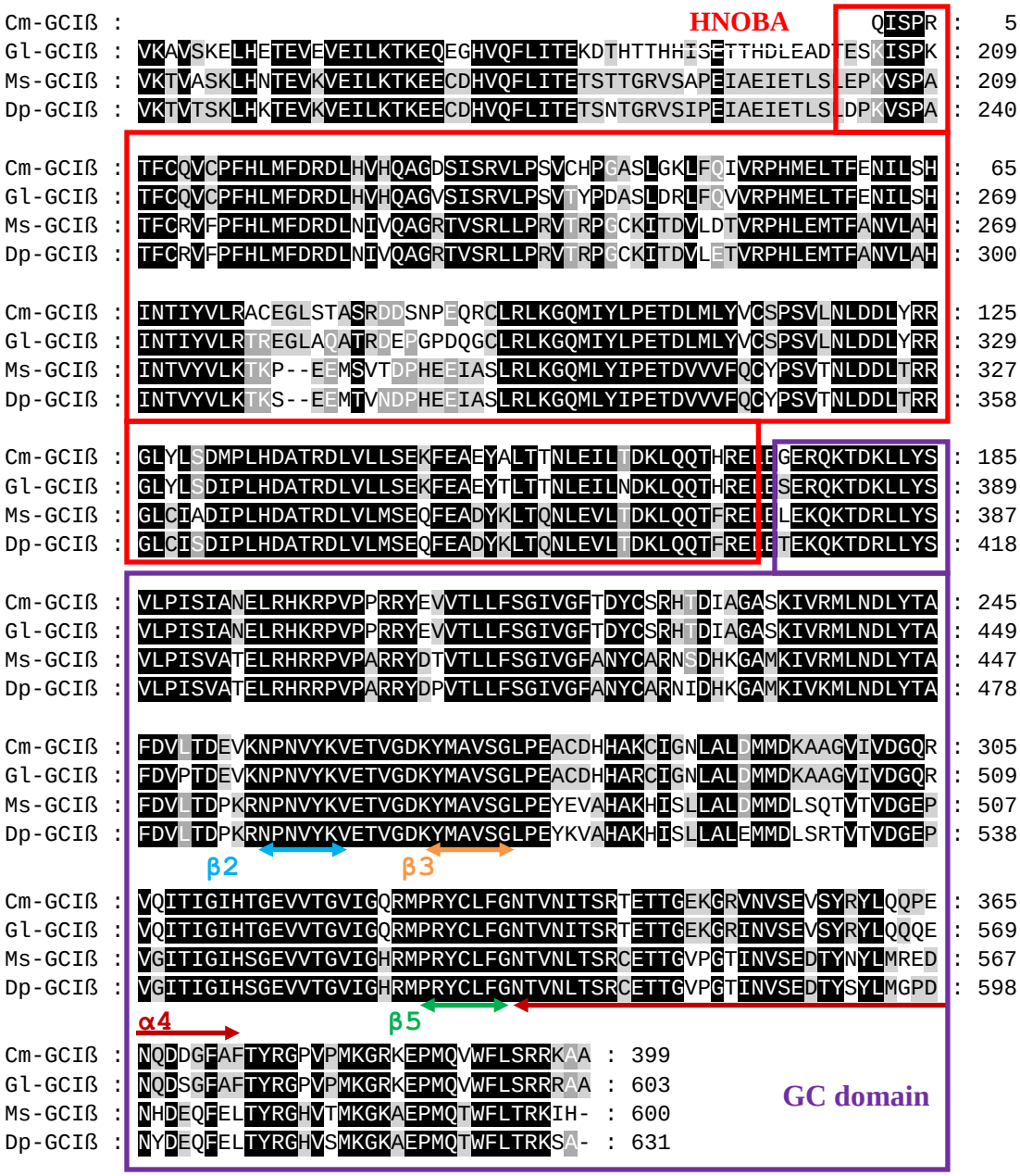

Figure 4. 3. Comparison of deduced amino acid sequences of the β subunit of NO-sensitive soluble guanylyl cyclase cDNAs from crustacean and insects. Amino acid sequence of green crab GC-Iβ (Cm-GC-Iβ; #JQ911525) was aligned with NO-sensitive GCs from land crab GC-Iβ (Gl-GC-Iβ; #DQ355434), *Manduca sexta* (Ms-GC-Iβ; #AAC61264), and *Danaus plexippus* (Dp-GC- Iβ, # EHJ74622) using ClustalX2 software. Amino acid residues that are identical or similar between all sequences are highlighted in black; residues identical or similar in two of the four sequences highlighted in gray. The catalytic GC domain (purple box) and the heme/NO-binding-associated HNOBA domain (red box) are indicated. The locations of secondary structures (α4, β2, β3, and β5) that form the GTP-binding pocket in the GC domain are indicated.

```
gtgtgtacggttaccgagtactgctcccgtggctccctcaaggacattctggacaacgag 60
 V  C  T  V  T  E  Y  C  S  R  G  S  L  K  D  I  L  D  N  E  20
gacgtgaagcttgacaacatgttcatagcttcactaattggagacatcgtgcagggtatg 120
 D  V  K  L  D  N  M  F  I  A  S  L  I  G  D  I  V  Q  G  M  40
atctaccttcacgattcccccgttaagtcccacggtaacctcaagtcatccaactgcctg 180
 I  Y  L  H  D  S  P  V  K  S  H  G  N  L  K  S  S  N  C  L  60
gtggattcccggtgggtggtgaagatcagtgactttgggcttcacgaacttaagtcaggc 240
 V  D  S  R  W  V  V  K  I  S  D  F  G  L  H  E  L  K  S  G  80
tatgaaacaacatcagtggcggaggcgggcgagacgcagaggaggtgtacagacctgctg 300
 Y  E  T  T  S  V  A  E  A  G  E  T  Q  R  R  C  T  D  L  L  100
taccgtgcccctgagctgctgagggacacgtcggcgccccctggagggacgcagaagggc 360
 Y  R  A  P  E  L  L  R  D  T  S  A  P  P  G  G  T  Q  K  G  120
gacgtgtactccttcgccatcatcctctacgaagttcacgtacgccacggcccctggggc 420
 D  V  Y  S  F  A  I  I  L  Y  E  V  H  V  R  H  G  P  W  G  140
gccacggaccaaagccccttgtccgtgattcgcctggtgatggcgggcgtacaaggctca 480
 A  T  D  Q  S  P  L  S  V  I  R  L  V  M  A  G  V  Q  G  S  160
aactctcccgtgagaccgtctgtggaagctatggggagttctctggactgtgtgcgtgtg 540
 N  S  P  V  R  P  S  V  E  A  M  G  S  S  L  D  C  V  R  V  180
gtgctgacggagtgctgggcggaggtacccgaggagaggccggacttcaggagcgtcaag 600
 V  L  T  E  C  W  A  E  V  P  E  E  R  P  D  F  R  S  V  K  200
atcaagctcagacccatgaggaaaggactgaagcccaacatcttcgacaacatgctggaa 660
 I  K  L  R  P  M  R  K  G  L  K  P  N  I  F  D  N  M  L  E  220
atgatggaaaagtacgccaataatctcgaggctctagtggatgagagaacggaccagctc 720
 M  M  E  K  Y  A  N  N  L  E  A  L  V  D  E  R  T  D  Q  L  240
atccaggagaagaagaaaacagaggcgctgctgtacgagatgctgccgccctatgtggct 780
 I  Q  E  K  K  K  T  E  A  L  L  Y  E  M  L  P  P  Y  V  A  260
gaacagctcaagaggggacgcaaggtacaggctgagagcttcgactgtgtcaccatctac 840
 E  Q  L  K  R  G  R  K  V  Q  A  E  S  F  D  C  V  T  I  Y  280
ttcagtgacattgtgggattcactgagatgtccgctgagtctacgccgctacaggtggtg 900
 F  S  D  I  V  G  F  T  E  M  S  A  E  S  T  P  L  Q  V  V  300
gatttcctgaacgacttgtacacctgtttcgactccatcatcggccactatgacgtgtac 960
 D  F  L  N  D  L  Y  T  C  F  D  S  I  I  G  H  Y  D  V  Y  320
aaggtggagacgatcggggacgcgcacatggtggtaagcgggctacctatccgtaacgag 1020
 K  V  E  T  I  G  D  A  H  M  V  V  S  G  L  P  I  R  N  E  340
gagcagcacgccggagaggtcgcgtccatgtccctccacctgttggacgccatcaacaag 1080
 E  Q  H  A  G  E  V  A  S  M  S  L  H  L  L  D  A  I  N  K  360
ttccagatccgccaccgtcccacagacaccctcaagcttcgtattggactccactcaggt 1140
 F  Q  I  R  H  R  P  T  D  T  L  K  L  R  I  G  L  H  S  G  380
ccagtgtgtgcaggcgtggtgggactcaagatgccgagatactgcctg             1188
 P  V  C  A  G  V  V  G  L  K  M  P  R  Y  C  L               396
```

Figure 4. 4. Nucleotide and amino acid sequences of cDNA encoding *C. maenas* GC-II. Initial sequence within the catalytic domain was obtained using nested degenerate primers (Table 1) directed toward conserved sequences in the catalytic domain of land crab and insect GCs. The3' UTR sequence was obtained using 3' RACE PCR. The glycine-rich site underlined in the KH domain. The locations of secondary structures (β2, β3, β5 and α4) that form the GTP-binding pocket in GC domain are indicated by font colors and underlines. The font colors correspond to the colors of the domains in Fig. 4. 1.

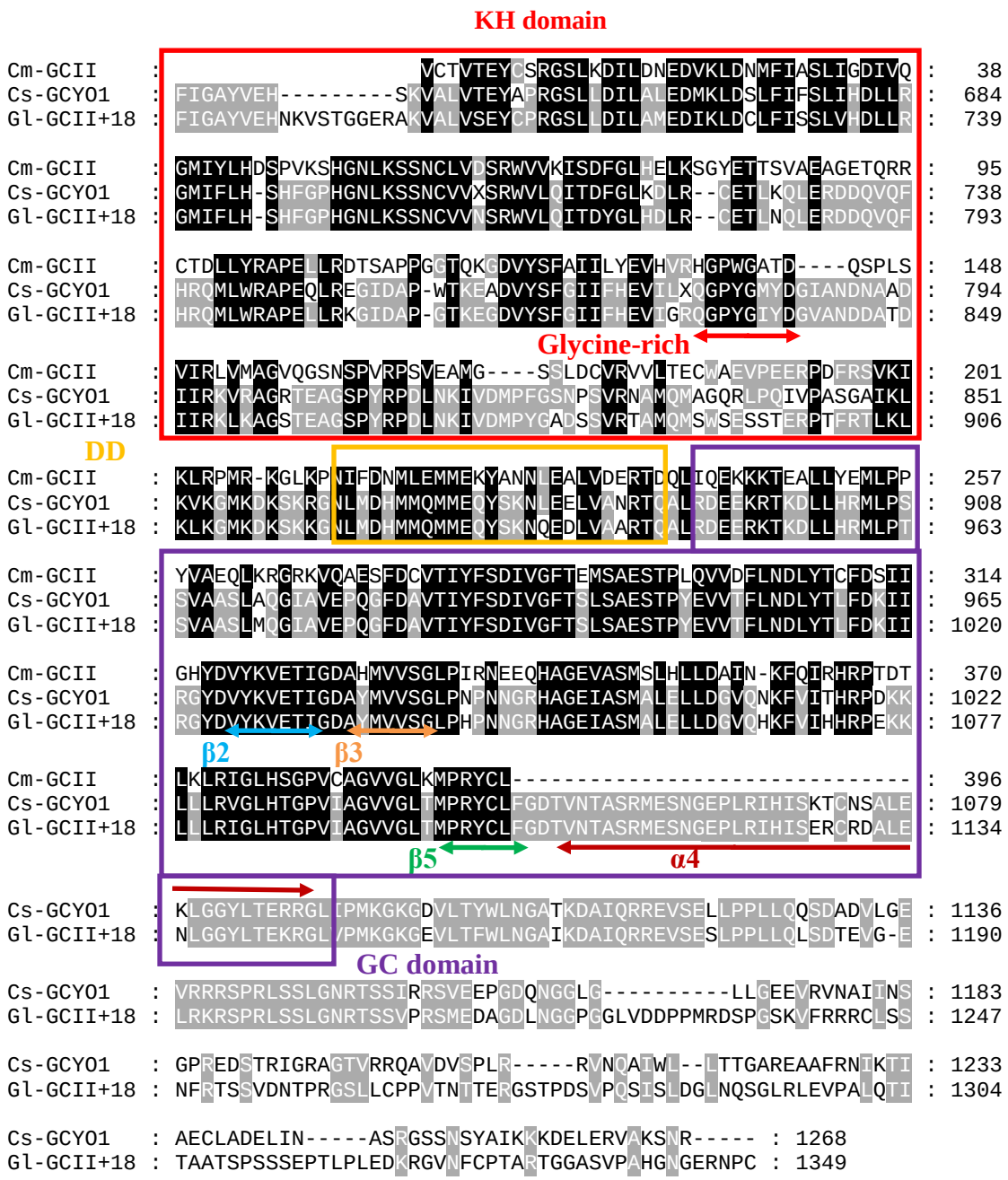

Figure 4. 5. Comparison of deduced amino acid sequences of crustacean membrane receptor guanylyl cyclase cDNAs. Amino acid sequence of green crab GC-II (Cm-GC-II; #JQ911527) was aligned with receptor GCs from of land crab (Gl-GC-II +18; #DQ355435) and blue crab (Cs-GC-YO1; #AY785292) using ClustalX2 software. Amino acid residues that are identical or similar between all the sequences are highlighted in black; residues identical or similar in two of the three sequences are highlighted in gray. There was a high degree of sequence identity in the kinase homology (KH; box with red line), dimerization (DD; box with green line), and catalytic (GC; box with purple line) domains. The glycine-rich subdomain in the KH domain is indicated. The locations of secondary structures (α4, β2, β3, and β5) that form the GTP-binding pocket in the GC domain are indicated.

```
cccaacatcttcgacaacatgctggaaatgatggaaaagtacgccaataatctcgaggct 60
 P  N  I  F  D  N  M  L  E  M  M  E  K  Y  A  N  N  L  E  A  20
ctagtggatgagagaacggaccagctcatccaggagaagaagaaaacagaggcgctgctg 120
 L  V  D  E  R  T  D  Q  L  I  Q  E  K  K  K  T  E  A  L  L  40
tacgagatgctgccgccctatgtggctgaacagctcaagaggggacgcaaggtacaggct 180
 Y  E  M  L  P  P  Y  V  A  E  Q  L  K  R  G  R  K  V  Q  A  60
gagagcttcgactgtgtcaccatctacttcagtgacattgtgggattcactgagatgtcc 240
 E  S  F  D  C  V  T  I  Y  F  S  D  I  V  G  F  T  E  M  S  80
gctgagtcaacgcccatgcaggtggtgcatctcctcaacgacctttacacacgcttcgac 300
 A  E  S  T  P  M  Q  V  V  H  L  L  N  D  L  Y  T  R  F  D  100
gctatcatcgagaacttcgacgtgtacaaggtggagactgtgggggacgcatacatggtg 360
 A  I  I  E  N  F  D  V  Y  K  V  E  T  I  G  D  A  Y  M  V  120
gtatccggacttccggtgaggaacggcactacacacacaagagagatcgcgaggatgtcc 420
 V  S  G  L  P  V  R  N  G  T  T  H  T  R  E  I  A  R  M  S  140
ttggcgctgctgcaagaggtagataccttcaccattgctcaccgtcctgaccacaaactg 480
 L  A  L  L  Q  E  V  D  T  F  T  I  A  H  R  P  D  H  K  L  160
aagctgaggatcgggatgcacacgggaccctgcgtggctggtgtggtgggcctcaaaatg 540
 K  L  R  I  G  M  H  T  G  P  C  V  A  G  V  V  G  L  K  M  180
cctagatactgcctgttcggcgacactgtcaacactgcctcgcggatggagagtaatgga 600
 P  R  Y  C  L  F  G  D  T  V  N  T  A  S  R  M  E  S  N  G  200
caaccactgaagatccatgtatccccctgcacccagaagttgttggctgagcactacccc 660
 Q  P  L  K  I  H  V  S  P  C  T  Q  K  L  L  A  E  H  Y  P  220
tccttcgtgttggagcttcgtggagaggttgacatgaagggcaaagggaggatgtacacc 720
 S  F  V  L  e  l  r  g  e  v  d  m  k  g  k  g  r  m  y  t  240
tactggttgcttggggagaacgattctggagcttaaggcaaagggaggatgtacacctac 780
 y  w  l  l  g  e  n  d  s  g  a  *                          251
tggttgcttggggagaacgattctggagcttaaggtgcaccatttcctcctcacacaaag 840
actccaacgcccagctggccactgtctctggctccacgcctccgccgctctgggtcgtag 900
catccgccgctcttgagaagcccatcactagaatatggactcaagaatccccttcccttc 960
agtttccaggcaccgcgacgcagccctcacgccttgcaccgtagcgctctcctcaacccg 1020
gcattaccgaaagcttgcaagatgtttataagccttgcgtatttctcgtctagtaacggc 1080
acacatgtgcgggattcagtaggatattgaatactataatgttctatgatagatgctcat 1140
tgaagaaaaaaaaaaaa                                             1157
```

Figure 4. 6. Nucleotide and amino acid sequences of cDNA encoding *C. maenas* GC-III. Initial sequence within the catalytic domain was obtained using nested degenerate primers (Table 1) directed toward conserved sequences in the catalytic domain of land crab and insect GCs. The 3' UTR sequence was obtained using 3' RACE PCR. Additional 5' sequence for *Cm-GCIII* was amplified using sequence-specific *Cm-GCII* gap bridging primers (Table 1; see Materials and methods). The locations of secondary structures (β2, β3, β5 and α4) that form the GTP-binding pocket in GC domain are indicated by font colors and underlines. The font colors correspond to the colors of the domains in Fig. 4. 1.

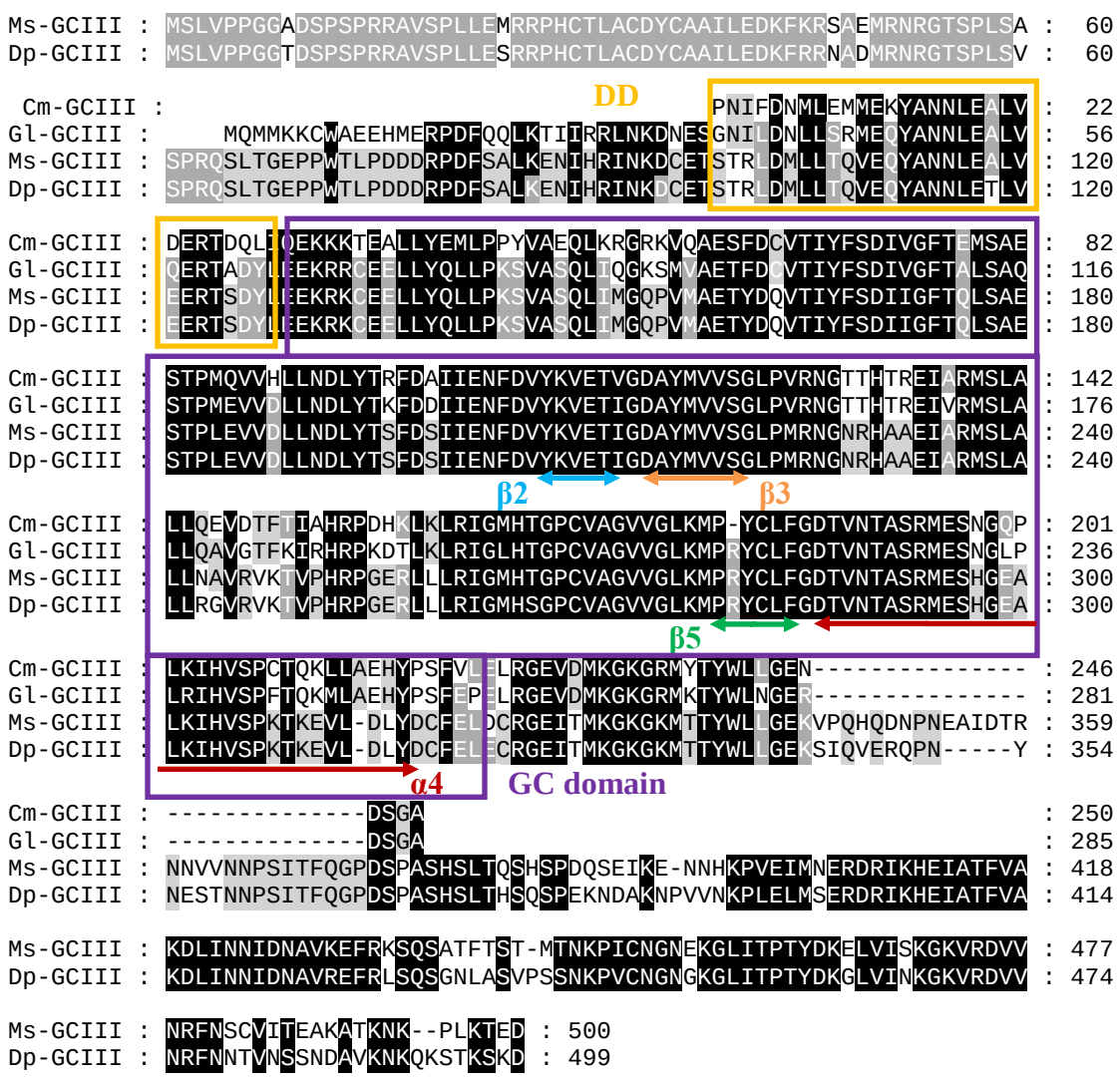

Figure 4. 7. Comparison of deduced amino acid sequences of NO-insensitive soluble guanylyl cyclase cDNAs from crustacean and insect. Amino acid sequence of the green crab GC-III (Cm-GC-III; #JQ911526) was aligned with soluble NO-insensitive GC from land crab GC-III (#DQ355438), *Manduca sexta* (Ms-GC-I, #AAC62238), and *Danaus plexippus* (Dp-GC, #EHJ68929) using ClustalX2 software. Amino acid residues that are identical or similar between all the sequences are highlighted in black. There was a high sequence identity in the dimerization (DD; green box), and catalytic GC (GC; purple box) domains. The locations of secondary structures (α4, β2, β3, and β5) that form the GTP-binding pocket in GC domain are indicated.

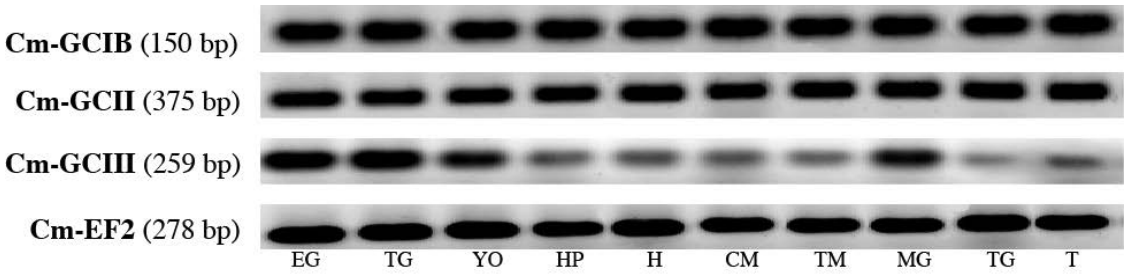

Figure 4. 8. Expression of guanylyl cyclases and elongation factor 2 (EF2), in *C. maenas* tissues. Endpoint PCR was used to determine the presence of Cm-EF2, Cm-GC-Iβ, Cm-GC-II, and Cm-GC-III in various tissues. Abbreviations: EG, eyestalk ganglia; TG, thoracic ganglia; YO, Y-organ; HP, hepatopancreas; H, hart; CM, claw muscle; TM, thoracic muscle; MG, midgut; HG, hindgut; and T, testis.

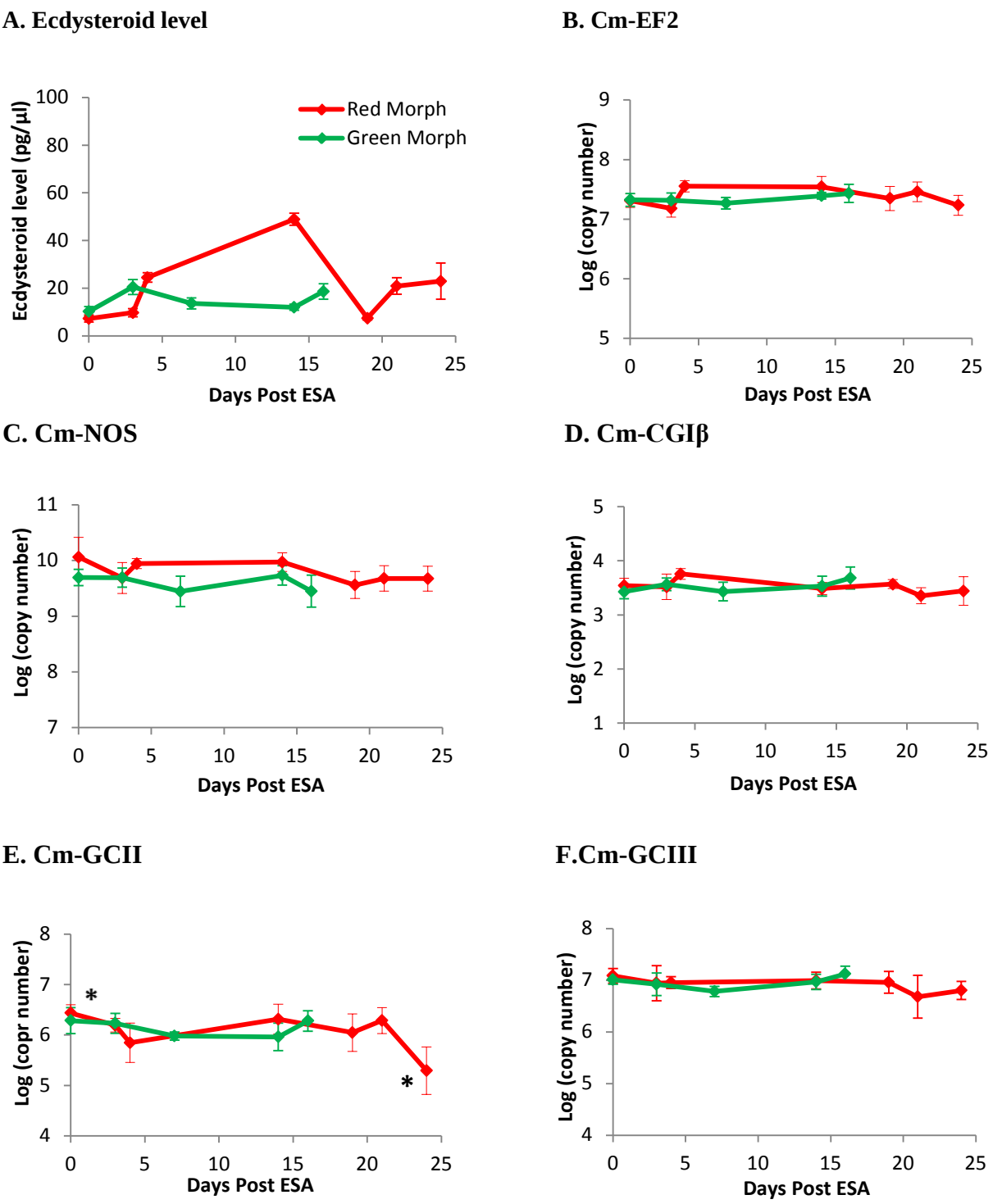

Figure 4. 9. Effects of ESA on hemolymph ecdysteroid and NOS and guanylyl cyclase expression in red (red symbol and line) and green (green symbol and line) morphs over 24 and 16 days, respectively. Animals were eyestalk-ablated at Day 0. YOs were harvested and hemolymph samples were taken at various intervals post-ESA. Ecdysteroid levels were quantified by ELISA. mRNA levels were quantified by real-time PCR. Data presented as mean

± 1. S.E. (red morph, n = 3 at Days 3 and n = 6 at Days 14; green morph, n = 4 at Days 7 and n = 6 at Days 3). Asterisks indicate significant differences between day 0 and 24 post ESA crabs at p < 0.017 (*) in *Cm-GCII* expression.

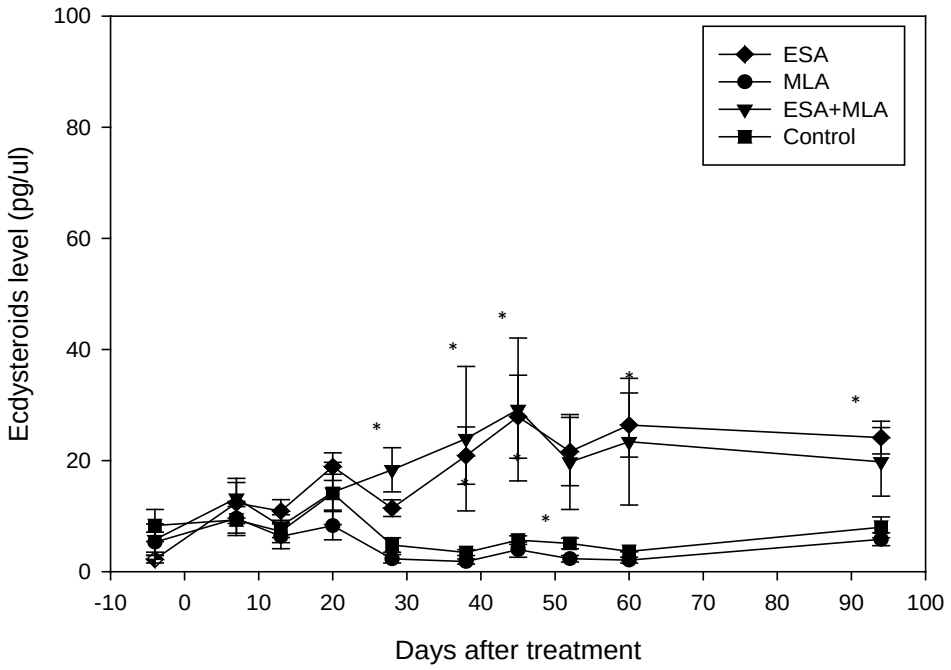

Figure 4. 10. Effects of ESA and MLA on *C. maenas* hemolymph ecdysteroid levels in red morphs. Intermolt red morphs were divided into intact (control), ESA, MLA, and ESA+MLA treatment groups and hemolymph samples were taken at weekly intervals during the 3-month period. Data presented as mean ± 1. S.E. (n=5).

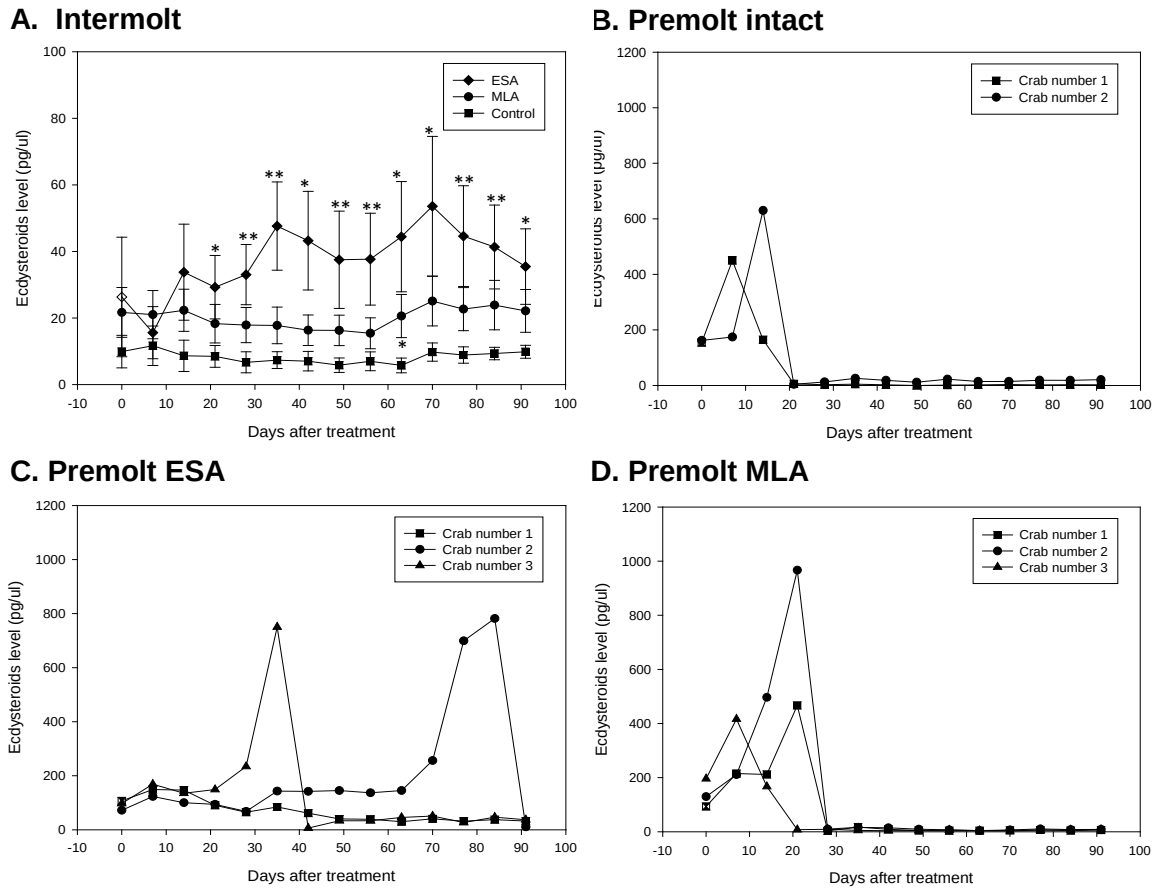

Figure 4. 11. Effects of ESA and MLA on *C. maenas* hemolymph ecdysteroid levels in green morphs. Green morphs were divided into intact, ESA, and MLA treatment groups and hemolymph samples were taken at weekly intervals during the 3-month period. Intermolt animals at Day 0 are graphed in (A); data presented as mean ± 1. S.E. (intact, n = 10; ESA, n=7 and MLA n=18). Premolt animals at Day 0 are graphed separately for individual crabs: (B) intact animals; (C) ESA animals; and (D) MLA animals.

A.

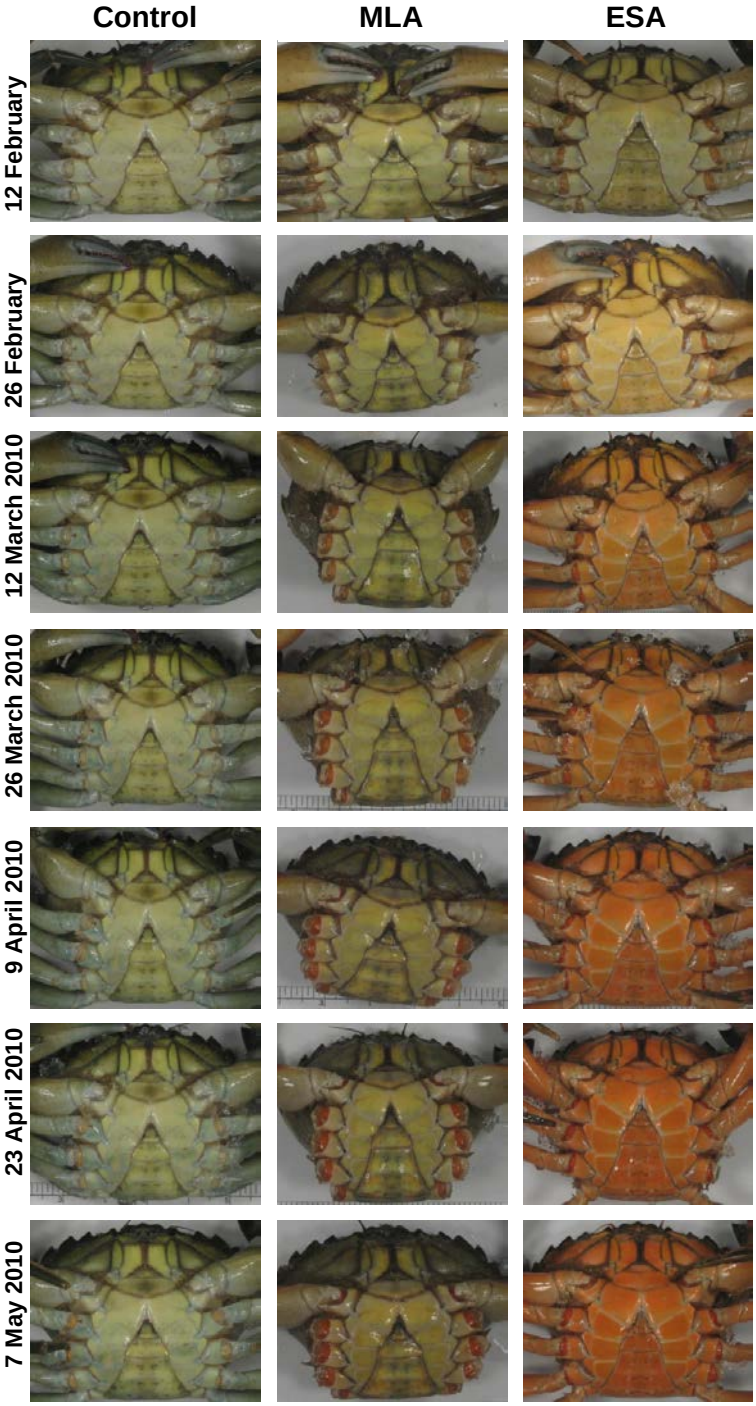
Control
MLA
ESA
12 February
26 February
12 March 2010
26 March 2010
9 April 2010
23 April 2010
7 May 2010

B.

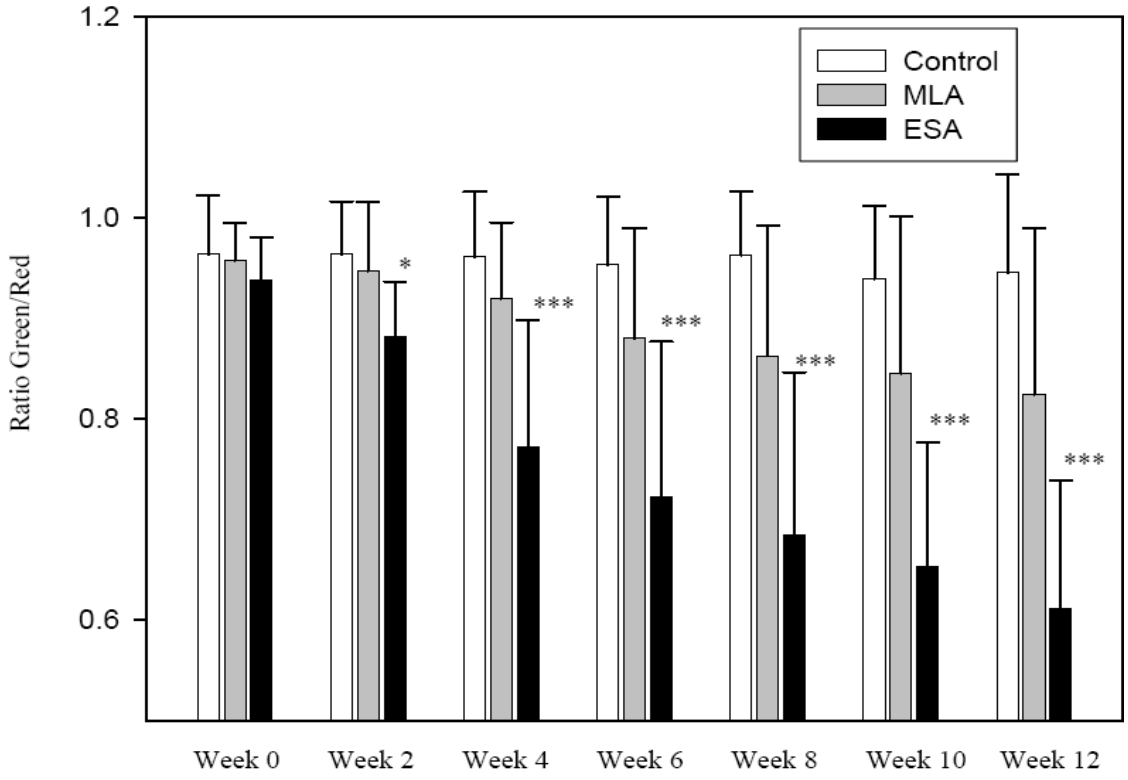

Figure 4. 12. Effects of eyestalk ablation (ESA) and multiple leg autotomy (MLA) on *C. maenas* green morph ventral pigmentation. (A) Representative images of individual crabs from intact, ESA, and MLA treatment groups captured at 2-week intervals for 12 weeks (see Materials and methods). Approximate width of each panel is equivalent to 5 cm. (B) Ratio of green to red color intensities of the left thoracic sternum of intact (n = 10), ESA (n = 10), and MLA (n = 20) animals (mean ± 1 S.D.; see Materials and methods). Asterisks indicate significant differences between the control and ESA crabs at $p < 0.05$ (*) and $p < 0.001$ (***). There were no significant differences between the intact and MLA animals.

A. Red Morph

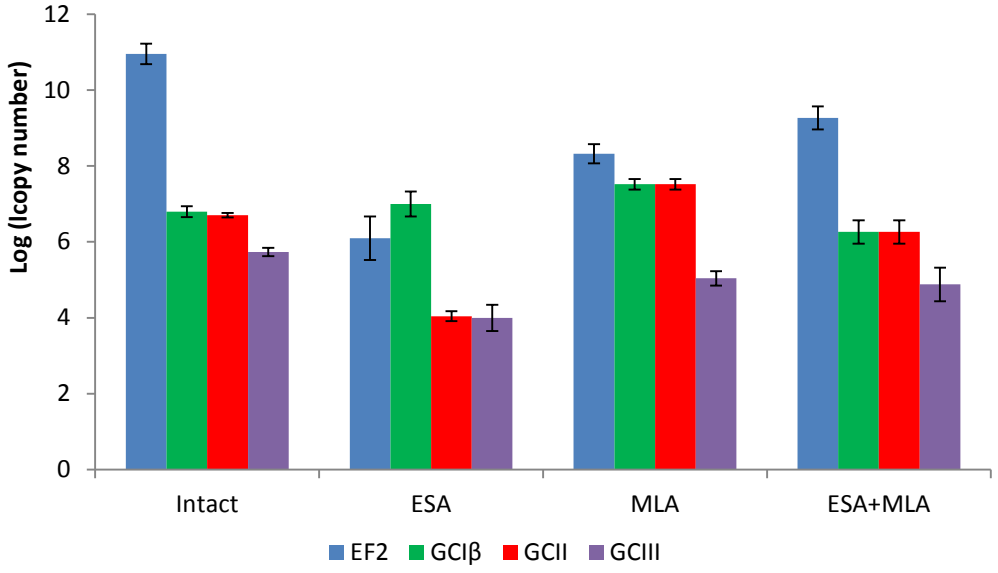

B. Green Morph

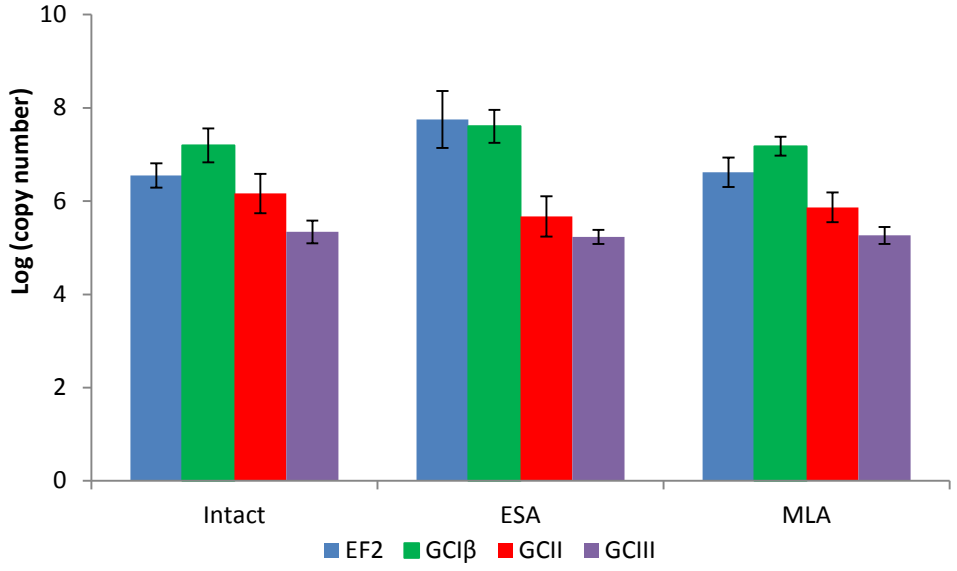

Figure 4. 13. Effects of ESA and MLA on YO expression of guanylyl cyclases (*GCIβ, GCII, and GCIII*) and *Cm-EF2* in red and green morphs. (A) Red morphs were divided into 4 treatment groups: intact (control), ESA, MLA, and ESA+MLA. (B) Green morphs were divided into 3 treatment groups: intact, ESA, and MLA. YOs were harvested 90 to 100 days post-treatment and transcripts were quantified by real-time PCR (see Materials and methods). Data are presented as mean ± 1. S.E. (red morph n = 3, 5 and green morph n = 8, 17).

A.

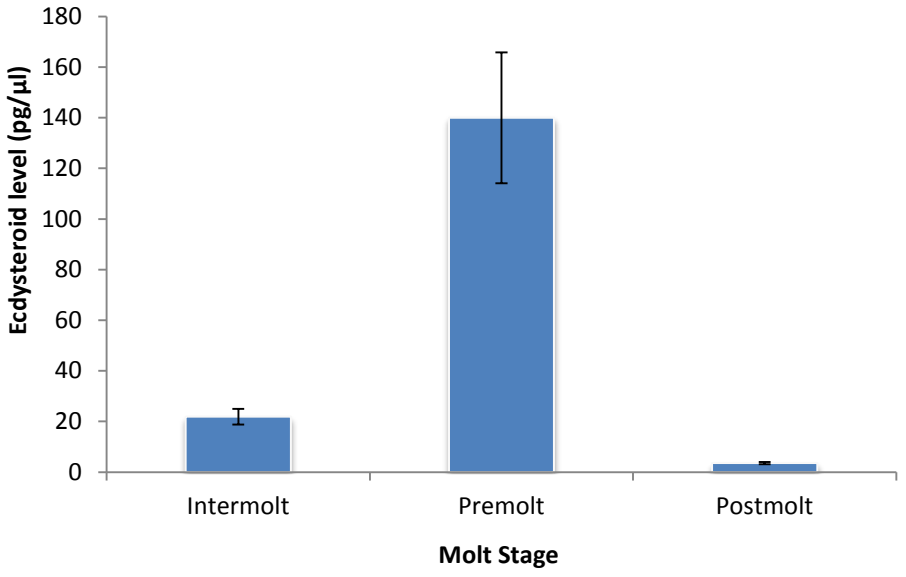

B.

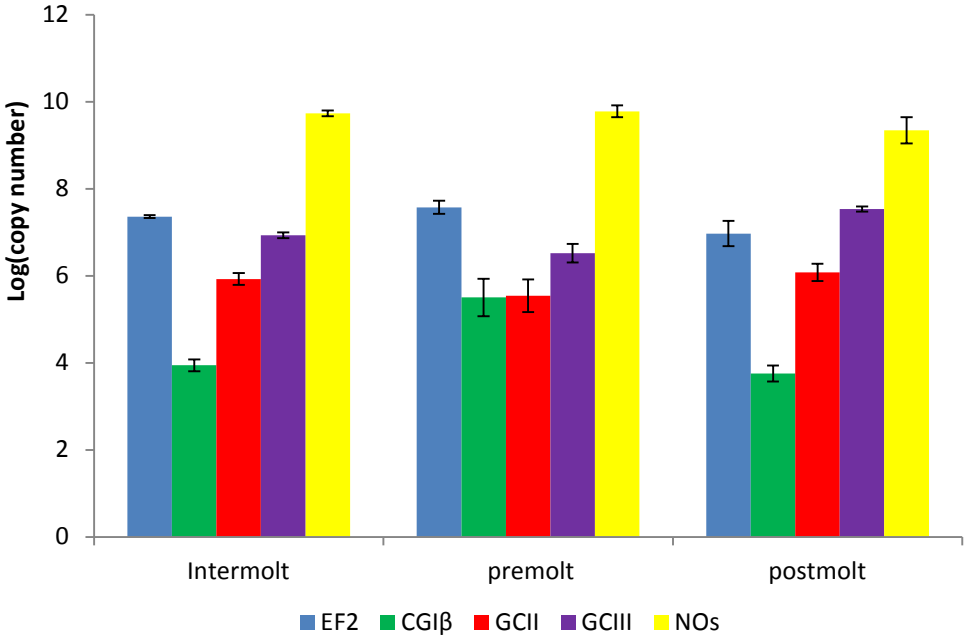

Figure 4. 14. Effects of molting on hemolymph ecdysteroid levels (A) and expression of guanylyl cyclases, and *Cm-NOS* in *C. maenas* YOs (B). Hemolymph and YOs were collected from spontaneously molting green morphs at 3 molt stages: intermolt, premolt, and posmolt (see Materials and methods). Data are presented as mean ± 1 S.E. (intermolt n = 62, premolt n= 18, and posmolt n = 4).

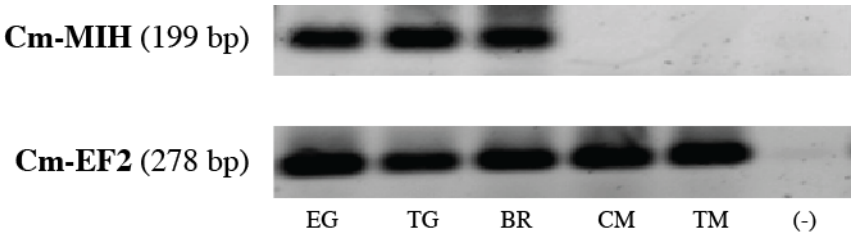

Figure 4. 15. Expression of *Cm-MIH* and *Cm-EF2* in eyestalk ganglia, brain, muscle, and thoracic ganglion from intermolt *C. maenas*. Nested end-point PCR was used to detect *Cm-MIH* transcript in cDNA from brain, thoracic ganglion, and muscle (35 cycles for each round). A single round of PCR was used to detect *Cm-MIH* in eyestalk ganglia (35 cycles with the inner primer pair) and *Cm-EF2* in cDNA from brain, thoracic ganglion, and muscle (35 cycles; see Materials and methods).

A. Ecdysteroid level

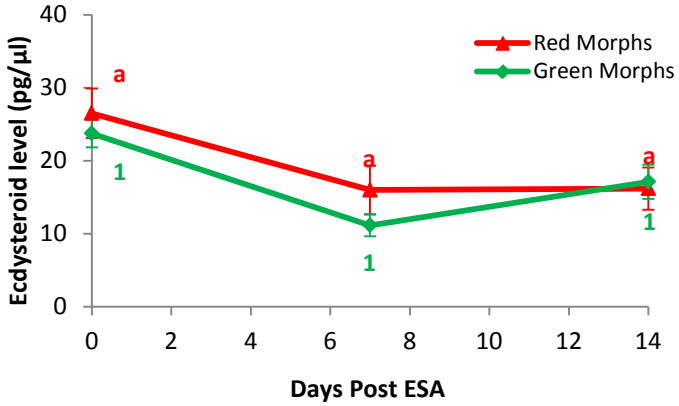

B. Cm-EF2

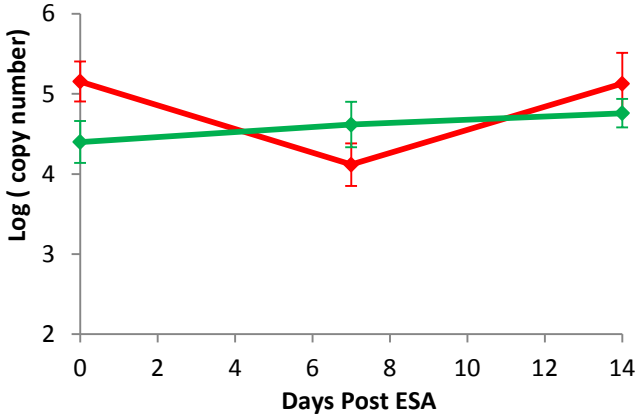

C. Cm-MIH

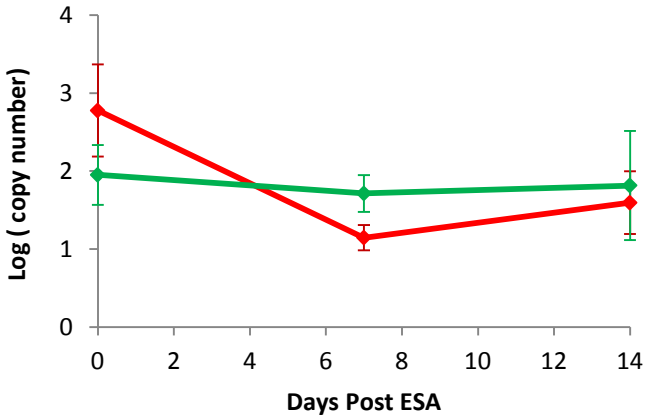

Figure 4. 16. Effects of ESA on hemolymph ecdysteroid (A), and expression of *Cm-EF2* (B), and *Cm-MIH* (C), in brain and thoracic ganglion from red and green morphs. Hemolymph and tissues were collected from intact (Day 0) and 7-day and 14-day ESA red and green morphs (see Materials and methods). Letters and numbers indicate significant differences between the control (intact) and ESA in hemolymph level (A), red morph at $p < 0.05$ (a & b) and green morph at $p < 0.001$ (1, 2 & 3). The samples from the brian and thoracic ganalion were combined for qPCR.

CHAPTER FIVE

SUMMARY AND FUTURE DIRECTIONS

The mechanistic target of rapamycin (mTOR) is a highly conserved protein kinase controlling cell growth in multicellular animals. Molting in decapod crustaceans is controlled by the X-organ/sinus gland complex, a neurosecretory center in the eyestalks (ES). The complex secretes molt-inhibiting hormone (MIH), a neuropeptide that suppresses production of molting hormone (ecdysteroids) by a pair of molting glands (Y-organs or YOs) located in the anterior of the body. MIH signaling is organized into a cAMP/Ca^{2+}-dependent "triggering" phase and a NO/cGMP-dependent "summation" phase linked by calmodulin. In the blackback land crab, *Gecarcinus lateralis*, molting can be induced by ES ablation (ESA) or autotomy of 5 or more walking legs (multiple leg autotomy or MLA). The up-regulation of mTOR signaling is necessary for YO hypertrophy and the molt-inhibiting hormone (MIH) down-regulates mTOR signaling in the YO of intermolt animals. cDNAs encoding Akt (protein kinase B), mTOR, Rheb, and p70 S6 kinase (S6k) were cloned from blackback land crab, *Gecarcinus lateralis*, and green shore crab, *Carcinus maenas*. The *G. lateralis* clones were obtained by RT-PCR and 3'RACE. Degenerate primers for *G. lateralis* were used in nested RT-PCR. We isolated partial cDNAs encoding 1051bp of the mTOR kinase domain, 827bp of the Akt pleckstrin and kinase domains and 810bp of the S6K N-terminal kinase domain. During the molt cycle, the YO transitions through four physiological states, which are mediated by endocrine and autocrine/paracrine factors: "basal" state at postmolt (molt stages A, B, C_{1-3}) and intermolt (C_4); "activated" state at early premolt (D_0); "committed" state at mid premolt ($D_{1,2}$); and "repressed" state at late premolt ($D_{3,4}$). The basal to activated state transition is triggered by a transient reduction in MIH; the

YOs hypertrophy, but remain sensitive to MIH, as premolt is suspended by MIH injection or by limb bud autotomy (LBA). Mechanistic Target of Rapamycin (mTOR), which controls global translation of mRNA into protein, appears to be involved in YO activation in early premolt. At the activated to committed state transition, the animal becomes committed to molt, as the YO is less sensitive to MIH and premolt is not suspended by LBA. YO commitment involves a putative TGFβ factor, as SB431542, a TGFβ receptor antagonist, lowers hemolymph ecdysteroid titers in mid premolt animals. At the committed to repressed state transition, high 20-hydroxyecdysone (20E) levels inhibit YO ecdysteroid secretion and hemolymph titers fall. Molting, or ecdysis, marks the regressed to basal state transition, during which the YO atrophies and regains sensitivity to MIH. Real-time PCR (qPCR) data for quantifying the effects of molting induced by eyestalk ablation (ESA) or multiple leg autotomy (MLA) on expression of mTOR components showed significant changes on EF2, mTOR at 3 and 7 days post ESA. The indicated up-regulation of Gl-EF2 and mTOR may reflect an increase in protein synthetic capacity in the premolt YO. The activated YO synthesizes required TGFβ-like factor for the mid-premolt transition and a sustained constitutive increase in ecdysteroid synthesis. These results provide the first evidence that an Activin-like TGFβ is involved in regulating YO ecdysteroidogenesis.

However, adult green shore crab (*Carcinus maenas*) is refractory to ESA. ESA causes a small increase in hemolymph ecdysteroid titers, but animals do not immediately enter premolt. Some ES-ablated animals molt after many months, but most fail to molt at all. We therefore hypothesized that other regions of the nervous system, specifically brain and/or thoracic ganglion, were secondary source(s) of MIH. Nested endpoint RT-PCR showed that MIH transcript is present in brain and thoracic ganglion of intermolt crabs. Sequencing of the PCR product confirmed its identity as MIH. Quantitative PCR was used to determine the effects of

ESA on MIH expression. Both green and red color morphs were ES-ablated and brain and thoracic ganglion were harvested at 7 days and 14 days post-ESA. Tissues from intact animals served as controls. MIH expression was similar between the color morphs and ESA had little effect on MIH transcript levels, indicating that the MIH gene was not regulated transcriptionally by the loss of the eyestalks. The data suggest that MIH secreted by neurons in the brain and thoracic ganglion is sufficient to prevent molt induction when the primary source of MIH is removed by ESA.

The project addresses the question: What are the endocrine and molecular mechanisms controlling molting in crustaceans? It focuses on the roles of the mTOR, MIH and TGFβ/Activin/Smad signaling pathways that mediate critical transitions in YO physiological states. We know very little about the signaling pathways regulating YO transitions, particularly those occurring in mid and late premolt. Now that key components of the mTOR signaling pathways have been identified and mTOR/TGFβ signaling were involved in YO activation, future studies can be directed to measure mTOR activity by S6k phosphorylation. S6k phosphorylation is determined by Western blotting using commercial antibodies that recognize S6k in insects; the ratio of phospho-S6k to total S6k is a measure of mTOR activity.

REFERENCES

Abramowitz, A. A. (1937). The chromatophorotropic hormone of the Crustacea: standardization, properties, and physiology of the eyestalk glands. Biol. Bull. 72: 344-365.

Albanella, J.; Rovira, A. and Rojob, F. (2007). mTOR signalling in human cancer. Clin Transl Oncol. 9: 484-493.

Alessi, D. R.; Kozlowski, M. T.; Weng, Q. P.; Morrice, N. and Avruch, J. (1998). 3-Phosphoinositidedependent protein kinase 1 (PDK1) phosphorylates and activates the p70 S6kinase in vivo and in vitro. Curr Biol. 8: 69–81.

Asazuma, H.; Nagata, S., and Nagasawa, H. (2009). Inhibitory effect of molt-inhibiting hormone on Phantom expression in the Y-organ of the kuruma prawn, Marsupenaeus japonicus. Arch. Insect Biochem. Physiol. 72: 220-233.

Bjedov, I.; Toivonen, J.M.; Kerr, F., Slack, C.; Jacobson, J.; Foley, A., and Partridge, L. (2010). Mechanisms of life span extension by rapamycin in the fruit fly *Drosophila melanogaster*. Cell Metab. 11: 35-46.

Bos, J. L. (1997). Ras-like GTPases. Biochim Biophys Acta. 1333; 2: M19-31.

Bosotti, R.; Isacchi, A. and Sonnhammer, E. (2000). FAT: a novel domain in PIK-related kinases. Trends Biochem Sci. 5: 225–227.

Bourne, H. R.; Sanders, D. A. and McCormick, F. (1990). The GTPase superfamily: a conserved switch for diverse cell functions. Nature. 348: 125 – 132.

Brown, F.A., Jr. (1961). Physiological rhythms. In: Waterman, T.H. (Ed.) The Physiology of Crustacea, vol. 2. Academic Press, New York, pp. 401-430

Caddy, J. (1987). Size-frequency analysis of crustacean: Molt increment and frequency models for stock assessment. Kuwait Bull. Mar. 9: 43-61.

Camargo, D.C.R.; Link, N.M. and Dames, S.A. (2012). The FKBP-rapamycin binding domain of human TOR undergoes strong conformational changes in the presence of membrane mimetics with and without the regulator phosphatidic acid. Biochem. 51: 4909-4921.

Carlson, S.P. (1936). Color changes in brachyuran crustaceans, especially in Uca pugilator. Proc. Roy. Physiograph. Soc. Lund. 6: 63-80.

Castro, A. F.; Rebhun, J. F.; Clark, G. J. and Quilliam, L. A. (2003) Rheb binds tuberous sclerosis complex 2 (TSC2) and promotes S6 kinase activation in a rapamycin- and farnesylation-dependent manner. J Biol Chem. 35 :32493-32496

Cazzamali, G.; Hauser, F.; Kobberup, S.; Williamson, M. and Grimmelikhuijzen, C.J.P. (2003). Molecular identification of a Drosophila G protein-coupled receptor specific for crustacean cardioactive peptide. Biochem. Biophys. Res. Commun. 303: 146-152.

Chandra, C. K. and Vincent, M. (2005). AKT crystal structure and AKT-specific inhibitors. Oncogene. 24: 7493–7501.

Chang, E. S. and M.J. Bruce. (1980). Ecdysteroid titers of juvenile lobsters following molt induction. J. Exp. Zool. 214: 157-160.

Chang, E.S. and Mykles, D.L. (2011). Regulation of crustacean molting: A review and our perspectives. Gen. Comp. Endocrinol. 172: 323-330.

Chang, E.S. (1989). Endocrine regulation of molting in Crustacea. Rev. Aquatic Sci. 1, 131-158.

Chuang, N. N. and Wang, P. C. (1994). Characterization of insulin receptor from the muscle of the shrimp *Penaeus japonicus* (Crustacea: Decapoda). Comp. Biochem. Physiol. 108C: 289-297.

Chung, J. S. and Webster, S.G. (2003). Moult cycle-related changes in biological activity of moult-inhibiting hormone (MIH) and crustacean hyperglycaemic hormone (CHH) in the crab, *Carcinus maenas*. From target to transcript. Eur. J. Biochem. 270: 3280-3288.

Chung, J.S., Zmora, N., Katayama, H., Tsutsui, N. (2010). Crustacean hyperglycemic hormone (CHH) neuropeptides family: Functions, titer, and binding to target tissues. Gen. Comp. Endocrinol. 166: 447-454.

Colombani, J., Bianchini, L., Layalle, S., Pondeville, E., Dauphin-Villemant, C., Antoniewski, C., Carre, C., Noselli, S., and Leopold, P. (2005). Antagonistic actions of ecdysone and insulins determine final size in *Drosophila*. Science 310: 667-670.

Covi, J. A.; Chang, E.S. and Mykles, D.L. (2009). Conserved role of cyclic nucleotides in the regulation of ecdysteroidogenesis by the crustacean molting gland. Comp. Biochem. Physiol. 152A: 470-477.

Covi, J. A.; Chang, E.S. and Mykles, D.L. (2012). Neuropeptide signaling mechanisms in crustacean and insect molting glands. Invert. Reprod. Dev. 56: 33-49.

Covi, J. A.; Bader,B., D.; Chang, E., S. and Mykles, D., L. (2010). Molt cycle regulation of protein synthesis in skeletal muscle of the blackback land crab, *Gecarcinus lateralis*, and the differential expression of myostatin-like factor during atrophy induced by mplting or unweighting. J.Exp. Biol. 213:172-183.

Covi, J.; Gomez, A.; Chang, S., Lee, K.; Chang, E., and Mykles, D. (2008). Repression of Y-organ ecdysteroidogenesis by cyclic nucleotides and agonists of NO-sensitive guanylyl cyclase, in 4th Meeting of Comparative Physiologists & Biochemists in Africa - Mara 2008 - "Molecules to Migration: The Pressures of Life", Morris, S. and Vosloo, A., Editors. Monduzzi Editore International: Bologna, Italy. pp. 37-46.

Daff, S. (2010). NO synthase: Structures and mechanisms. Nitric Oxide 23: 1-11.

Dall, W. and M. C. Barclay. (1977). Induction of viable ecdysis in the Western rock lobster by 20-hydroxyecdysone. General and Comparative Endocrinology 31: 323-334.

de Rivera, C.E.; Grosholz, E.D. and Ruiz, G.M. (2011). Multiple and long-term effects of an introduced predatory crab. Mar. Ecol. Progr. Ser. 429: 145-155.

Dell, S.; Sedlmeier, D.; Böcking, D., and Dauphin-Villemant, C. (1999). Ecdysteroid biosynthesis in crayfish Y-organs: Feedback regulation by circulating ecdysteroids. Arch. Insect Biochem. Physiol. 41: 148-155.

Dibble, C. C.; Asara, J.M. abd Manning, B. D. (2009). Characterization of rictor phosphorylationsites reveals direct regulation of mTOR complex 2 by S6K1. Mol Cell Biol. 29:5657–5670.

Dodd, K.M. and Tee, A.R. (2012). Leucine and mTORC1: a complex relationship. Am. J. Physiol. 302: E1329-E1342.

Drach, P. (1939). Mue et cycle d'intermue chez les Crustaces Decapodes. Annls. Inst. Oceanogr. 19: 103-391.

Dunlop, E. A.; Dodd, K. M.; Seymour, L. A. and Tee, A. R. (2009) Mammalian target of rapamycin complex 1-mediated phosphorylation of eukaryotic initiation factor 4E-binding protein 1 requires multiple protein-protein interactions for substrate recognition. Cell Signal. 7: 1073-84.

Fanjul-Moles, M.L. (2006). Biochemical and functional aspects of crustacean hyperglycemic hormone in decapod crustaceans: Review and update. Comp. Biochem. Physiol. 142C: 390-400.

Fingerman, M. (1965). Chromatophores. Physiol. Rev. 45.

Fowler, S. W.; Small, L. F. and Keckes, S. (1971). Effects of temperature and size on molting of euphausiid crustaceans. Mar. Biol. 11: 45—51.

Gallardo, N.; Carrillo, O.; Molto, E.; Deas, M.; Gonzalez-Suarez, R.; Carrascosa, J.M.; Ros, M. and Andres, A. (2003). Isolation and biological characterization of a 6-kDa protein from hepatopancreas of lobster Panulirus argus with insulin-like effects. Gen. Comp. Endocrinol. 131: 284-290.

Gentzler, R.D.; Altman, J.K. and Platanias, L.C. (2012). An overview of the mTOR pathway as a target in cancer therapy. Expert Opin. Ther. Targets 16: 481-489.

Gibbens, Y.Y.; Warren, J.T.; Gilbert, L.I. and O'Connor, M.B. (2011). Neuroendocrine regulation of *Drosophila* metamorphosis requires TGF beta/Activin signaling. Devel. 138: 2693-2703.

Gilbert, L. I. and Rewitz, K.F. (2009). The function and evolution of the halloween genes: The pathway to the arthropod molting hormone, in Ecdysone: Structures and Function, Smagghe, G., Editor. Spri. Nethe.pp: 231-269.

Goodwin, T.W. (1960). Biochemistry of pigments. In: Waterman, T.H. (Ed.) The Physiology of Crustacea, vol. 1. Academic Press, New York. pp: 101-140

Grewal, S. S. (2009). Insulin/TOR signaling in growth and homeostasis: A view from the fly world. Int. J. Biochem. Cell Biol. 41: 1006-1010.

Grosholz, E.D.; Ruiz, G.M. (1995). Spread and potential impact of the recently introduced European green crab, *Carcinus maenas*, in Central California. Mar. Biol. 122: 239-247.

Grosholz, E.D. and Ruiz, G.M. (1996). Predicting the impact of introduced marine species: Lessons from the multiple invasions of the European green crab, *Carcinus maenas*. Biol. Conserv. 78: 59-66.

Grove J. R.; Banerjee P.; Balasubramanyam A.; Coffer P. J.; Price D. J.; Avruch J. and Woodgett J. R. (1991). Cloning and expression of two human p70 S6 kinase polypeptides differing only at their amino termini. Mol. Cell. Biol. 11: 5541–5550.

Gu, S. H.; Lin, J.L.; Lin, P.L. and Chen, C.H. (2009). Insulin stimulates ecdysteroidogenesis by prothoracic glands in the silkworm, Bombyx mori. Insect Biochem. Molec. Biol. 39: 171-179.

Gu, S.H.; Yeh, W.L.; Young, S.C.; Lin, P.L. and Li, S. (2012). TOR signaling is involved in PTTH stimulated ecdysteroidogenesis by prothoracic glands in the silkworm, *Bombyx mori*. Insect Biochem. Molec. Biol. 42: 296-303.

Gu, S.H.; Young, S.C.; Lin, J.L. and Lin, P.L. (2011). Involvement of PI3K/Akt signaling in PTTH stimulated ecdysteroidogenesis by prothoracic glands of the silkworm, *Bombyx mori*. Insect Biochem. Molec. Biol. 41: 197-202.

Hall, D. J.; Grewal, S. S.; de la Cruz, A. F. A. and Edgar, B. A. (2007). Rheb-TOR signaling promotes protein synthesis, but not glucose or amino acid import, in *Drosophila*. BMC Biol. 5: 10.

Hanfling, B.; Edwards, F. and Gherardi, F. (2011). Invasive alien Crustacea: dispersal, establishment, impact and control. Biocont. 56: 73-595.

Harris, T. E. and Lawrence, J. C. (2003). TOR signaling. Sci STKE. 212: re15.

Hatt, P. J.; Liebon, C.; Morinière, M.; Oberlander, H. and Porcheron, P. (1997). Activity of insulin growth factors and shrimp neurosecretory organ extracts on a lepdopteran cell line. Arch. Insect Biochem. Physio. 34: 313-328.

Heldin, C.H. and Moustakas, A. (2012). Role of Smads in TGF beta signaling. Cell Tiss. Res. 347: 21-36.

Hietakangas, V. and Cohen, S. M. (2009). Regulation of tissue growth through nutrient sensing. Ann. Rev. Genet. 43: 389-410.

Hopkins, P. M. (2009). Crustacean ecdysteroids and their receptors, in Ecdysone: Structures and Functions, Smagghe, G., Editor. Spr. Netherl.pp: 73-97.

Hopkins, P.M. (2012). The eyes have it: A brief history of crustacean neuroendocrinology. Gen. Comp. Endocrinol. 175: 357-366.

Hughes, J. T.; Sullivan, J. J., and Shleser, R. (1972). Enhancement of lobster growth. Science. 177: 1110-1111.

Inada, M.; Mekata, T.; Sudhakaran, R., Okugawa, S.; Kono, T.; El Asely, A.M.; Linh, N.T.H.; Yoshida, T.; Sakai, M.; Yui, T. and Itami, T. (2010). Molecular cloning and characterization of the nitric oxide synthase gene from kuruma shrimp, *Marsupenaeus japonicus*. Fish Shellfish Immunol. 28: 701-711.

Jacinto, E. and Hall, M.N. (2003*).* TOR signaling in bugs, brain, and brawn. Nature Reviews. Mol.Cell.Biol. 4*:* 117-126.

Julien, L. A.; Carriere, A.; Moreau, J. and Roux, P. P. (2010). mTORC1-activated S6K1 phosphorylates rictor on threonine 1135 and regulates mTORC2 signaling. Mol Cell Biol. 30: 908–21.

Kean, L.; Cazenave, W.; Costes, L.; Broderick, K.E.; Graham, S.; Pollock, V.P.; Davies, S.A.; Veenstra, J.A. and Dow, J.A.T. (2002). Two nitridergic peptides are encoded by the gene capability in *Drosophila melanogaster*. Am. J. Physiol. 282: R1297-R1307.

Kim, H. W.; Batista, L.A.; Hoppes, J.L.; Lee, K.J. and Mykles, D.L. (2004). A crustacean nitric oxide synthase expressed in nerve ganglia, Y-organ, gill and gonad of the tropical land crab, *Gecarcinus lateralis*. J. Exp. Biol. 207: 2845-2857.

Kingan, T.G. (1989). A competitive enzyme-linked immunosorbent assay - Applications in the assay of peptides, steroids, and cyclic nucleotides. Anal. Biochem. 183: 283-289.

Klein, J.M.; Mangerich, S.; De Kleijn, D.P.V.; Keller, R. and Weidemann, W.M. (1993). Molecular cloning of crustacean putative molt-inhibiting hormone (MIH) precursor. FEBS Lett. 334: 139-142.

Kleinholz, L.H. (1961). Pigmentary effectors. In: Waterman, T.H. (Ed.) Physiol. Crust. 2. Academic Press, New York. pp: 133-169

Kone, B. C. (2001). Molecular biology of natriuretic peptides and nitric oxide synthases. Cardiovasc. Res. 51: 429-441.

Kucharski, L.C.; Capp, E.; Chittó, A.L.F.; Trapp, M.; Da Silva, R.S.M. and Marques, M. (1999). Insulin signaling: Tyrosine kinase activity in the crab *Chasmagnathus granulata* gills. J. Exp. Zool. 283: 91-94.

Kucharski, L.C.; Schein, V.; Capp, E. and Da Silva, R.S.M. (2002). In vitro insulin stimulatory effect on glucose uptake and glycogen synthesis in the gills of the estuarine crab *Chasmagnathus granulata*. Gen. Comp. Endocrinol. 125: 256-263.

Labbe, P.; McTaggart, S.J. and Little, T.J. (2009). An ancient immunity gene duplication in *Daphnia magna*: RNA expression and sequence analysis of two nitric oxide synthase genes. Dev. Comp. Immunol. 33: 1000-1010.

Lachaise, A.; Le Roux, A.; Hubert, M. and Lafont, R. (1993). The molting gland of crustaceans: localization, activity, and endocrine control. J. Crust. Biol. 13: 198-234.

Lai, E. C.; Burks, C. and Posakony, J. W. (1998). The K box, a conserved 3’ UTR sequence motif, negatively regulates accumulation of enhancer of split complex transcripts. Devel. 125: 4077-4088.

Laplante, M. and Sabatini, D.M. (2012). mTOR signaling in growth control and disease. Cell. 149: 274-293.

Laplante, M. and Sabatini, M. D. (2009). mTOR signaling at a glance. J. Cell Sci. 122: 3589–3594.

Layalle, S., Arquier, N., and Leopold, P. (2008). The TOR pathway couples nutrition and developmental timing in Drosophila. . Dev. Cell(15), 568-577.

Lee, S. G. and Mykles, D.L. (2006). Proteomics and signal transduction in the crustacean molting gland. Integr. Comp. Biol. 46: 965-977.

Lee, S.G.; Bader, B.D.; Chang, E.S. and Mykles, D.L. (2004). High-throughput proteomic approaches for identifying molt-associated proteins in crustacean molting gland. Integr. Comp. Biol. 44: 717.

Lee, S.G.; Bader, B.D.; Chang, E.S. and Mykles, D.L. (2007a). Effects of elevated ecdysteroid on tissue expression of three guanylyl cyclases in the tropical land crab *Gecarcinus lateralis*: possible roles of neuropeptide signaling in the molting gland. J. Exp. Biol. 210: 3245-3254.

Lee, S.G.; Kim, H.W. and Mykles, D.L. (2007b). Guanylyl cyclases in the tropical land crab, *Gecarcinus lateralis*: Cloning of soluble (NO-sensitive and -insensitive) and membrane receptor forms. Comp. Biochem. Physiol. 2D: 332-344.

Lenel, R., Veillet, A. (1951). Effects de l'ablation des pédoncules oculaires sur les pigments caroténoïdes du crabe Carcinus maenas. C. R. Acad. Sci. Paris 233, 1064-1065.

Li, S.K.; Zhang, Z.; Li, C.B.; Zhou, L.Z.; Liu, W.H.; Li, Y.Y.; Zhang, Y.L.; Zheng, H.P. and Wen, X.B. (2012). Molecular cloning and expression profiles of nitric oxide synthase (NOS) in mud crab *Scylla paramamosain*. Fish Shellfish Immunol. 32: 503-512.

Lin, C.L.; Wang, P.C. and Chuang, N.N. (1993). Specific phosphorylation of membrane proteins of Mr 44,000 and Mr 32,000 by the autophosphorylated insulin receptor from the hepatopancreas of the shrimp *Penaeus monodon* (Crustacea, Decapoda). J. Exp. Zool. 267: 113-119.

Liu, H.F.; Lai, C.Y.; Watson, R.D. and Lee, C.Y. (2004). Molecular cloning of a putative membrane form guanylyl cyclase from the crayfish *Procambarus clarkii*. J. Exp. Zool. 301A: 512-520.

Lu, W.Q.; Wainwright, G.; Olohan, L.A.; Webster, S.G.; Rees, H.H. and Turner, P.C. (2001). Characterization of cDNA encoding molt-inhibiting hormone of the crab, *Cancer pagurus*; expression of MIH in non-X-organ tissues. Gene 278: 149-159.

Ma, D.; Bai, X.; Guo, S. and Jiang, Y. (2008). The switch I region of Rheb is critical for its interaction with FKBP38. J Biol Chem. 38:25963-25970.

MacLea, K.S.; Abuhagr, A.M.; Pitts, N.L.; Covi, J.A.; Bader, B.D.; Chang, E.S., and Mykles, D.L. (2012). Rheb, an activator of Target of Rapamycin, in the blackback land crab, *Gecarcinus lateralis*: cloning and effects of molting and unweighting on expression in skeletal muscle. J. Exp. Biol. 215: 590-604.

Maestro, J.L.; Cobo, J. and Belles, X. (2009). Target of rapamycin (TOR) mediates the transduction of nutritional signals into juvenile hormone production. J. Biol. Chem. 284: 5506-5513.

Malarkey, K.; Coker, K. J. and Sturgill, T. W. (1998). Ribosomal S6 kinase is activated as an early event in preemergence development of encysted embryos of *Artemia salina*. Eur J Biochem. 1-2: 269-274.

Manor, R.; Weil, S.; Oren, S.; Glazer, L.; Aflalo, E.D.; Ventura, T.; Chalifa-Caspi, V.; Lapidot, M. and Sagi, A. (2007). Insulin and gender: An insulin-like gene expressed exclusively in the androgenic gland of the male crayfish. Gen. Comp. Endocrinol. 150: 326-336.

Markov, G. V.; Tavares, R.; Dauphin-Villemant, C.; Demeneix, B.A.; Baker, M.E. and Laudet, V. (2009). Independent elaboration of steroid hormone signaling pathways in metazoans. Proc. Natl. Acad. Sci. 106: 11913-11918.

Marte, B.M. and Downward, J. (1997). PKB/Akt: connecting phosphoinositide 3-kinase to cell survival and beyond. Trends Biochem. Sci. 22: 355–358.

Masahito, H.; Jianhua, F. and Brian, A. H. (2004). Structure, regulation and function of PKB/AKT-a major major therapeutic target. Biochim. Biophy. Acta. 1697: 3–16.

McDonald, A. A.; Chang, E. S. and Mykles, D. L. (2011). Cloning of a nitric oxide synthase from green shore crab, *Carcinus maenas*: a comparative study of the effects of eyestalk ablation on expression in the molting glands (Y-organs) of *C.maenas*, and blackback land crab *Gecarcinus lateralis*. Comp. Biochem. Physiol.158A: 150-162.

McGaw, I.J. and Naylor, E. (1992a). Distribution and rhythmic locomotor patterns of estuarine and open-shore populations of *Carcinus maenas*. J. Mar. Biol. Assoc. U. K. 72, 599-609.

McGaw, I.J. and Naylor, E. (1992b). Salinity preference of the shore crab *Carcinus maenas* in relation to coloration during intermolt and to prior acclimation. J. Exp. Mar. Biol. Ecol. 155: 145-159.

Medler, S.; Brown, K.J.; Chang, E.S. and Mykles, D.L. (2005). Eyestalk ablation has little effect on actin and myosin heavy chain gene expression in adult lobster skeletal muscles. Biol. Bull. 208: 127-137.

Mirth, C.; Truman, J.W. and Riddiford, L.M. (2005). The role of the prothoracic gland in determining critical weight to metamorphosis in *Drosophila melanogaster*. Curr. Biol. 15: 1796-1807.

Mirth, C.K. and Shingleton, A.W. (2012). Integrating body and organ size in *Drosophila*: recent advances and outstanding problems. Front. Endocrinol. 3: Article 49.

Montagne, J.; Lecerf, C.; Parvy, J.P.; Bennion, J.M.; Radimerski, T.; Ruhf, M.L.; Zilbermann, F.; Vouilloz, N.; Stocker, H.; Hafen, E.; Kozma, S.C. and Thomas, G. (2010). The nuclear receptor DHR3 modulates dS6 kinase-dependent growth in *Drosophila*. Plos Genetics 6. 5: e1000937.

Morton, D.B. (2004). Invertebrates yield a plethora of atypical guanylyl cyclases. Molecular Neurobiology 29: 97-115.

Morton, D.B. (2011). Behavioral responses to hypoxia and hyperoxia in Drosophila larvae Molecular and neuronal sensors. Fly 5: 119-125.

Morton, D.B. and Hudson, M.L. (2002). Cyclic GMP regulation and function in insects. In: Advances in Insect Physiology, Vol 29: 1-54

Mykles, D. L.; Adams, M.E.; Gade, G.; Lange, A.B.; Marco, H.G. and Orchard, I. (2010). Neuropeptide action in insects and crustaceans. Physiol. Biochem. Zool. 83: 836-846.

Mykles, D.L. (2011). Ecdysteroid metabolism in crustaceans. J. Steroid Biochem. Molec. Biol. 127: 196-203.

Mykles, D.L. (1997). Crustacean muscle plasticity: Molecular mechanisms determining mass and contractile properties. Comp. Biochem. Physiol. 117B, 367-378.

Mykles, D.L. (2001). Interactions between limb regeneration and molting in decapod crustaceans. Am. Zool. 41: 399-406.

Nakatsuji, T. and Sonobe, H. (2004). Regulation of ecdysteroid secretion from the Y-organ by molt-inhibiting hormone in the American crayfish, *Procambarus clarkii*. Gen. Comp. Endocrinol. 135: 358-364.

Nakatsuji, T.; Lee, C.Y. and Watson, R.D. (2009). Crustacean molt-inhibiting hormone: Structure, function, and cellular mode of action. Comp. Biochem. Physiol. 152A: 139-148.

Nimitkul, S.; Mykles, D.L. and Chang, E.S. (2010). Feedback regulation of ecdysteroid analog on Y-organs of the green crab *Carcinus maenas*. Integr. Comp. Biol. 50: E274.

Niwa, R.; Namiki, T.; Ito, K.; Shimada-Niwa, Y.; Kiuchi, M.; Kawaoka, S.; Kayukawa, T.; Banno, Y.; Fujimoto, Y.; Shigenobu, S.; Kobayashi, S.; Shimada, T.; Katsuma, S. and Shinoda, T. (2010). Non-molting glossy/shroud encodes a shot-chain dehydrogenase/reductase that functions in the "Black Box" of the ecdysteroid biosynthesis pathway. Devel. 137: 1991-1999.

Passano, L. M. (1960). Molting and its control. In T. H. Waterman (ed.). The physiology of Crustacea, Vol. I, pp: 473-536.

Patel, P. H.; Thapar, N.; Guo, L.; Martinez, M.; Maris, J.; Gau, C. L.; Lengyel, J. A. and Tamanoi, F. (2003). *Drosophila* Rheb GTPase is required for cell cycleprogression and cell growth. J. Cell Sci. 116: 3601-3610.

Peebles, J. B. (1977). A Rapid Technique for Molt staging in live Macrobra-chium rosenbergii. Aquacult. 12: 173-180.

Perrt, J. and Klechkner, N. (2003). The ATRs, ATMs, and TORs are giant HEAT repeat proteins, Cell 112: 151-155.

Potter, L.R. (2011). Guanylyl cyclase structure, function and regulation. Cell. Signal. 23: 1921-1926.

Pouchet, G. (1872). Sur les rapides changements de coloration provoqués expérimentalement, chez les Crustacés et sur les colorations bleues des poissons. J. Anat. 8: 401-407.

Proud, C. G. (2009). mTORC1 signalling and mRNA translation. Biochem. Soc. Trans. 37: 227-231.

Pullen, N.; Dennis, P. B.; Andjelkovic, M.; Dufner, A.; Kozma, S. C. and Hemmings, B. A. (1998). Phosphorylation and activation of p70s6k by PDK1. Sci. 279: 707–10.

Reid, D.G.; Abello, P.; Kaiser, M.J. and Warman, C.G. (1997). Carapace colour, inter-moult duration and the behavioural and physiological ecology of the shore crab Carcinus maenas. Estuar. Coast. Shelf Sci. 44: 203-211.

Rewitz, K. F. and Gilbert, L.I. (2008). Daphnia Halloween genes that encode cytochrome P450s mediating the synthesis of the arthropod molting hormone: Evolutionary implications. BMC Evol. Biol. 8: 60.

Rodriguez-Ramos, T.; Carpio, Y.; Bolivar, J.; Espinosa, G.; Hernandez-Lopez, J.; Gollas-Galvan, T.; Ramos, L.; Pendon, C. and Estrada, M.P. (2010). An inducible nitric oxide synthase (NOS) is expressed in hemocytes of the spiny lobster *Panulirus argus*: Cloning, characterization and expression analysis. Fish Shellfish Immunol. 29: 469-479.

Santiago, J. and Sturgill, T.W. (2001). Identification of the S6 kinase activity stimulated in quiescent brine shrimp embryos upon entry to preemergence development as p70 ribosomal protein S6 kinase: Isolation of *Artemia franciscana* p70(S6k) cDNA. Biochem. Cell Biol. 79: 141-152.

Schlattner, U.; Vafopoulou, X.; Steel, C.G.H., Hormann, R.E. and Lezzi, M. (2006). Non-genomic ecdysone effects and the invertebrate nuclear steroid hormone receptor EcR – new role for an “old” receptor? Molec. Cell. Endocrinol. 247: 64-72.

Shibley, G.A. (1968). Eyestalk function in chromatophore control in a crab, Cancer magister. Physiol. Zool. 41: 268-279.

Skinner, D. M. (1962). The structure and metabolism of a crustacean integumentary tissue during a molt cycle. Biol. Bull. 123: 635-647.

Skinner, D. M. (1985). Molting and regeneration, in The Biology of Crustacea, Bliss, D.E. and Mantel, L.H., Editors. Academic Press: New York. pp: 43-146.

Skinner, D.M., Graham, D.E. (1972). Loss of limbs as a stimulus to ecdysis in Brachyura (true crabs). Biol. Bull. 143: 222-233.

Small, L. F., and Habard, J. F. (1967). Respiration of a vertically migrating marine crustacean Euphausia pacifica HANSEN. Limnoh Ocean. 12: 272-280.

Sonja, A. D.; Jose, M. M.; Klara, R.; Michael, N. H. and Stephan, G. (2005). The Solution Structure of the FATC Domain of the Protein Kinase TOR Suggests a Role for Redox-Dependent Structural and Cellular Stability. J Biol Chem. 21: 20558-20564.

Soulard, A., Cohen, A. and Hall, M. N. (2009). TOR signaling in invertebrates. Curr.Opin. Cell Biol. 21: 825-836.

Soyez, D., and Kleinholz, L. H. (1977). Molt-inhibiting factor from the crustacean eyestalk. Gen. Comp. Endocrin. 31: 233-242.

Spaziani, E.; Jegla, T. C.; Wang. W. L.; Booth, J. A.; Connolly, S. M.; Conrad, C. C.; Dewall, M. J.; Sarno, C. M.; Stone, D. K. and Montgomery, R. (2001). Further studies on

signalling pathways for ecdysteroidogenesis in crustacean Y-organs. Ameri. Zool. 41: 418-429.

Srivastava, D.P.; Yu, E.J.; Kennedy, K.; Chatwin, H.; Reale, V.; Hamon, M.; Smith, T. and Evans, P.D. (2005). Rapid, nongenomic responses to ecdysteroids and catecholamines mediated by a novel *Drosophila* G-protein-coupled receptor. J. Neurosci. 25: 6145-6155.

Tamone, S.L.; Taggart, S.J.; Andrews, A.G.; Mondragon, J. and Nielsen, J.K. (2007). The relationship between circulating ecdysteroids and chela allometry in male tanner crabs: Evidence for a terminal molt in the genus Chionoecetes. J. Crustacean Biol. 27, 635-642.

Taylor, G.M.; Keyghobadi, N. and Schmidt, P.S. (2009). The geography of crushing: Variation in claw performance of the invasive crab *Carcinus maenas*. J. Exp. Ma. Biol. Ecol. 377: 48-53.

Teleman, A. A. (2010). Molecular mechanisms of metabolic regulation by insulin in Drosophila. J. Biochem. 425: 13-26.

Tepolt, C.K.; Darling, J.A.; Bagley, M.J.; Geller, J.B.; Blum, M.J. and Grosholz, E.D. (2009). European green crabs, *Carcinus maenas* in the northeastern Pacific: genetic evidence for high population connectivity and current-mediated expansion from a single introduced source population. Diver. Distrib. 15: 997-1009.

Thompson, J. D.; Gibson, T. J.; Plewniak, F.; Jeanmougin, F. and Higgins, D. G. (1997). The CLUSTAL_X windows interface: flexible strategies for multiple sequence alignment aided by quality analysis tools. Nucleic Acids Res. 25: 4876-4882.

Tim, R. F. and Ivan, T. G. (2011). Functions and regulation of the 70 kDa ribosomal S6 kinases. Biochem. Cell Biol. 43: 47–59.

Tiu, S.H.K. and Chan, S.M. (2007). The use of recombinant protein and RNA interference approaches to study the reproductive functions of a gonad-stimulating hormone from the shrimp *Metapenaeus ensis*. J. FEBS. 274: 4385-4395.

Toker, A. and Newton, A.C. (2000). Akt/protein kinase B is regulated by autophosphorylation at the hypothetical PDK-2 site. J. Biol. Chem. 275: 8271–8274.

Towle, D. W. and Smith, C. M. (2006). Gene discovery in *Carcinus maenas* and *Homarus americanus via* expressed sequence tags. Integr. Comp. Biol. 46: 912-918.

Treins, C.; Warne, P. H.; Magnuson, M. A.; Pende, M. and Downward, J. (2009). Rictor is a novel target of p70 S6 kinase-1. Oncog. 29: 1003–1016.

Ventura, T.; Manor, R.; Aflalo, E.D.; Weil, S.; Raviv, S.; Glazer, L. and Sagi, A. (2009). Temporal silencing of an androgenic gland-specific insulin-like gene affecting phenotypical gender differences and spermatogenesis. Endocrinol. 150: 1278-1286.

Veverka, V.; Crabbe, T.; Bird, I.; Lennie, G.; Muskett, F.; Taylor R. and Carr, M. (2008). Structural characterization of the interaction of mTOR with phosphatidic acid and a novel class of inhibitor: compelling evidence for a central role of the FRB domain in small molecule-mediated regulation of mTOR. Oncog. 5: 585–95.

Walkiewicz, M.A. and Stern, M. (2009). Increased insulin/insulin growth factor signaling advances the onset of metamorphosis in *Drosophila*. Plos One 4.

Wang, X.; Fonseca, B. D.; Tang, H.; Liu, R.; Elia, A.; Clemens, M. J. and Bommer, U. A. (2008) Proud CG. Re-evaluating the roles of proposed modulators of mammalian target of rapamycin complex 1 (mTORC1) signaling. J Biol Chem. 45: 30482-30492.

Webster, S.G. (1993). High-affinity binding of putative moult-inhibiting hormone (MIH) and crustacean hyperglycaemic hormone (CHH) to membrane-bound receptors on the Y-organ of theshore crab *Carcinus maenus*. Proc. R. Soc. Lond. Biol. 251: 53-59.

Webster, S.G.; Keller, R. and Dircksen, H., (2012). The CHH-superfamily of multifunctional peptide hormones controlling crustacean metabolism, osmoregulation, moulting, and reproduction. Gen. Comp. Endocrinol. 175: 217-233.

Won, J. H. and Estele, J. (2011). mTOR complex 2 signaling and functions. Cell Cyc. 14: 2305–2316.

Wullschleger,S.; Loewith, R. and Hall, M., N. (2006). TOR signaling in growth and metabolism. Cell 124: 471484.

Xin, H.; Michael, B.; Kurt, A. M.; Yan, G.; Paul, R.; Huilin, Z. and Xiaotian, Z. (2003). Crystal Structure of an Inactive Akt2 Kinase Domain. Struct. 1: 21–30.

Xu, P.L.; Liu, J.M. and Derynck, R. (2012). Post-translational regulation of TGF-beta receptor receptor and Smad signaling. FEBS Letters. 586: 1871–1884.

Yao, C.L.; Ji, P.F.; Wang, Z.Y.; Li, F.H. and Xiang, J.H. (2010). Molecular cloning and expression of NOS in shrimp, *Litopenaeus vannamei*. Fish Shellfish Immunol. 28: 453-460.

Zhao B.; Lehr R.; Smallwood A. M.; Ho T. F.; Maley K.; Randall T.; Head M. S.; Koretke K. K. and Schnackenberg C. G. (2007). Crystal structure of the kinase domain of serum and glucocorticoid-regulated kinase 1 in complex with AMP–PNP. Prote. Sci. 16: 2761–2769.

Zheng, J.Y.; Lee, C.Y. and Watson, R. D. (2006). Molecular cloning of a putative receptor guanylyl cyclase from Y-organs of the blue crab, *Callinectes sapidus*. Gen. Comp. Endocrinol. 146: 329-336.

Zhou, C.F.; Zhang, J.; Zheng, Y. and Zhu, Z.G. (2012). Pancreatic neuroendocrine tumors: A comprehensive review. Int. J. Cancer 131: 1013-1022.

Zhu, D.F.; Hu, Z.H. and Shen, J.M. (2011). Moult-inhibiting hormone from the swimming crab, *Portunus trituberulatus* (Miers, 1876); PCR cloning, tissue distribution, and expression of recombinant protein in Escherichia coli (Migula, 1895). Crus. 84: 1481-1496.

Zoncu, R.; Efeyan, A. and Sabatini, D.M. (2011). mTOR: from growth signal integration to cancer, diabetes and ageing. Nature Rev. Molec. Cell Biol. 12: 21-35.

APPENDICES

Appendix I. Cloing partial sequences for American lobster, *Homarus americanus* ribosomal protein S6 kinase (Ha-S6k).

```
gttaacttgacggggaagggccgtgtggacatggcgcatttcgaactgctcaaagtttta 60
 V  N  L  T  G  K  G  R  V  D  M  A  H  F  E  L  L  K  V  L  20
ggcacgggagcatatggaaaagtgtttcttgtgagaaaaatatcagggaaagatgcagga 120
 G  T  G  A  Y  G  K  V  F  L  V  R  K  I  S  G  K  D  A  G  40
aaactgtatgccatgaaggtcttgaagaaggcaaccatcatccagaagaaaaagacgaca 180
 K  L  Y  A  M  K  V  L  K  K  A  T  I  I  Q  K  K  K  T  T  60
gaacacacaaagacagagcgtcaagtcttggaggctgtgcgacaaagtcctttcctagtt 240
 E  H  T  K  T  E  R  Q  V  L  E  A  V  R  Q  S  P  F  L  V  80
actcttcactatgccttccaaactgatgccaagcttcatctaattttagattatgttagt 300
 T  L  H  Y  A  F  Q  T  D  A  K  L  H  L  I  L  D  Y  V  S  100
ggaggagaactatttacacacctgtatcagcgtgaaagatttcgtgaggatgaagtgcgt 360
 G  G  E  L  F  T  H  L  Y  Q  R  E  R  F  R  E  D  E  V  R  120
ctctatattggagaaatcatccttgcccttgagcatttgcacaaactgggcataatatat 420
 L  Y  I  G  E  I  I  L  A  L  E  H  L  H  K  L  G  I  I  Y  140
cgtgatatcaaacttgagaacattctcctagactctgatggccatgtagtgctaacagat 480
 R  D  I  K  L  E  N  I  L  L  D  S  D  G  H  V  V  L  T  D  160
tttggcctaagcaaggattttctgtcacatgacacagaacatcgtgcttactctttttgt 540
 F  G  L  S  K  D  F  L  S  H  D  T  E  H  R  A  Y  S  F  C  180
ggtactattgaatatatggcaccagaggtagttcgtggaggatctcatgggcatgaccag 600
 G  T  I  E  Y  M  A  P  E  V  V  R  G  G  S  H  G  H  D  Q  200
gcagtagactggtggagtgttggtgtgctgacttacgaacttttaacgggagcgtcacca 660
 A  V  D  W  W  S  V  G  V  L  T  Y  E  L  L  T  G  A  S  P  220
ttcactgttgagggagagaaaaataaccaacaggagatctcaaggcgaatcctgaaaaca 720
 F  T  V  E  G  E  K  N  N  Q  Q  E  I  S  R  R  I  L  K  T  240
caacctcctctaccgagtgaactgtccccagaagtttgtgatttcatttcccgtttactt 780
 Q  P  P  L  P  S  E  L  S  P  E  V  C  D  F  I  S  R  L  L  260
gtgaaagatccccgtcaacga                                         801
 V  K  D  P  R  Q  R                                          267
```

I. A. Nucleotide and amino acid sequences of cDNA encoding Ha-S6k. The cDNA encoded an incomplete ORF.

```
Cm-S6k : ----------------------------------QKMTGGRGGGSIFAMKVLKKATIVRN :  26
Ha-S6k : ---VNLTGKGRVDMAHFELLKVLGTGAYGKVFLVRKISGKDAG-KLYAMKVLKKATIIQK :  56
Gl-S6k : SDSTVNPGREKVRPSDFQLLKVLGKGGYGKVFQVRKMTGGRGGGKIFAMKVLKKATIVRN :  73
Aa-S6k : SEEIVNPGRMKLGPQDFELKKVLGKGGYGKVFQVRKTTGADAN-SYFAMKVLKKASIVRN : 109
Dp-S6k : SETTVNPGAEKTGPQDFELRRVLGRGGYGKVFQVRKLTGKDSG-HIFAMKVLKKATIVRN :  71
Dm-S6k : CEENVNPGKIKLGPKDFELKKVLGKGGYGKVFQVRKTAGRDAN-KYFAMKVLKKASIVTN : 119

Cm-S6k : QKDTAHTKAERNILEAVKH-PFIVDLVYAFQTGGKLYLILEYLSGGELFMHLEREGIFME :  85
Ha-S6k : KKTTEHTKTERQVLEAVRQSPFLVTLHYAFQTDAKLHLILDYVSGGELFTHLYQRERFRE : 116
Gl-S6k : QKDTAHTKAERNILEAVKH-PFILDLVYAFQTGGKLYLILEYLSGGELFMHLEREGIFME : 132
Aa-S6k : QKDTAHTRAERNILEAVRH-PFIVELVYAFQTGGKLYLILEYLSGGELFMHLEREGIFLE : 168
Dp-S6k : QKDTAHTKAERNILEAVKH-PFIVDLIYAFQTGGKLYLILEYLSGGELFMHLEREGIFME : 130
Dm-S6k : QKDTAHTRAERNILEAVKH-PFIVELVYAFQTDGKLYLILEYLSGGELFMHLEREGIFLE : 178

Cm-S6k : DTACFYISEIILALEHLHSEGIIYRDLKPENILLDSYGHVKLTDFGLCKEKIQDDSVT-- : 143
Ha-S6k : DEVRLYIGEIILALEHLHKLGIIYRDIKLENILLDSDGHVVLTDFGLSKDFLSHDTEHRA : 176
Gl-S6k : DTACFYISEIILALEHLHSEGIIYRDLKPENILLDAFGHVKLTDFGLCKEKIQDDSVT-- : 190
Aa-S6k : DTTCFYLCEIILALEHLHNLGIIYRDLKPENVLLDAQGHVKLTDFGLCKEHIQEGIVT-- : 226
Dp-S6k : DTASFYLAEIILALEHLHCQGIIYRDLKPENILLDAHGHVKLTDFGLCKESVEDGGVT-- : 188
Dm-S6k : DTTCFYLSEIIFALGHLHKLGIIYRDLKPENILLDAQGHVKLTDFGLCKEHIQEGIVT-- : 236

Cm-S6k : HTFCGTIEYMAPEILTR--TGHGKAVDWWSLGALMYDVLTGAPPFTAE----NRKKTIEK : 197
Ha-S6k : YSFCGTIEYMAPEVVRGGSHGHDQAVDWWSVGVLTYELLTGASPFTVEGEKNNQQEISRR : 236
Gl-S6k : HTFCGTIEYMAPEILTR--TGHGKAVDWWSLGALMYDMLTGAPPFTAE----NRKKTIEK : 244
Aa-S6k : HTFCGTIEYMAPEILTR--SGHGKAVDWWSLGALMFDMLTGMPPFTAD----NRKNTIDA : 280
Dp-S6k : HTFCGTIEYMAPEILTR--SGHGKAVDWWSLGALMYDMLTGAPPFTAE----NRKKTIEK : 242
Dm-S6k : HTFCGTIEYMAPEILTR--SGHGKAVDWWSLGALMFDMLTGVPPFTAE----NRKKTIET : 290

Cm-S6k : ILKGKLNLPPYLTPDSRDLIRKLLKRQVSQRLGSGSDDGEPIKRHLFFKLINWDEVINRK : 257
Ha-S6k : ILKTQPPLPSELSPEVCDFISRLLVKDPRQR----------------------------- : 267
Gl-S6k : ILKGKLNLPPYLTPDARDLIRKLLKRQVSQRLGSGPDDGEPIKRHLFFKLINWD-VINRK : 303
Aa-S6k : ILKGKLNIPAYLAADSRDLIRRLMKRQVSQRLGSGPTDGQAVRSHSFFKNVNWDDVLARR : 340
Dp-S6k : ILKGKLNLPPYLTPDARDLIRRLLKRGVVSRLGSTVADGEPVRMHPFFKTIDWNEVACRR : 302
Dm-S6k : ILKAKLNLPAYLTPEARDLVRRLMKRQEPQRLGSGPEDAAAVQIHPFFKHVNWDDVLARR : 350
```

I. B. Multiple alignment of deduced amino acid sequences of S6k proteins in four crustacean species and two insect species. Abbreviations: Ha, *H. americanus*; Aa, *A. aegypti* (XP001650653); Cm, *C. maenas* (JQ864250); Dm, *D. melanogaster* (AAC47429); Dp,. *D. pulxe* (EFX86042); and Gl, *G. lateralis* (HM989975). Amino acid residues that are identical or similar in all sequences are shaded in black; gray shading indicates identical or similar amino acids in most of the sequences. Dashes indicate gaps introduced to optimize the alignment.